



TECHNISCHE
UNIVERSITÄT
DARMSTADT

Refined generation of chimeric antigen receptor T cells by dasatinib and urolithin A


**vom Fachbereich Chemie
der Technischen Universität Darmstadt**

zur Erlangung des akademischen Grades
Doctor rerum naturalium
(Dr. rer. nat.)

**Dissertation von
Angela Hannah Braun, M. Sc.**
Aus Langen, Hessen

Erstgutachter: Prof. Dr. Harald Kolmar
Zweitgutachter: Prof. Dr. Christian J. Buchholz

Darmstadt 2024



Braun, Angela Hannah: Refined generation of chimeric antigen receptor T cells by dasatinib and urolithin A

Darmstadt, Technische Universität Darmstadt

Jahr der Veröffentlichung der Dissertation auf TUpriints: 2024

URN: urn:nbn:de:tuda-tuprints-265465

Tag der Einreichung: 05.10.2023

Tag der mündlichen Prüfung: 12.01.2024

Veröffentlicht unter CC BY-SA 4.0 International

<https://creativecommons.org/licenses/>

I. Summary

In recent years, genetic modification of T lymphocytes has revolutionized the treatment of certain types of hematopoietic cancer. Equipping T lymphocytes with chimeric antigen receptors (CARs) directed towards tumor-associated antigens (TAAs) has shown great clinical success in tumor cell elimination. However, there are still limitations to CAR T cell therapy that hinder its broader application and clinical efficacy. These limitations include the laborious manufacturing process and the quality of the resulting CAR T cells in terms of their efficacy and persistence. During manufacturing, the transduction of T cells, most often using lentiviral vectors (LVs), comprises extensive isolation and activation of T cells to ensure safe and efficient gene delivery. To reduce the risk of unwanted transduction and allow transduction of non-activated T cells, T cell-targeted LVs have been developed. Among these, CD3-LV is of potential relevance since the CD3 receptor in complex with the T cell receptor (TCR) is exclusively expressed on T cells and CD3-LV has been shown to activate and transduce non-activated T cells. However, CD3-LV-induced T cell activation increases CD3:TCR complex downregulation, eventually dampening gene transfer rates and preventing its clinical application.

Regarding the quality of the CAR T cell product, CAR T cell activity is often hampered by limited engraftment and persistence caused by differentiation and exhaustion of the CAR T cells. Therefore, CAR T cells with the favorable T stem cell memory (T_{SCM}) phenotype, have shown to be superior over conventional CAR T cells, as they greatly expand *in vivo* and have prolonged antitumor response. So far, attempts to increase the frequency of CAR T_{SCM} cells have been restricted to introducing additional steps to the manufacturing process, such as cell sorting, enrichment, and reprogramming.

To address the two limitations explained above, the small molecules dasatinib and urolithin A (UA) were used to help refine the generation of CAR T cells. Dasatinib is a tyrosine kinase inhibitor (TKI) known to inhibit phosphorylation by the T cell specific tyrosine kinase Lck and thereby preventing T cell activation. UA on the other hand, has been shown to induce mitophagy which is associated with immunomodulatory effects such as an enhanced antitumor efficacy.

Incubation of activated peripheral blood mononuclear cells (PBMCs) with dasatinib prior to transduction with CD3-LV(GFP) significantly increased transduction efficiency by 3- to 10-fold in a time- and dose-dependent manner. The maximal enhancing effect was achieved when 50 nM dasatinib was applied for five hours during transduction, resulting in over 60% transduced cells. The transduction enhancing effect of dasatinib, did not impair viability or cell proliferation and was further increased when combined with the transduction enhancer vectofusin-1 (VF-1). Importantly, dasatinib also increased the transduction of cytokine-only stimulated PBMCs and non-activated PBMCs in whole blood. In an *in vivo* approach, treatment with dasatinib did not interfere with the selectivity of CD3-LV, and one mouse treated with dasatinib prior to CD3-LV administration showed a higher transduction level and vector genome integration compared to untreated mice. While dasatinib increased transduction efficiency of CD3-LV in all these setups, it had no effect on transduction using CD4-, CD8- or VSV-LV. The inhibition of endocytosis or other tyrosine kinases did not enhance transduction by CD3-LV. Instead, preventing CD3-LV-induced T cell activation with dasatinib increased CD3 receptor availability and improved CD3-LV binding to the cells, most likely being the cause for dasatinib's enhancing effect. When CD19.CAR was delivered instead of the *gfp* reporter gene, dasatinib had the same effect on enhancing CD3-LV transduction. The presence of dasatinib during transduction with CD3-LV resulted in CAR T cell levels similar to those achieved with VSV-LV. These CAR T cells were able to efficiently kill tumor cells while expressing lower levels of exhaustion markers and exhibiting a slightly more naïve phenotype. While tumor cell killing was not affected by dasatinib, the secretion of pro-inflammatory cytokines during killing was reduced for CAR T cells generated in presence of dasatinib, regardless of whether they were transduced with CD3- or VSV-LV. Thus, dasatinib not only reduced CD3-LV-induced stimulation, resulting in increased CD3-LV-mediated gene transfer, but also reduced transduction-induced stimulation by LVs in general.

The second part of this thesis focused on the effect of UA on T cells and the generation of CAR T cells. Cultivation of T cells directly after transduction with LVs in medium containing 25 μ M UA resulted in a 10-fold expansion of T_{SCM} cells which among CAR-expressing T cells resulted in 50% T_{SCM} cells. This shift in phenotype is most likely attributed to the induction of mitophagy. Cultivation in UA-containing medium had no effect on the transduction efficiency or CAR expression. The high proportion of CAR T_{SCM} cells did not impair killing efficacy of neither CD19.CAR nor

CEA.CAR T cells. Accordingly, the transduction enhancing effect of dasatinib with CD3-LV was combined with the expansion of CEA.CAR T_{SCM} cells by UA, which allowed the selective transduction of 40% of the T cells, of which 30% showed to have the T_{SCM} phenotype, resulting in a high proportion of functional CAR T_{SCM} cells.

This work represents the first description of dasatinib as transduction enhancer for CD3-LV thus identifying a new class of transduction enhancers. Dasatinib is a member of a here firstly described class of transduction enhancers that do not act by facilitating vector-cell interaction outside the cell, but instead increase the availability of the target receptor through intracellular mechanisms, in this case Lck inhibition. Thereby, dasatinib prevents CD3:TCR downregulation, increases the binding of CD3-LV to the cell and by fusion of more CD3-LV particles with the cell, helps evade possible intrinsic restriction factors (RFs).

In addition, a simple protocol for the expansion of CAR T_{SCM} cells was developed in this work. The cultivation of cells in UA-containing medium significantly increases the amount of CAR T_{SCM} cells and provides a simplified method to enrich T_{SCM} cells compared to methods described so far. This demonstrates the ability of UA to reprogram human T cells towards the T_{SCM} phenotype by inducing mitophagy, thereby enhancing T cell fitness and providing a valuable source for future tumor therapies.

Taken together, the results obtained in this work demonstrate the potency of small molecules to further refine CAR T cell generation by representing a viable approach to facilitate gene delivery and generate a favorable CAR T cell phenotype, helping to improve therapeutic outcomes.

II. Zusammenfassung

In den letzten Jahren hat die Immuntherapie die Behandlung bestimmter Blutkrebsarten revolutioniert. Durch die Ausstattung von T-Lymphozyten mit chimären Antigenrezeptoren (CAR), die gegen tumorassoziierte Antigene gerichtet sind, wurden große klinische Erfolge bei der Eliminierung von Tumorzellen erzielt. Die CAR-T-Zelltherapie stößt jedoch weiterhin auf Hindernisse, die einer breiteren Anwendung und höheren klinischen Wirksamkeit im Wege stehen. Dazu gehören primär der hohe Aufwand bei der Herstellung sowie die Qualität der resultierenden CAR-T-Zellen in Bezug auf Wirksamkeit und *in vivo*-Persistenz. Die genetische Modifikation von T-Zellen erfolgt in der Regel durch Transduktion mit lentiviralem Vektor (LV). Im Herstellungsprozess gehen der Transduktion umfangreiche Isolierungs- und Aktivierungsschritte voraus, um einen sicheren und effizienten Gentransfer in ausschließlich T-Zellen zu gewährleisten. Die Verwendung von T-Zell-spezifischen LV könnte diese Schritte umgehen, das Risiko einer unerwünschten Transduktion verringern und die Transduktion nicht-aktivierter T Zellen ermöglichen. Der CD3-Rezeptor-targetierte LV (CD3-LV) ist hier von potentieller Bedeutung, da der CD3-Rezeptor im Komplex mit dem T-Zell-Rezeptor (engl. *T cell receptor*, TCR) ausschließlich auf T-Zellen exprimiert wird und CD3-LV nachweislich nicht-aktivierte T-Zellen aktiviert und transduziert. Die CD3-LV-induzierte T-Zellaktivierung führt jedoch zu einer verstärkten Runterregulierung des CD3:TCR-Komplexes, was letztlich die Gentransferraten dämpft und somit die klinische Anwendung verhindert.

Im Hinblick auf die Qualität des CAR-T-Zellprodukts wird die CAR-T-Zellaktivität häufig durch eine begrenzte Expansion und Persistenz der Zellen im Patienten beeinträchtigt, die durch die Differenzierung und frühe Erschöpfung der CAR-T-Zellen verursacht wird. So haben sich CAR-T-Zellen mit dem T-Gedächtnis-Stammzell Phänotyp (engl. *T stem cell memory*, T_{SCM}) gegenüber konventionellen CAR-T-Zellen als überlegen erwiesen, da sie eine starke Proliferation und eine verlängerte Antitumorantwort im Patienten zeigen. Bisherige Versuche die Häufigkeit von CAR-T_{SCM}-Zellen zu erhöhen, beschränkten sich auf die Einführung zusätzlicher Schritte im Herstellungsprozess. Um die genannten Hindernisse der CAR-T-Zelltherapie zu überwinden, wurden in dieser Arbeit die Moleküle Dasatinib und Urolithin A (UA) auf ihre Anwendbarkeit im Zusammenhang mit CAR-T-Zellen und

deren Herstellung getestet. Dasatinib ist ein Tyrosinkinase-Inhibitor (TKI), der die Phosphorylierung durch die T-Zell-spezifischen Tyrosinkinase Lck hemmt und somit die Aktivierung der T-Zellen verhindert. Im Gegensatz dazu induziert UA nachweislich Mitophagie, was mit positiven immunmodulatorischen Effekten wie einer verbesserten Antitumorwirkung assoziiert ist.

Die Inkubation von peripheren mononuklearen Blutzellen (engl. *peripheral blood mononuclear cells*, PBMCs) mit Dasatinib vor der Transduktion mit CD3-LV(GFP) steigerte die Transduktionseffizienz um das 3- bis 10-fache. Der Effekt war zeit- und konzentrationsabhängig und zeigte eine maximale Verstärkung nach fünfstündiger Inkubation der Zellen mit 50 nM Dasatinib, resultierend in über 60% transduzierter T-Zellen. Die transduktionsverstärkende Wirkung von Dasatinib beeinträchtigte weder die Zellviabilität noch die Zellproliferation und wurde durch die Kombination mit dem Transduktionsverstärker Vectofusin-1 (VF-1) noch verstärkt. Dasatinib steigerte zudem die Transduktion von Zytokin-stimulierten PBMCs und nicht-aktivierten PBMCs in Vollblut. Im Mausmodell zeigte sich, dass die Behandlung mit Dasatinib die Selektivität von CD3-LV nicht beeinträchtigt. Darüber hinaus zeigte eine Maus, die vor der Verabreichung von CD3-LV mit Dasatinib behandelt wurde, im Vergleich zu unbehandelten Mäusen eine leicht erhöhte Transduktionsrate und Integration des Vektorgenoms. Während Dasatinib die Transduktionseffizienz von CD3-LV in den verschiedenen Experimenten erhöhte, hatte es keine Auswirkungen auf die Transduktion mit CD4-, CD8- oder VSV-LV. Die Hemmung der Endozytose oder anderer Tyrosinkinasen verstärkte die Transduktion durch CD3-LV nicht. Stattdessen erhöhte die Inhibierung der CD3-LV-induzierten T-Zellaktivierung mit Dasatinib die Oberflächenexpression des CD3-Rezeptors und verbesserte die Bindung von CD3-LV an die Zellen. Dies ist höchstwahrscheinlich die Ursache für die transduktionsverstärkende Wirkung von Dasatinib. Die Generierung von CAR-T-Zellen durch Transduktion mit CD3-LV in Gegenwart von Dasatinib führte zu hohen CAR-T-Zellzahlen, vergleichbar mit denen die mit herkömmlichen LV erzielt werden. Diese CAR-T-Zellen waren in der Lage, Tumorzellen effizient zu eliminieren, während sie weniger Erschöpfungsmarker exprimierten und einen geringfügig naiveren Phänotyp aufwiesen. Während die zytotoxische Aktivität der CAR-T-Zellen gegen die Tumorzellen nicht beeinträchtigt wurde, war die Sekretion von proinflammatorischen Zytokinen bei CAR-T-Zellen, die in Gegenwart von Dasatinib generiert wurden,

reduziert. Dies war unabhängig davon, ob die CAR-T-Zellen mit CD3- oder VSV-LV transduziert wurden. Dasatinib reduzierte also nicht nur die durch CD3-LV-induzierte Stimulation, sondern auch die durch LV-Transduktion induzierte Stimulation im Allgemeinen.

Im zweiten Teil dieser Thesis wurde die Wirkung von UA auf T-Zellen und die Generierung von CAR-T-Zellen untersucht. Hierfür, wurden T-Zellen kurz nach der Transduktion mit LV in Medium mit 25 μ M UA über mehrere Tage kultiviert. Die Kultivierung der Zellen in UA-haltigem Medium führte zu einer 10-fachen Expansion der T_{SCM}-Zellen, was bei CAR-exprimierenden T-Zellen zu 50% T_{SCM}-Zellen führte. Diese Veränderung des Phänotyps ist höchstwahrscheinlich auf die Induktion der Mitophagie zurückzuführen ist. Die Kultivierung der Zellen in UA-haltigem Medium hatte keinen Einfluss auf die Transduktionseffizienz oder CAR Expression. Der hohe Anteil an CAR-T_{SCM}-Zellen beeinflusste weder die zytotoxische Aktivität von CD19.CAR- noch von CEA.CAR-T-Zellen. Anschließend wurde der transduktionsverstärkende Effekt von Dasatinib mit CD3-LV und der Expansion der CEA.CAR-T_{SCM}-Zellen durch UA kombiniert. Die Kombination beider Behandlungen ermöglichte die selektive Transduktion von 40% der T-Zellen, von denen 30% den T_{SCM}-Phänotyp aufwiesen, und führte dadurch zur Generierung zytotoxischer CAR-T_{SCM}-Zellen.

Diese Arbeit beschreibt erstmals die Funktion von Dasatinib als Transduktionsverstärker für CD3-LV und identifiziert eine neue Klasse von Transduktionsverstärkern. Dasatinib gehört zu einer hier erstmals beschriebenen Klasse von Transduktionsverstärkern, die nicht durch Erleichterung der Vektor-Zell-Interaktion außerhalb der Zelle wirken, sondern die Verfügbarkeit des Zielrezeptors durch intrazelluläre Mechanismen, in diesem Fall Lck-Inhibition, erhöhen. Auf diese Weise verhindert Dasatinib die Runterregulierung des CD3:TCR Rezeptorkomplexes, erhöht die Bindung von CD3-LV an die Zelle und hilft durch die Fusion von mehr CD3-LV-Partikeln mit der Zelle, mögliche intrinsische Restriktionsfaktoren (RFs) zu umgehen.

Darüber hinaus wurde in dieser Arbeit ein einfaches Protokoll für die Expansion von CAR-T_{SCM}-Zellen entwickelt. Die Kultivierung von Zellen in UA-haltigem Medium erhöht die Menge der CAR-T_{SCM}-Zellen signifikant und bietet eine vereinfachte Methode zur Anreicherung von T_{SCM}-Zellen im Vergleich zu bestehenden Methoden.

Dies zeigt, dass UA in der Lage ist, menschliche T-Zellen durch Induktion von Mitophagie in Richtung des T_{SCM}-Phänotyps umzuprogrammieren, wodurch die Fitness der T-Zellen verbessert und eine wertvolle Quelle für zukünftige Tumortherapien geschaffen wird.

Zusammenfassend zeigt diese Arbeit das Potenzial niedermolekularer Verbindungen (engl. *small molecules*) zur weiteren Verbesserung der CAR-T-Zellgenerierung. Die Kombination von Dasatinib und UA beschreibt einen praktikablen Ansatz, um den Gentransfer zu erleichtern und einen bevorzugten CAR-T-Zell-Phänotyp zu erzeugen, der die therapeutischen Ergebnisse womöglich verbessern wird.

Table of contents

I.	Summary	I
II.	Zusammenfassung	IV
1	Introduction	12
1.1	T lymphocytes	12
1.1.1	T cell receptor	12
1.1.2	T cell activation	13
1.1.3	T cell differentiation and exhaustion.....	15
1.2	CAR T cell therapy	17
1.2.1	CAR T cells	18
1.2.2	Manufacturing	20
1.2.3	Limitations of manufacturing and CAR T cell therapy	22
1.3	T cell-targeted gene transfer	23
1.3.1	Lentiviral vectors	24
1.3.2	T cell targeted lentiviral vectors.....	26
1.3.3	Transduction enhancers for lentiviral vectors.....	28
1.4	Objective	31
2	Results	32
2.1	Dasatinib as transduction enhancer for CD3-LV	32
2.1.1	Transduction of primary T cells in presence of dasatinib	33
2.1.2	Dasatinib's effect on viability and proliferation	36
2.1.3	Synergistic effect of dasatinib and vectofusin-1	37
2.1.4	Transduction of non-activated human T cells.....	39
2.1.5	Dasatinib enhances <i>in vivo</i> transduction in some mice.....	41
2.2	Mechanism of transduction enhancement by dasatinib.....	44
2.2.1	CD3-LV transduction is endocytosis independent.....	45
2.2.2	Dasatinib exclusively enhances CD3-LV gene transfer	46
2.2.3	Dasatinib prevents CD3-LV induced T cell activation	47

2.2.4	Dasatinib increases CD3 receptor availability and improves vector particle binding.....	49
2.2.5	The effect of tyrosine kinase inhibitors on LV gene delivery	51
2.3	Generation of CAR T cells in presence of dasatinib.....	52
2.3.1	Dasatinib enhances CD3-targeted CD19.CAR gene delivery in a time- and dose-dependent manner	53
2.3.2	Dasatinib enhances CAR expression in a co-culture with tumor cells, allowing long-term killing activity	56
2.3.3	Dasatinib mediates generation of functional and less exhausted CAR T cells	58
2.3.3.1	Comparing CD3-LV generated CAR T cells with and without dasatinib.....	58
2.3.3.2	Comparing CD3-LV to VSV-LV generated CAR T cells with and without dasatinib	62
2.3.3.3	Cytokine secretion after CD19.CAR T cell killing assay.....	65
2.4	Urolithin A promotes the expansion of CAR T _{SCM} cells	67
2.4.1	Urolithin A facilitates generation of CD19.CAR T _{SCM} cells	68
2.4.2	Urolithin A facilitates the generation of CEA.CAR T _{SCM} cells and can be combined with dasatinib	71
3	Discussion	78
3.1	A novel class of transduction enhancers.....	78
3.1.1	Dasatinib as transduction enhancer.....	78
3.1.2	The importance of receptor availability and particle binding for successful transduction.....	81
3.2	Towards better CAR T cells	86
3.2.1	Improved CAR T cell manufacturing using CD3-LV with dasatinib	86
3.2.2	CAR T cell subset and phenotype.....	88
3.3	Combining small molecules with CAR T cell therapy	90
4	Material and methods	93

4.1	Material	93
4.1.1	Chemicals and reagents	93
4.1.2	Kits	94
4.1.3	Buffers and solutions	94
4.1.4	Cell culture media	95
4.1.5	Cell lines	95
4.1.6	Antibodies	95
4.1.7	Plasmids	96
4.1.8	Oligonucleotide primers	97
4.1.9	Consumables	97
4.1.10	Instruments	98
4.1.11	Software	99
4.2	Methods	99
4.2.1	Molecular biology	99
4.2.1.1	Isolation of genomic DNA	99
4.2.1.2	Quantitative polymerase chain reaction	99
4.2.2	Cell culture	100
4.2.2.1	Freezing and thawing of cells	100
4.2.2.2	Cultivation of cell lines	101
4.2.2.3	Lentiviral vector production	101
4.2.2.4	Titration and particle number detection	102
4.2.2.5	Isolation of human primary blood mononuclear cells	103
4.2.2.6	Activation and cultivation of human PBMCs	104
4.2.2.7	Transduction of activated and cytokine-stimulated PBMCs	104
4.2.2.8	Transduction of whole blood	105
4.2.2.9	LV binding assay	105
4.2.2.10	T cell proliferation assay	105
4.2.2.11	Long-term killing assay	106

4.2.2.12	Cytotoxicity assay	106
4.2.2.13	Cytokine assay.....	107
4.2.2.14	Antibody staining and flow cytometry	107
4.2.3	Experimental mouse work.....	107
4.2.3.1	PBMC administration	108
4.2.3.2	Blood sampling and cell preparation	108
4.2.3.3	Drug formulation and administration	108
4.2.3.4	Administration of vector particles	109
4.2.3.5	Organ harvest and cell preparation	109
4.2.4	Statistical analysis.....	110
5	References	111
6	Abbreviations	129
7	List of figures and tables	133
7.1	Figures	133
7.2	Tables	135
8	List of publications	136
8.1	Original research articles.....	136
8.2	Conference poster presentations	136
8.3	Awards	137
8.4	Patents.....	137
9	Acknowledgement.....	138
10	Ehrenwörtliche Erklärung.....	139

1 Introduction

1.1 T lymphocytes

T lymphocytes, also known as T cells, are key players of the adaptive immune system, which provides protection against infection and malignancy. T cells are involved in the acquired or antigen-specific immune response. They arise from the bone marrow and mature in the thymus, where they undergo random T cell receptor (TCR) rearrangement resulting in unique TCRs that are negatively selected for autoreactivity and allow recognition of a diverse repertoire of antigens (Murphy et al., 2012). From the thymus, naïve T cells migrate continuously to the secondary lymphoid organs, such as spleen and lymph nodes, where they are primed and differentiate into effector cells with specific functions (Germain, 2002).

There are two primary subsets of T cells: Cluster of differentiation (CD)4⁺ T cells and CD8⁺ T cells. They are distinguished by the presence of the surface proteins, CD4 or CD8, which function as co-receptors and associate with distinct major histocompatibility complex (MHC) molecules. CD8⁺ T cells are also known as cytotoxic T cells as they directly kill recognized target cells that present the respective antigen on MHC class I molecules on their surface. CD4⁺ T cells, known as T helper cells, secrete pro-inflammatory chemokines and cytokines upon antigen recognition on MHC-II, to help induce the humoral immune response by activating B cells and other immune cell subsets. More recently, it has been shown that CD4⁺ T cells also possess cytotoxic activity (Agarwal et al., 2020; Akhmetzyanova et al., 2013; Li et al., 2020).

1.1.1 T cell receptor

The TCR is a heterodimeric cell surface receptor consisting of an α -chain and a β -chain. The TCR α and TCR β chains are linked by a disulfide bond, with their variable domains forming the antigen recognition site. Antigens are recognized as peptide fragments presented on MHC molecules displayed on antigen presenting cells (APCs). With the exception of a small subset of T cells characterized by an alternate pair of polypeptides, known as $\gamma:\delta$ T cells, which make up 1-5% of the circulating T cell population (Carding & Egan, 2002), the majority of T cells possess the $\alpha\beta$ -TCR. The TCR itself is not able to induce T cell activation due to missing intracellular signaling

motifs (Call et al., 2002). Therefore, the TCR is non-covalently associated to the CD3 receptor consisting of two heterodimers CD3 $\epsilon\gamma$ and CD3 $\epsilon\delta$, and one CD3 $\zeta\zeta$ homodimer (Figure 1, left) (Sušac et al., 2022). These CD3 signaling components bear immunoreceptor tyrosine-based activation motifs (ITAMs) in their cytoplasmic domains, which are phosphorylated by extrinsic Src-family kinases after antigen recognition (Call & Wucherpfennig, 2004; Palacios & Weiss, 2004; Straus & Weiss, 1992).

Though overall arrangement of TCR- $\alpha\beta$ /CD3 subunits and fully assembled ligand-bound structure of the receptor have recently been resolved (Dong et al., 2019; Sušac et al., 2022), the initiation of T cell signaling upon ligand binding remains to be a great enigma in immunology.

1.1.2 T cell activation

Prior to encountering an antigen, naïve T cells remain in their quiescent state, having low metabolic, transcriptional and translation activity (Chapman et al., 2020). This is rapidly changed upon antigen stimulation and co-stimulation of the cells, after which the cells transition from G0 into G2-S-M phase, and increase proliferation, cellular size, gene expression profile, surface receptor repertoire, mitochondrial activity and cytokine receptor production (Chapman et al., 2020; Chapman & Chi, 2018). All these properties are necessary for efficient response towards respective antigens. Since encounters with foreign antigens are relatively rare, T cell activation requires sensitive recognition of the antigen and the ability to rapidly increase the number of activated T cells in response to the stimulus (Huang et al., 2013).

Upon recognition and binding of the TCR to the peptide-loaded MHC complex, the co-receptors CD4/CD8 bind to the MHC molecules and bring the co-receptor associated tyrosine kinase Lck into close proximity to the ITAMs (Figure 1, right). Lck subsequently phosphorylates the tyrosine residues of the ITAMs, which is the first step in T cell activation and plays a crucial role in T cell receptor signaling in naïve T cells (Murphy et al., 2012; Palacios & Weiss, 2004). Next, the phosphorylated ITAMs recruit the Syk-family kinase ZAP-70, which is further phosphorylated and activated by Lck, along with undergoing autophosphorylation. Once activated, ZAP-70 phosphorylates the T cell specific adapters, LAT and SLP-76. This leads to the recruitment and activation of additional kinase families and enzymes, ultimately amplifying the stimulus

and culminating in the activation of T cells, providing signal 1 of the classical T cell activation pathway (Palacios & Weiss, 2004).

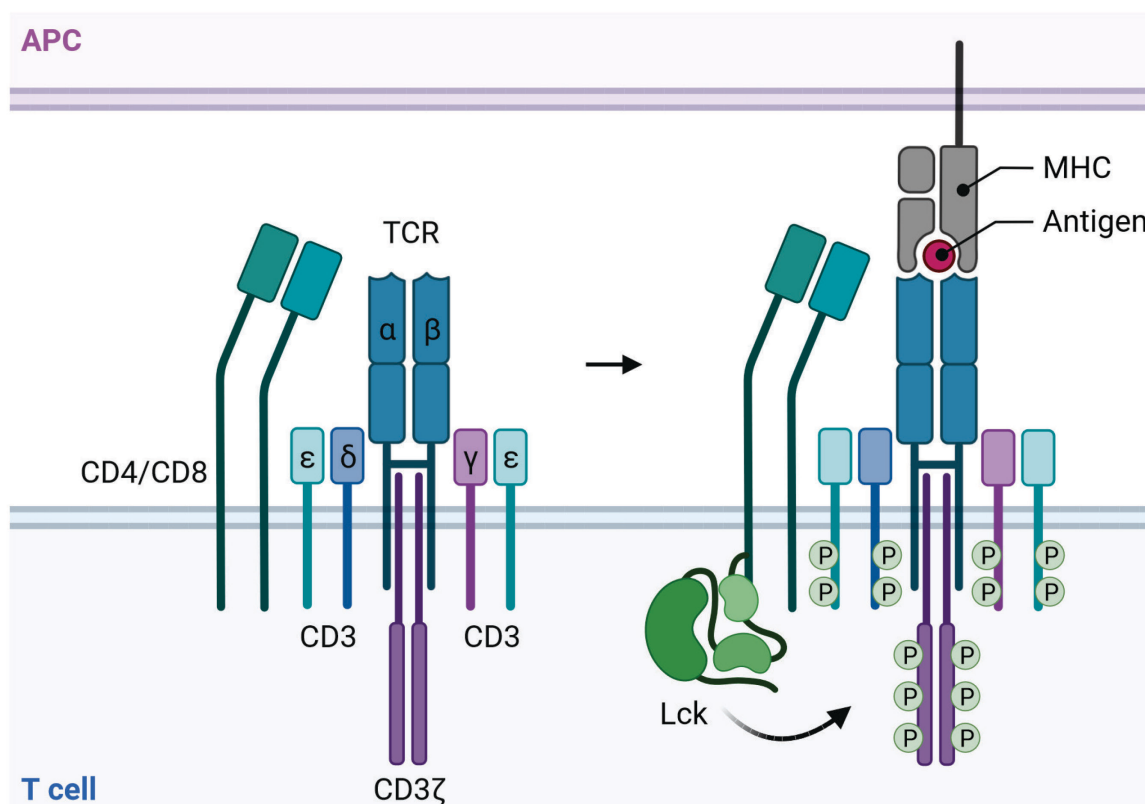


Figure 1: CD3 receptor: T cell receptor complex.

The antigen presenting cell (APC) membrane (lilac) is shown above and the membrane of the cytotoxic T cell (blue) is shown below. **(Left)** Schematic representation of the CD3 receptor domains (CD3 ϵ , CD3 δ , CD3 γ and CD3 ζ) in complex with the T cell receptor (TCR; TCR α and TCR β), supported by the co-receptor CD4 or CD8. **(Right)** Upon interaction of the TCR with the major histocompatibility complex (MHC) presenting an antigen, the tyrosine residues in the intracellular tyrosine activation motifs (ITAMs) of the CD3 domains become phosphorylated by the tyrosine kinase Lck. P:phosphorylation

For complete and sustained T cell activation, two additional signals are required, namely co-stimulation (signal 2) and inflammatory cytokines (signal 3). Signal 2 is mainly mediated by the co-receptor CD28, which upon binding to its ligands CD80 or CD86 on APCs, is phosphorylated by Lck and activates phosphatidylinositide 3-kinase (PI3K) (Acuto & Michel, 2003). Co-stimulation provided by CD28 functions as an amplifier for the relatively weak TCR signal. When combined with signal 1, co-stimulation activates second messengers, leading to the activation of three distinct transcription factors: NFAT, AP-1, and NF κ B. These transcription factors converge on the interleukin (IL)-2 promoter, inducing IL-2 production necessary for cell proliferation and differentiation, which in turn serves as signal 3 of T cell activation. Other pro-inflammatory cytokines can act directly on T cells and provide the signal 3 of T cell

activation (Curtsinger et al., 1999). Successful activation can be witnessed by the upregulation of several activation markers such as CD69, the IL-2 receptor α -chain (CD25), CD40 ligand and cytotoxic T-lymphocyte-associated protein 4 (CTLA-4) (Cibrián & Sánchez-Madrid, 2017; Murphy et al., 2012). Also, the secretion of pro-inflammatory cytokines such as interferon- γ (IFN- γ), tumor necrosis factor- α (TNF- α) and IL-2 is increased after activation, which enables survival of the T cells and converts effector function towards target cells (Brehm et al., 2005).

T cells can be activated through an MHC-independent pathway in the absence of APCs, triggered by agonistic monoclonal antibodies (Meuer et al., 1983). In cell culture, T cells are therefore commonly activated by incubation with α CD3 (clone OKT-3) antibody as signal 1 together with α CD28 antibody as signal 2 and inflammatory cytokines such as IL-2 or IL-7 and IL-15 as signal 3 (Vormittag et al., 2018).

To prevent pathogenesis caused by unwanted over-activation of T cells in the case of autoimmune disease, graft-versus-host disease (GvHD) or transplant rejection, inhibitory molecules such as dasatinib can be administered to patients. Dasatinib is a multitarget tyrosine kinase inhibitor of the Src/Abl kinase inhibitor family that binds to the T cell specific tyrosine kinase Lck and prevents phosphorylation upon antigen recognition (Lissina et al., 2009; Schade et al., 2008). Blocking Lck and thereby inhibiting phosphorylation of the ITAMs and continuously ZAP-70 prevents T cell activation.

1.1.3 T cell differentiation and exhaustion

The ability of T cells to fight disease relies on their capability to migrate to specific sites of inflammation, persist and carry out various effector functions. These characteristics are reflected in their distinct phenotypes, which develop over the course of T cell response.

Once naïve T cells (T_N) encounter APCs presenting a pathogenic antigen, T cells become activated, proliferate and differentiate into T stem cell memory (T_{SCM}), T central memory (T_{CM}), T effector memory (T_{EM}) and T effector (T_{EFF}) cells (Golubovskaya & Wu, 2016; Tantaló et al., 2021). In the process of differentiation, the effector functions increase while memory and proliferative function decrease, leading to terminally differentiate T_{EFF} cells which rapidly undergo apoptosis after pathogen clearance (Figure 2). The differentiation status is influenced by the type of stimulation,

the intensity of the signal, and the cytokine environment, and can be discriminated by phenotypic cell surface markers (Gattinoni et al., 2012; Golubovskaya & Wu, 2016).

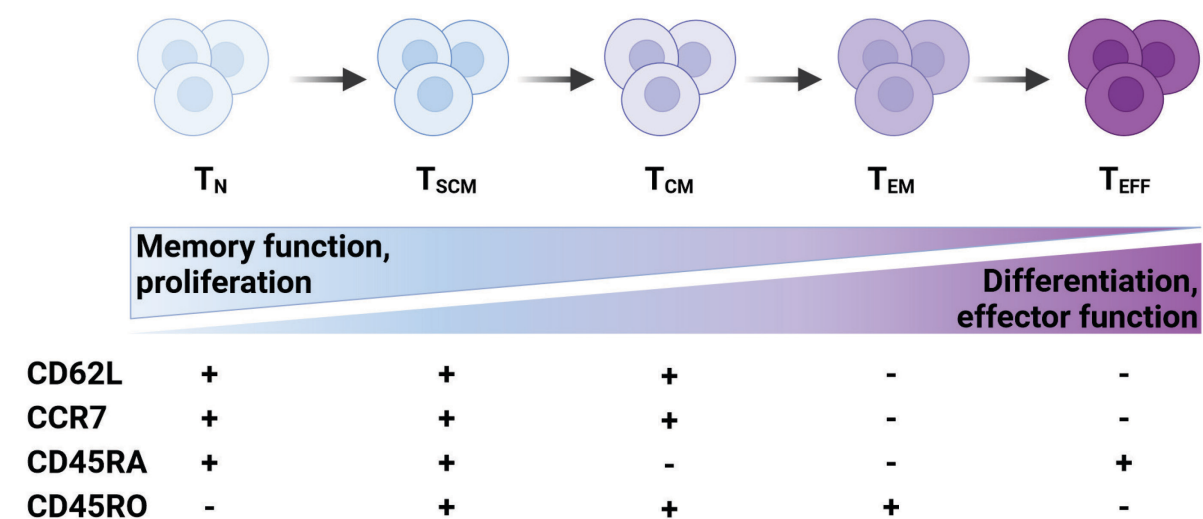


Figure 2: T cell differentiation.

The differentiation status of T cells can be distinguished by the expression of the cell surface receptors CD62L, CCR7, CD45RA and CD45RO. From left to right, the memory function and proliferative capacity of the T cells decrease while the effector function increases during differentiation. T_N : naïve T cell, T_{SCM} : stem cell memory T cell, T_{CM} : central memory T cell, T_{EM} : effector memory T cell, T_{EFF} : effector T cell. Figure adapted from (Golubovskaya & Wu, 2016).

The least differentiated T cells are T_N cells ($CD62L^+CCR7^+CD45RA^+$), which express the homing receptors CD62L and CCR7, and reside in the blood and lymphoid organs. They are antigen unexperienced and can persist in the lymph nodes for several years (5-10 years) prior to encountering their respective antigen (den Braber et al., 2012; Vrisekoop et al., 2008). Upon strong and prolonged antigen stimulation, T_N cells differentiate into T_{EFF} ($CD62L^-CCR7^-CD45RA^+$) cells, which migrate to the area of inflammation, produce high amounts of pro-inflammatory cytokines, and kill target cells. After target cell clearance, T_{EFF} cells rapidly undergo apoptosis, while some cells differentiate from T_{EFF} into T memory (T_M) cells. Alternatively, a proportion of activated T_N cells, which did not experience full-strength effector state, differentiate into T_M cells (Tantalo et al., 2021). These antigen-experienced, partially differentiated T_M cells, characterized by the expression of CD45RO, can continuously persist in absence of further antigen stimulation, maintaining both their proliferative and cytotoxic capacity (Verdon et al., 2020). T_M cells can be divided into the three memory subsets T_{SCM} , T_{CM} and T_{EM} cells. T_{CM} ($CD62L^+CCR7^+CD45RO^+$) cells express the lymph node homing receptors CD62L and CCR7, which retain them within the secondary lymphoid organs. These cells display an improved capacity for self-renewal and proliferation, while their

effector function is limited (Tantalo et al., 2021). T_{EM} (CD62L⁻CCR7⁻CD45RO⁺) cells are more effector-like, as they migrate to the site of inflammation, where they secrete cytokines and enforce effector function. More recently the T_{SCM} (CD62L⁺CCR7⁺CD45RA⁺RO⁺) cell phenotype was discovered, which is the least differentiated T_M cell type and makes up the rarest memory subset with only 2-3% of circulating T cells (Tantalo et al., 2021). Compared to T_N cells, T_{SCM} cells show increased proliferation and an enhanced ability to respond to their target antigen (Gattinoni et al., 2012; Gattinoni et al., 2011). Additionally, T_{SCM} cells exhibit enduring longevity, possess the capability for self-renewal, and can restore the full range of T_M and T_{EFF} cell subsets.

Under conditions of persistent high antigen stimulation or repeated engagement of the TCR without proper co-stimulation, T cells transition into a state of exhaustion, irrespective of their differentiation state (Blank et al., 2019; Tantalo et al., 2021). Exhausted T cells experience compromised effector functions, undergo changes in metabolic and transcriptional profiles, exhibit impaired cytokine production, and express a range of co-inhibitory receptors, including T cell immunoglobulin and mucin domain-containing protein 3 (TIM-3), lymphocyte activation gene 3 (LAG-3), and programmed cell death protein 1 (PD-1) (Verdon et al., 2020). The co-expression of these inhibitory receptors on exhausted and therefore dysfunctional T cells can induce tolerance and inhibit antitumor function towards malignant cells (Tantalo et al., 2021; Verdon et al., 2020).

1.2 CAR T cell therapy

Adoptive immunotherapy has revolutionized the treatment of certain types of cancer in the past years. In the 1990s, the first gene transfer techniques evolved, redirecting the specificity of T cells by genetically introducing TCRs or chimeric antigen receptors (CARs) (Gross et al., 1989; June & Sadelain, 2018). Such T cell-based immunotherapies are meant to reengage the immune system in recognizing and eliminating malignant cells. Up to date, six CAR T cell products are approved by the Food and Drug Administration (FDA) and the European Medicines Agency (EMA). All products target hematological malignancies and are approved for the treatment of several indications including B cell acute lymphatic leukemia (B-ALL), multiple myeloma, large B cell lymphoma, follicular lymphoma, and mantle-cell lymphoma

(Labanieh & Mackall, 2023). Four of the six CAR T cell products target the B cell marker CD19 (Kymriah, Yescarta, Tecartus and Breyanzi) and two target the B cell maturation antigen (BCMA) (Abecma and Carvykti). Many more tumor markers and treatment indications are under investigation, including other B cell markers such as CD20 or CD22, T cell markers such as CD7 for treatment of T cell acute lymphoblastic leukemia (T-ALL), but also solid tumor markers such as disialoganglioside 2 (GD2), epidermal growth factor receptor-2 (HER2), epithelial growth factor receptor (EGFR), and carcinoembryonic antigen (CEA) (Labanieh & Mackall, 2023; Chengcheng Zhang et al., 2017). The use of CAR T cells for the treatment of solid tumors remains challenging, due to several factors including the lack of truly exclusive solid tumor antigens leading to on-target off-tumor toxicity, impaired CAR T cell trafficking and tumor infiltration, and early T cell exhaustion conferred by the tumor microenvironment (L. Wang et al., 2019). While clinical results are still much less encouraging, a growing number of studies indicate the applicability and safety of CAR T cells in solid tumors (Holzinger & Abken, 2017; Newick et al., 2016; Chengcheng Zhang et al., 2017).

1.2.1 CAR T cells

In order to mediate sufficient killing of tumor cells, CARs must selectively recognize and bind to the tumor cells, and subsequently trigger T cell activation to induce cytotoxicity. CARs provide the unique ability for T cells to recognize target cells independently of MHC molecules through the full-length cell surface receptors. This MHC-independent recognition broadens the range of potential targets that CAR T cells can identify and eliminate (Holzinger & Abken, 2019). CARs contain an extracellular antigen binding domain commonly consisting of an antibody-derived single chain variable fragment (scFv) necessary for antigen recognition and binding (Figure 3). The binding domain is connected via hinge region to the transmembrane domain (TMD) derived from CD28, CD8 or CD4 (Holzinger & Abken, 2019). The TMD connects the targeting moiety to the intracellular signaling and activation domain (ICD). The ICD of first generation CAR T cells solely contains the CD3 ζ signaling domain derived from the TCR. Upon binding of the CAR to the target, the CD3 ζ ITAMs are phosphorylated and mediate antigen-specific stimulation, providing signal 1 for T cell activation (Eshhar et al., 1993; Vormittag et al., 2018). To ensure a sustained T cell response, second-generation CAR T cells incorporate a co-stimulatory domain, commonly

derived from CD28 or 4-1BB, to provide signal 2. This addition provides the essential signal 2 during T cell activation. Third-generation CAR T cells combine two costimulatory domains with the primary signal, which is believed to enhance CAR T cell survival and maturation (Srivastava & Riddell, 2015; Weinkove et al., 2019). Overall, co-stimulatory domains have been shown to increase effector function and persistence, allowing for a pronounced and durable clinical effect (Ramos et al., 2018; Weinkove et al., 2019). Next generation designs are being developed, containing additional antigen specificities or co-expressing biologically active proteins (Holzinger & Abken, 2019). At the moment, all authorized products use second generation constructs delivered by viral vectors. However, they differ in specific domains within the CAR structure, the viral vector used for CAR gene delivery, and certain manufacturing steps (Cappell & Kochenderfer, 2023).

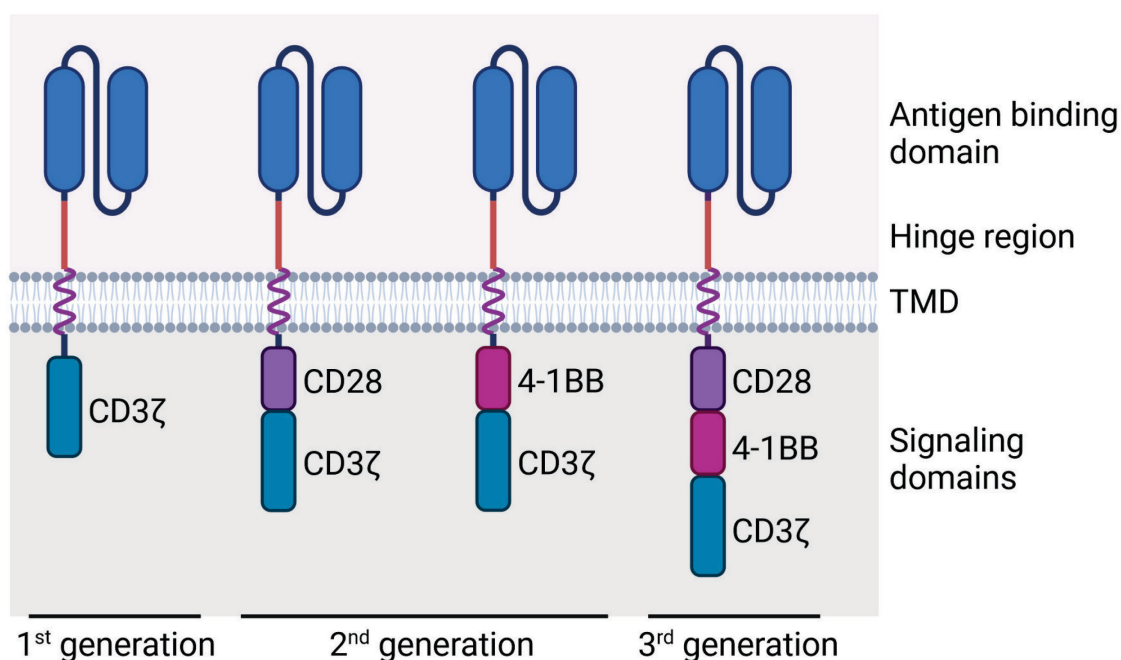


Figure 3: Chimeric antigen receptor designs.

Chimeric antigen receptors (CARs) are equipped with an antigen binding domain, often a single chain variable fragment (scFv), that allows binding to a tumor antigen of choice. The scFv is connected via a hinge region to the transmembrane domain (TMD) and the intracellular signaling domains. The 1st generation of CARs solely contain a CD3ζ signaling domain, while 2nd generation CARs incorporate an additional co-stimulatory domain derived from CD28 or 4-1BB. The 3rd generation of CARs combine the two co-stimulatory domains along with the CD3ζ signaling domain.

To achieve exclusive tumor cell recognition without inducing on-target off-tumor toxicity, the selection of an appropriate target antigen is crucial for therapeutic efficacy (Sterner & Sterner, 2021). While B cell-specific CAR T cells show strong antitumor effects with tremendous response rates and manageable side effects, the clinical

outcomes in solid tumors are not satisfactory and side effects due to on-target off tumor activity remain to be one of the major hurdles in CAR T cell therapy against solid tumors (June & Sadelain, 2018; Labanieh & Mackall, 2023).

Nevertheless, clinical efficacy in treatment of gastrointestinal adenocarcinoma with CEA.CAR T cells has been demonstrated (Holzinger & Abken, 2017; Katz et al., 2015; Thistlethwaite et al., 2017; Chengcheng Zhang et al., 2017). CEA is a promising tumor associated antigen (TAA) for colorectal cancer (CRC) as it is nearly not detectable in healthy adult tissue. It is expressed at low levels on the apical surface of the gastrointestinal tract, making it invisible to immune cells (Chengcheng Zhang et al., 2017). In cancer cells, CEA is upregulated and expressed over the entire cell, making it a feasible target for CAR T cells without inducing severe tissue destruction (Katz et al., 2015; Thistlethwaite et al., 2017; Chengcheng Zhang et al., 2017).

1.2.2 Manufacturing

Currently, CAR T cell manufacturing is carried out in a multi-stage workflow with several production steps, combined with extensive quality controls (Figure 4). The first step of CAR T cell manufacturing is the isolation of white blood cells from the patient's blood by leukapheresis. Optionally, the isolated leukocytes can be cryopreserved or downstream manufacturing can be directly conducted with the fresh product. Next, T cells are isolated and enriched by fluorescent or magnetic cell sorting and can be sorted for specific T cell subsets or phenotypes to obtain a defined T cell composition (Levine et al., 2017; X. Wang & Riviere, 2016). For efficient expansion and transduction, the T cells are activated through the endogenous CD3:TCR receptor by stimulation with recombinant antibodies against CD3 and CD28 (soluble, plate-, or bead-bound) in combination with IL-2 or IL-7 and IL-15 (Vormittag et al., 2018). The activated T cells are then genetically modified using viral vectors encoding the CAR. Most commonly, lentiviral vectors (LVs) or gamma-retroviral vectors (γ -RV) are used as they stably integrate the CAR gene and allow for long-lasting gene expression. Additionally, transduction enhancers are routinely used to improve transduction efficiency (Abou-El-Enein et al., 2021). More recently, non-viral transposon/transposase gene delivery systems have been applied to generate CAR T cells and clinical trials are ongoing (Bishop et al., 2021; Caruso et al., 2019; Lock et al., 2022). After transduction or transfection, the T cell product is expanded *ex vivo* for

several days (6-14 days), during which the cells are frequently washed and the medium is changed to remove residual vector particles and maintain optimal conditions for T cell expansion (Ghassemi et al., 2022; Ghassemi et al., 2018). Before reinfusion into the patients, the cellular products undergo in process and release quality control. In these measurements, the absence of contaminations, the percentage of CAR T cells, and the vector copy numbers (VCN) per cell genome, are determined (X. Wang & Riviere, 2016). The concentrated cells are then cryopreserved and delivered to the site of administration, where the product is reinfused into the lymphodepleted patient. In total, the entire process, takes three to five weeks, from the time of leukapheresis to the production of the CAR T cells, the quality control, and final reinfusion of the product (Geethakumari et al., 2021).

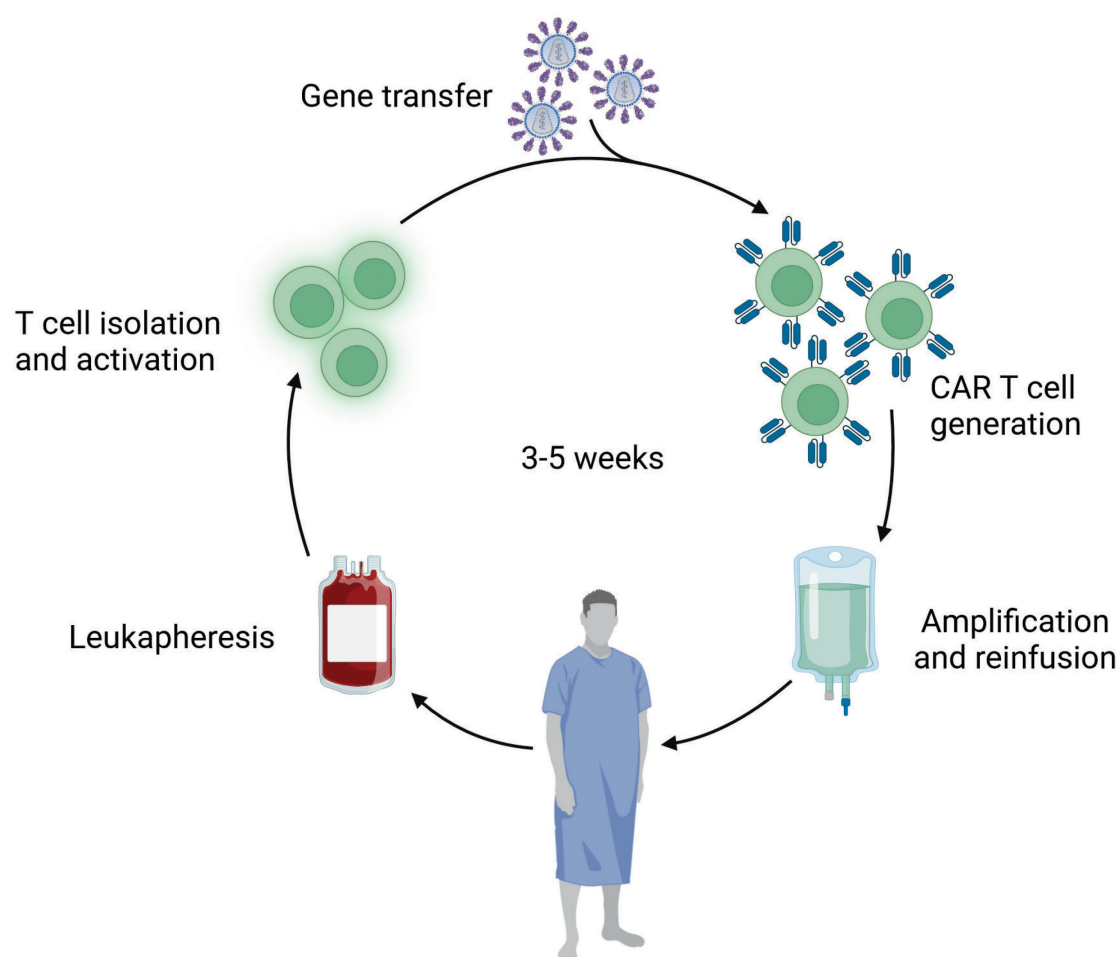


Figure 4: CAR T cell manufacturing.

Patients undergo leukapheresis and T cells are subsequently isolated and activated. Activated T cells are genetically modified using a viral vector to express the CAR. CAR T cells are amplified and reinfused into the patient.

1.2.3 Limitations of manufacturing and CAR T cell therapy

Ex vivo manufacturing of CAR T cells is complex, time-consuming and therefore expensive. Several factors and production steps restrain the availability, safety and efficiency of the product. The long manufacturing time reduces the chance of successfully treating severely ill patients with progressing disease (Yang et al., 2022). Additionally, the composition and quality of the starting material has a major impact on the resulting product, as highly diseased and treated patients often have a low yield of T cells with an exhausted and highly differentiated phenotype (Abou-El-Enein et al., 2021). Apart from that, the manufacturing process itself causes accelerated differentiation, exhaustion and senescence of the cells, and was recently described to induce dysfunctional methylation programs (Salz et al., 2023; Watanabe et al., 2022). For instance, the step of T cell activation is time-consuming and causes progressive differentiation, shown to be associated with loss of anti-leukemic efficacy (Ghassemi et al., 2018). The stimulation during T cell transduction, tonic signaling by the CAR and cytokine signaling during expansion can further drive differentiation and exhaustion (Watanabe et al., 2022). This progressive loss of stemness induced by *ex vivo* cultivation has shown to reduce potency and persistence of the product *in vivo* (Ghassemi et al., 2022; Ghassemi et al., 2018), and factors such as expansion, persistence and phenotype have been identified to directly correlate with the clinical response (Fraietta et al., 2018). While the initial response rate of complete remission in patients treated with CAR T cells is around 70-90%, about 40-60% of these patients experience relapse and tumor progression (Gu et al., 2022; Larson & Maus, 2021; Yang et al., 2022). Many groups are therefore working to shorten the manufacturing process to just a few days (Ghassemi et al., 2022; Ghassemi et al., 2018; Yang et al., 2022; Cheng Zhang et al., 2022) or enrich for a more favorable phenotype (Arcangeli et al., 2022; Jung et al., 2023; Meyran et al., 2023), in the hope of improving clinical outcomes.

Further, safety considerations persist in the production and administration of CAR T cell therapy. Precise isolation and selection of T cells prior to genetic modification are critical during the manufacturing process, as the presence of non-target cells, specifically malignant cells, can give rise to significant safety concerns during gene transfer. The transduction of a single leukemic cell has demonstrated the ability to confer resistance to CAR T cells, leading to relapse and ultimately death of

the patient (Ruella et al., 2018). An additional risk is associated with the infusion of large numbers of CAR T cells into the patients. The patients frequently develop side effects characterized as cytokine release syndrome (CRS) and immune effector cell associated neurotoxicity syndrome (ICANS). These side effects arise due to the rapid proliferation and activation of the infused CAR T cells, resulting in the secretion of elevated levels of cytokines, which can progress to life-threatening grades (Lee et al., 2014; Shimabukuro-Vornhagen et al., 2018).

The increasing demand of CAR T cells in the upcoming years will require improved manufacturing platforms and methods to refine the clinical product (Abou-El-Enein et al., 2021). The main strategies hereby being: shortening manufacturing time, selecting a preferred T cell phenotype and T cell composition as starting material, and further improving the product's safety.

To meet the clinical need, there is growing interest in transitioning from the personalized towards an off-the-shelf product using allogeneic T cells as a readily available and often better source for CAR T cell therapy. Moreover, advancements in gene delivery techniques have opened new avenues for delivering the genetic information of the CAR directly *in vivo*, bypassing the *ex vivo* modification step altogether (Michels et al., 2022). Therefore, T cells can be genetically modified *in vivo*, by systemic administration of T cell-targeted vectors delivering the CAR transgene (Pfeiffer et al., 2018). This approach eliminates the need for *ex vivo* handling of the cells, thereby preventing cultivation induced exhaustion and differentiation. In addition, it circumvents the risk of cytokine secretion during CAR T cell administration, significantly shortens the time until treatment, and has the potential to expand the availability of the treatment. To date, T cell-targeted gene delivery *in vivo* has been achieved using polymer nanocarriers, lipid nanoparticles, and most often viral vectors in preclinical mouse models (Michels et al., 2022).

1.3 T cell-targeted gene transfer

The most promising approach for T cell-targeted gene transfer is the use of viral vectors, mainly γ -RVs or LVs, as they stably integrate into the genome and lead to sustained expression of the transgene (Naldini et al., 2016). For this purpose, LVs are especially favorable since they are able to transduce resting cells and show lower genotoxicity, as they integrate semi-randomly into sites away from active promoter

regions (Abou-El-Enein et al., 2021; Gogol-Döring et al., 2016; Levine et al., 2017). To enable cell specific gene transfer, LVs have been engineered to recognize selected surface markers as entry receptors and have shown to be effective in transducing T cells *in vitro* and *in vivo* (Agarwal et al., 2020; Frank et al., 2020; Pfeiffer et al., 2018).

1.3.1 Lentiviral vectors

LVs are most commonly derived from the human immunodeficiency virus-1 (HIV-1), an enveloped, single-stranded ribonucleic acid (ssRNA) virus of the *Retroviridae* family. With a packaging capacity of 10 kb, it contains two copies of positive sense ssRNA encoding nine viral proteins (Sakuma et al., 2012).

To prevent replication competence of engineered LVs, the genome of HIV-1 is modified by removing the self-replicative elements and splitting the viral genome onto different plasmids (Figure 5). Genes non-essential for particle formation, such as the accessory genes *vif*, *vpr*, *vpu* and *nef* are eliminated (Zufferey et al., 1997). Consequently, genes necessary for particle assembly namely, *gag*, *pol*, and *env* are co-expressed to produce the viral vectors (Blessing & Deglon, 2016). Therefore, the three primary structural genes are separated onto distinct plasmids to avoid recombination. *Gag/pol* are encoded on the packaging plasmids, providing the information for the viral core proteins and viral enzymes needed for replication, while the glycoproteins are encoded on the envelope plasmid. These two plasmids contain a strong constitutive promoter of choice and lack the packaging signal Ψ to prevent incorporation of the genes into the viral particles, ensuring replication deficiency of the vectors. The transfer plasmid contains the transgene under the control of an internal promoter of choice, flanked by 5' and 3' long terminal repeats (LTRs) for genome integration. Only the transfer vector plasmid with the gene of interest contains the packaging signal Ψ and is integrated into the vector particles. In addition, the U3 region of the 3'-end LTR, known to confer promoter and enhancer activity, is deleted resulting in a self-inactivating (SIN) LV that cannot be fully mobilized following integration into the host genome (Miyoshi et al., 1998; Zufferey et al., 1998).

The three plasmids are transiently co-transfected into human embryonic kidney (HEK) producer cells, where the genes are transcribed and translated. The proteins expressed from the packaging plasmid assemble the viral capsid into which the ssRNA transgene is incorporated via its packaging signal Ψ (Sakuma et al., 2012). The

glycoproteins expressed from the envelope plasmid are trafficked to and presented on the cell membrane, where the assembled viral capsids bud from the cells equipped with the transmembrane and receptor binding proteins. The released viral particles can be harvested from the supernatant and used as gene delivery vectors after further purification and concentration.

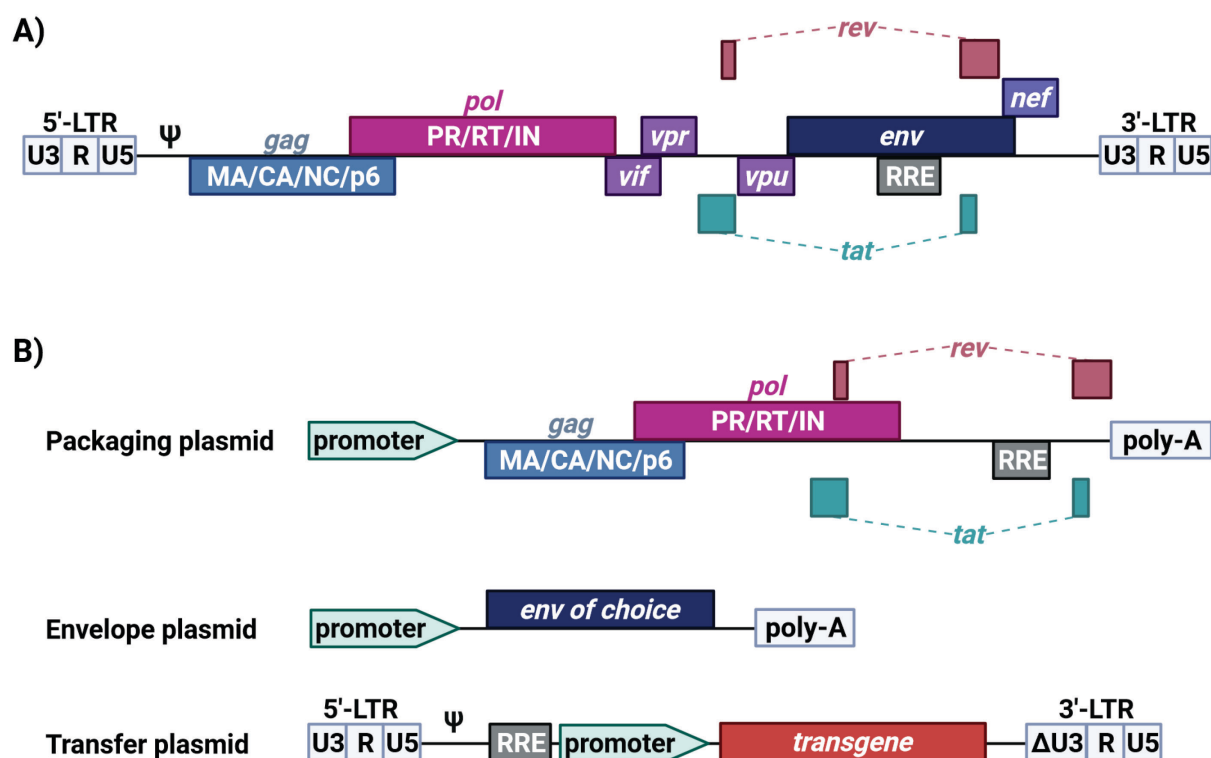


Figure 5: Genetic information of HIV-1 and HIV-1 derived 2nd generation lentiviral vectors.

(A) The HIV-1 genome is flanked by 5'- and 3'-long-terminal repeats (LTR). The packaging signal ψ is followed by the structural genes *gag*, *pol* and *env*, the regulatory genes *rev* and *tat*, and the accessory genes *vif*, *vpr*, *vpu* and *nef*. *Gag* encodes the viral core proteins. *Pol* codes for viral protease (PR), reverse transcriptase (RT) and integrase (IN). The envelope glycoproteins gp120 surface subunit (SU) and gp41 transmembrane subunit (TM) are encoded by *env*. The four genes *vif*, *vpr*, *vpu* and *nef* encode virulence factors. **(B)** The genetic information for 2nd generation lentiviral vectors (LVs) is split onto three plasmids, the packaging, the envelope and the transfer plasmid, and all genes non-essential for particle formation are deleted. Gene expression is driven by promoters of choice and only the transfer plasmid with the transgene contains the packaging signal ψ and is incorporated into the viral particles. Poly-A: polyadenylation signal, RRE: rev-responsive element. Figure adapted from (Sakuma et al., 2012).

To broaden the range of cellular targets, LVs can be equipped with glycoproteins from various virus families with different receptor specificities. The process of altering the native envelope protein to a glycoprotein that is derived from other enveloped viruses is termed pseudotyping. This modification enables the vectors to effectively bind to and transduce specific cell types.

The most commonly used glycoprotein is the vesicular stomatitis virus glycoprotein (VSV-G), a member of the *Rhabdoviridae* family (Finkelshtein et al., 2013). It serves

as the gold standard for LV transduction due to its high stability, broad tropism and good efficiency to transduce cells. The high stability of the glycoprotein allows the concentration of the harvested VSV-G pseudotyped LVs (VSV-LVs) generating stocks with high titers. VSV-LV targets the low density lipoprotein (LDL) receptor, which is expressed on many cell types. Some cells such as resting T cells, show very low levels of LDL receptor and are therefore not susceptible to efficient transduction with VSV-LV, despite VSV-LV's broad tropism (Amirache et al., 2014). On the other hand, the broad tropism of VSV-LV limits its use mainly to *in vitro* application of pre-selected cells and precludes *in vivo* administration (Finkelshtein et al., 2013).

1.3.2 T cell targeted lentiviral vectors

In order to improve viral gene transfer by making it safer and eventually enabling *in vivo* gene delivery, it is necessary to selectively transduce the cells of interest. In this context, glycoproteins from the *Paramyxoviridae* family have raised interest. These are negative-stranded RNA viruses with the unique feature of having two viral glycoproteins, one responsible for receptor recognition and binding, and one responsible for cell fusion (fusion (F) protein). Therefore, receptor recognition can be altered, while membrane fusion is not affected. The modification of paramyxoviral glycoproteins to selectively target cells was firstly described for the measles virus (MV) envelope protein hemagglutinin (H protein) (Funke et al., 2008) and extended to Nipah virus (NiV) glycoprotein (G protein) (Bender et al., 2016). To achieve successful engineering of these glycoproteins, deliberate mutations need to be introduced at the receptor contact residues of the natural receptor binding site, making the glycoprotein incapable of binding to its original receptors (Figure 6). Next, the glycoproteins can be equipped with a new specificity by genetically fusing targeting ligands such as scFv (Funke et al., 2008) or DARPin (Münch et al., 2011), which recognize a receptor of choice, to the blinded glycoproteins H_{mut} or G_{mut}. In addition, the cytoplasmic domains of the glycoproteins need to be truncated to allow successful integration into the viral particle.

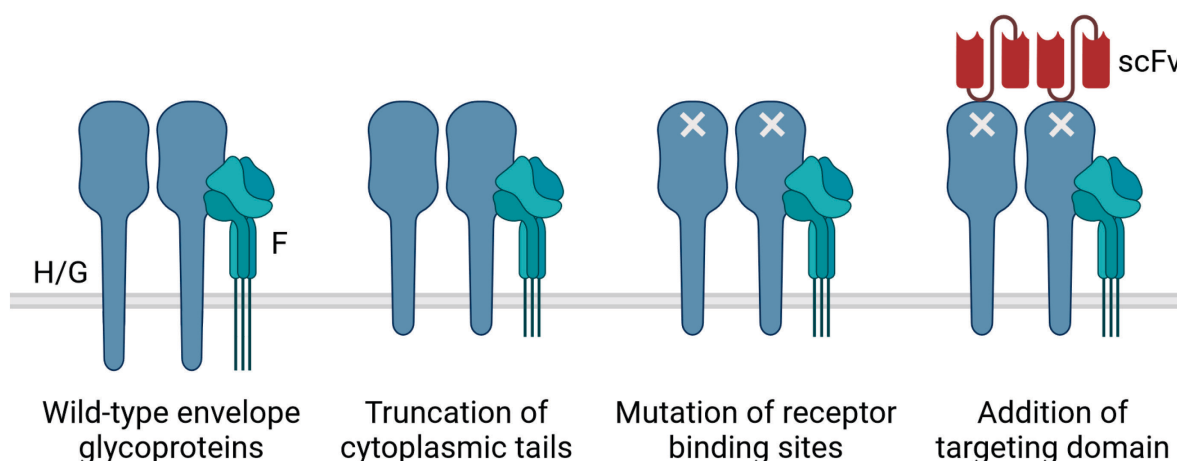


Figure 6: Engineering of paramyxoviral envelope glycoproteins for receptor targeting.

The wild-type paramyxoviral envelope glycoproteins hemagglutinin (H) from measles virus (MV) or glycoprotein (G) from Nipah virus (NiV) with their fusion protein (F) are truncated at the cytoplasmic tails. Next, the receptor binding sites are blinded towards their natural receptor by mutation and can then be equipped with a targeting domain of choice, often a single chain variable fragment (scFv).

LVs pseudotyped with various glycoproteins, not only acquire the receptor selectivity of the specific glycoprotein but also adopt its unique cell entry mechanism. As a consequence, there are fundamental distinctions in how the targeted LVs enter the cells. For instance, VSV-LV undergoes pH-dependent membrane fusion through endocytosis. In contrast, LVs pseudotyped with paramyxoviral glycoproteins like NiV-LV and MV-LV initiate cell entry by receptor recognition, leading to direct fusion at the cell membrane in a pH-independent manner (Frank & Buchholz, 2018). Blocking endocytosis, reduces gene delivery by VSV-LV, while it does not primarily affect paramyxoviral glycoprotein mediated gene transfer (Rasbach et al., 2013). This feature is particularly important to consider when targeting specific receptors that are frequently endocytosed.

So far, this platform has been used to target a variety of cell surface receptors with the main focus on T cell specific receptors. For this purpose, a human CD8-LV containing a scFv derived from the monoclonal antibody OKT-8 fused to MV glycoprotein was firstly described to selectively transduce T cells (Zhou et al., 2012). Transduction efficiency and vector titers could be significantly improved for CD8-LV by exchanging the MV glycoprotein to the one of NiV (Bender et al., 2016). Additionally, CD4⁺ T cells were addressed using a high affinity CD4 DARPin fused to the MV glycoprotein (Zhou et al., 2015). Both CD4- and CD8-LVs have been demonstrated to be highly selective for cells expressing their target receptor, as determined in initial studies (Zhou et al., 2012; Zhou et al., 2015) and verified by single-cell transcriptomics

(Charitidis et al., 2021). These vectors were also functional for selective *in vivo* gene delivery, generating functional CAR T cells in preclinical mouse models (Agarwal et al., 2020; Pfeiffer et al., 2018).

Though the T cell-targeted LVs have been proven to be selective towards the targeted receptor, CD4 and CD8 are not exclusive for T cells and have been described to be expressed on other cell types, such as dendritic cells (DCs), macrophages, monocytes and natural killer (NK) cells (Gibbings & Befus, 2009). The potential consequences of targeted delivery of therapeutic genes to these immune cells are not yet fully understood. For the exclusive transduction of T cells, CD3-targeted LVs have recently been described that target the ϵ -chain of the CD3 receptor expressed on T cells as part of the CD3:TCR receptor complex (Frank et al., 2020). This T cell-exclusive targeting strategy allows for the transduction of both CD4⁺ and CD8⁺ T cell subsets, which has been demonstrated to offer advantages for CAR T cell products and effective tumor cell elimination (Sommermeyer et al., 2016). In addition to its high selectivity and specificity for T cells, the CD3-LV exerts a strong agonistic effect upon binding to the CD3:TCR complex, leading to T cell activation and downmodulation of the complex. Due to the agonistic nature of the CD3-LV, the vector was shown to efficiently transduce not only fully activated but also quiescent cells. However, its gene transfer activity towards activated T cells remained to be lower than that of the CD4- and CD8-LV (Frank et al., 2020).

1.3.3 Transduction enhancers for lentiviral vectors

To achieve optimal transduction efficiency with targeted LVs, transduction enhancers are commonly used to facilitate co-localization and to boost vector cell entry. This is particularly important for receptor-targeted LVs, which rely on efficient cell contact to trigger pH-independent membrane fusion and cell entry. In order to promote vector-to-cell binding, various substances are commonly employed. These include cationic polymers, lipids and peptides, such as polybrene, protamine sulfate, vectofusin-1 (VF-1) or fibronectin (Hanenbergh et al., 1996; Höfig et al., 2012; Kaygisiz & Synatschke, 2020; Vermeer et al., 2017). The mechanism of action involves nanofibrill-mediated cell contact, neutralization of charge repulsion, or permeabilization of the cell membrane (Figure 7).

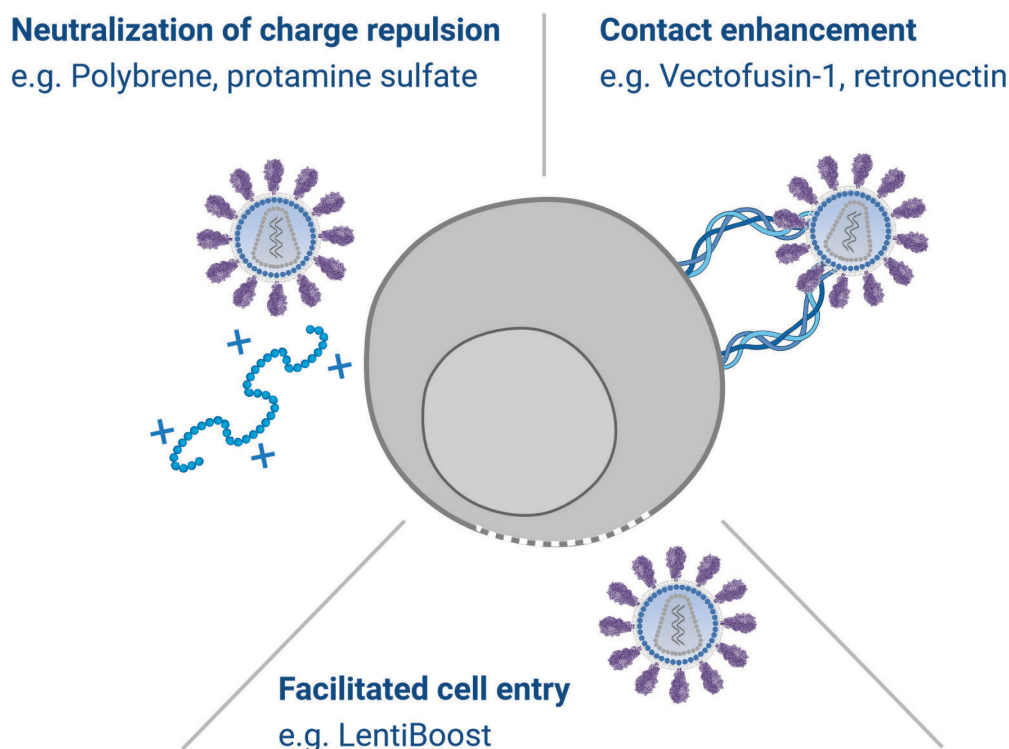


Figure 7: Transduction enhancers for viral vectors.

Transduction enhancers facilitate vector-to-cell interaction by neutralizing the charge repulsion, enhancing contact by forming nanofibrils, or facilitating cell entry by reducing the membrane microviscosity. Exemplary transduction enhancers are listed according to their function.

Cationic polymers, such as polybrene or protamine sulfate, are employed to neutralize membrane charges, thereby reducing charge repulsion and promoting effective vector-to-cell contact (Cornetta & Anderson, 1989; Toyoshima & Vogt, 1969). However, their use is limited due to the potential toxicity resulting from the disruption of transmembrane potential. The amphiphilic poloxamer synperonic F108, known as LentiBoost, has demonstrated superior performance over polybrene due to its lower toxicity and higher efficiency (Höfig et al., 2012). Poloxamers reduce the membrane microviscosity by reorganizing the membrane microstructure. This enhances lipid exchange and facilitates transmembrane transport, ultimately contributing to its transduction enhancing capabilities. While retronectin mediates co-localization of the vector and cell at specific adhesion domains (Hanenberg et al., 1996), the histidine-rich cationic amphipathic short peptide VF-1 forms nanofibrils that associate with the viral particles, resulting in sedimentation and increased local concentration at the cell surface (Fenard et al., 2013; Vermeer et al., 2017). VF-1 was shown to enhance transduction of all T cell-targeted LVs (CD4-, CD8- and CD3-LV) by 2- to 3 fold without compromising their selectivity (Frank et al., 2020; Jamali et al., 2019). However, even with the enhancing effect of VF-1, the transduction efficiency of CD3-LV remains

notably lower when compared to VSV-LV or other T cell-targeted LVs (Frank et al., 2020).

All of the transduction compounds described here share a common mechanism of facilitating cell binding in a receptor-independent manner, primarily by modifying the vector-to-cell interaction. However, their use is often associated with cell toxicity, which makes them unsuitable for *in vivo* administration.

1.4 Objective

The growing success and interest in CAR T cell therapy requires further improvements in manufacturing, safety and persistence of the product. CD3-targeted LVs have shown to selectively transduce T cells *in vitro* and *in vivo*, and though having moderate efficacy, they reduce the risk of transducing malignant cells (Frank et al., 2020). Upon transduction, CD3-LVs trigger T cell activation and CD3:TCR downregulation, potentially reducing transduction efficiency. Inhibition of activation induced downregulation of the CD3:TCR complex, using the Lck inhibitor dasatinib, might enhance gene delivery by T cell-targeted LVs.

At first, the optimal concentration and incubation time of dasatinib had to be determined and the effect on transduction efficiency using CD3-LV *in vitro* and *in vivo* had to be evaluated. Next, the mechanism behind the transduction enhancement by dasatinib had to be resolved. Therefore, the effect of dasatinib and other tyrosine kinase inhibitors on the transduction with targeted LVs had to be tested and the treatment with dasatinib on the availability of the CD3 receptor had to be determined. Also, the impact of dasatinib on the generation of CD19.CAR T cells using CD3-LV or VSV-LV had to be compared. Therefore, CAR T cells had to be evaluated for functionality, phenotype, and exhaustion when challenged in repetitive stimulation assays or conventional killing assays.

On the other hand, poor expansion and persistence of CAR T cells is one of the main causes for relapse and tumor progression in patients. Promotion of mitophagy has been demonstrated to boost T cell fitness and anti-tumor immunity (Buck et al., 2016). The metabolite compound urolithin A (UA) has been described to induce mitophagy and has shown to have immunomodulatory effects, attenuating inflammation and the progression of age-related diseases (D'Amico et al., 2021; Toney et al., 2021).

Therefore, the immunomodulatory effect of UA on CD19.CAR T cells and CEA.CAR T cells, in terms of phenotype, transduction and killing efficacy, had to be investigated. At last, the combinability of the transduction enhancing effect of dasatinib together with the immunomodulatory function of UA on CAR T cells had to be assessed. Therefore, the proportion of T_{SCM} cells, the killing efficacy and the cytokine secretion of CAR T cells generated under the different treatment regimens had to be compared.

2 Results

This thesis describes the evaluation of small molecules, dasatinib and urolithin A (UA), in the context of T cell directed gene transfer using lentiviral vectors (LVs) for the generation of refined therapeutic T cells.

While acting very differently both molecules, dasatinib and UA, were determined to have a positive impact on genetically modified T cells, either by increasing CD3-targeted gene transfer or by facilitating the generation of chimeric antigen receptor (CAR) T stem cell memory (T_{SCM}) cells. The use of dasatinib during transduction with the CD3-targeted LV (CD3-LV) led to an increase in transduction efficiency by blocking CD3-LV-mediated T cell activation followed by CD3:TCR downmodulation. This effect was time- and concentration-dependent and exclusive for the transduction with CD3-LVs. When delivering a therapeutically relevant transgene, dasatinib increased the number of functional CAR T cells, allowing the generation of functional and less exhausted CAR T cells. The presence of UA during transduction with LVs and further cultivation of the cells, promoted the expansion of T_{SCM} cells, facilitating the generation of CD19.CAR T_{SCM} and carcinoembryonic antigen (CEA) CAR T_{SCM} cells. The effect of UA was independent of the LV used and could be combined with the transduction enhancing effect of dasatinib on CD3-LV. The CAR T_{SCM} cells were functionally active in tumor cell elimination, showing no difference in cytokine secretion compared to conventional CAR T cells.

The following chapters contain data previously published in (Braun et al., 2023) and (Denk et al., 2022). Figures derived from the mentioned publications are indicated as such.

2.1 Dasatinib as transduction enhancer for CD3-LV

At first, the effect of dasatinib on the transduction of primary human T cells with LVs was evaluated. To test if dasatinib increases CD3-LV-mediated gene transfer, a Nipah virus (NiV) glycoprotein G_{mut} pseudotyped LV displaying a single chain variable fragment (scFv) derived from the CD3-specific agonistic antibody TR66 (TR66.opt) was used. The reporter gene *gfp* was delivered under control of the SFFV promoter. Therefore, the optimal time and concentration of dasatinib treatment needed to be

determined. Next, the effect of dasatinib on the transduction of non-activated T cells such as *in vivo* gene delivery in presence of dasatinib was demonstrated.

2.1.1 Transduction of primary T cells in presence of dasatinib

To date, dasatinib has been used in cell culture for a number of different reasons. In the T cell context, dasatinib has been applied to prevent T cell activation (Schade et al., 2008) and as on/off switch for cytotoxic CAR T cells (Mestermann et al., 2019). Never before has its effect on T cell transduction been tested, specifically on transduction with targeted LVs. Therefore, an experimental setup to evaluate the effect of dasatinib on T cell directed gene transfer had to be established. First, human peripheral blood mononuclear cells (PBMCs) were activated in presence of plate-bound α CD3 (clone OKT-3) and soluble α CD28 antibodies in medium containing IL-7 and IL-15 for three days. Upon activation, cells were exposed to dasatinib one hour prior to addition of LVs. Dasatinib and residual vector particles were removed from the cells by medium exchange at the indicated time points, and transduction efficiency was determined by flow cytometry three days post treatment (Figure 8).

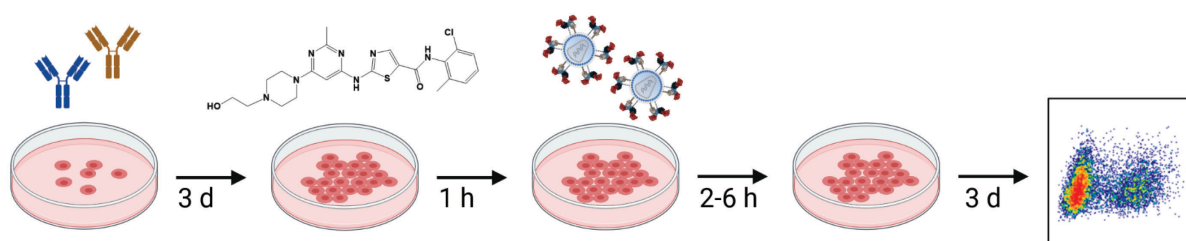


Figure 8: Experimental setup for PBMC transduction in presence of dasatinib.

Human PBMCs were activated with α CD3/ α CD28 in medium supplemented with IL-7/15. After three days the cells were treated with dasatinib and subsequently incubated with LVs. The medium was refreshed after two to six hours (h) and transgene expression was analyzed, three days post transduction.

To determine the transduction efficiency of different CD3-LV stocks in presence or absence of 50 nM dasatinib, a serial dilution of vector particles was added to the cells and medium was changed four hours after LV addition. On day three post transduction, incubation with dasatinib increased CD3-LV titers by an average of 8-fold (Figure 9A). In detail, the transduction enhancement ranged from 3- to 10-fold, dependent on the number of vector particles. At low particle numbers (500 per cell) the increase was particularly pronounced (8-fold on average), compared to high particle numbers of

3.3×10^5 particles per cell, for which a 4.5-fold increase was achieved (Figure 9B). Representative dot plots of a CD3-LV stock titrated in presence or absence of dasatinib, clearly demonstrate the effect of dasatinib on transduction (Figure 9C). GFP expression ranged from 5.7% at the lowest particle concentration up to 65.6% at the highest particle concentration, compared to 0.8% to 15.9% GFP expression in the absence of dasatinib.

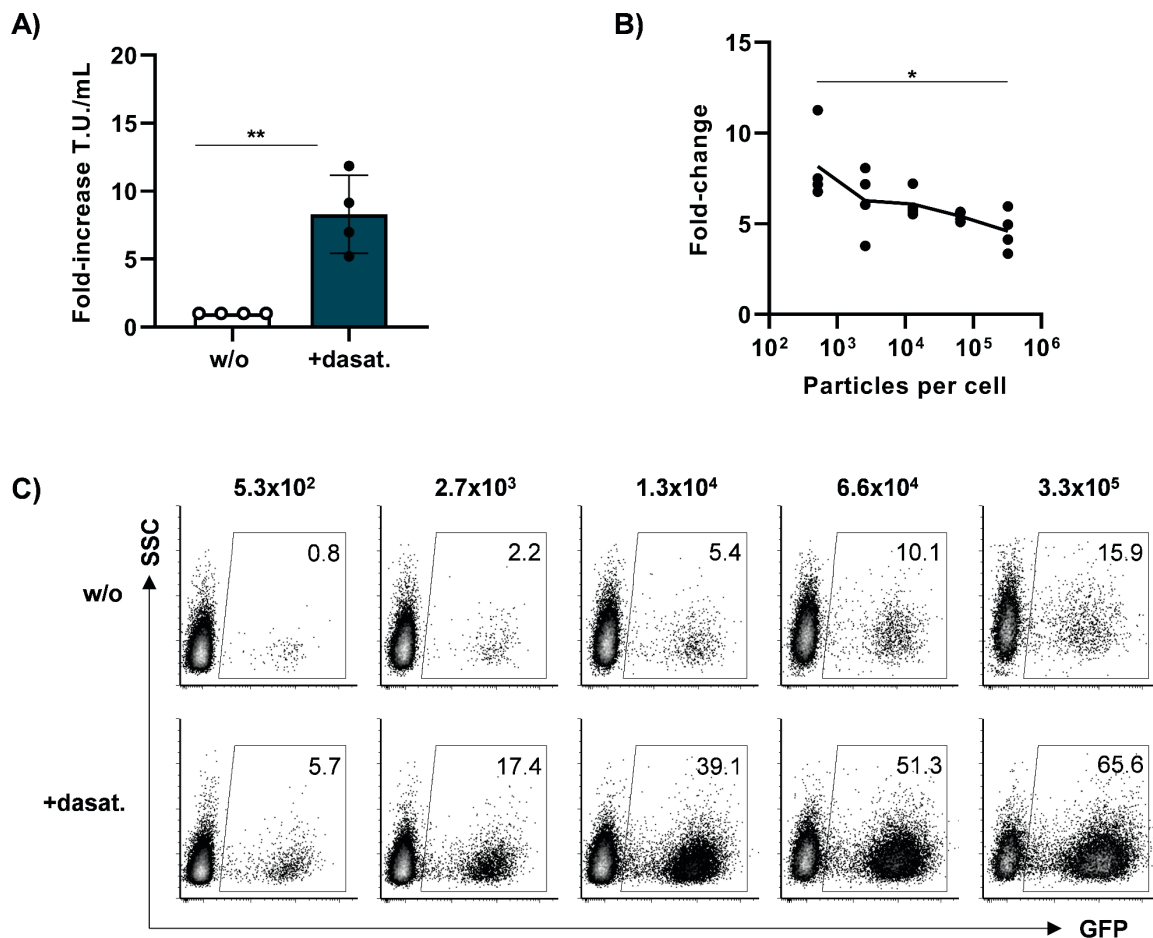


Figure 9: Dasatinib increases CD3-LV titers.

Fully activated human PBMCs were incubated with a serial dilution of CD3-LV in presence or absence of 50 nM dasatinib for five hours. GFP expression was determined three days post transduction by flow cytometry. **(A)** Bar diagrams show the fold-increase in functional titers (T.U./mL) determined after transduction in absence (w/o) or in presence of dasatinib (+dasat.). Each data point represents an average value referring to a particular vector stock tested on one to four donors. Values are shown as mean \pm standard deviation (SD). ** $p < .01$, by ratio paired t-test. **(B)** Fold-change in GFP expression is shown for the number of particles applied during transduction in presence compared to in absence of dasatinib. Each data point is an average value referring to a particular vector stock tested on one to four donors. * $p < .05$, by one-way analysis of variance (ANOVA) followed by Tukey's multiple comparisons test. **(C)** Representative dot plots show GFP expression of cells transduced with increasing amounts of vector particles in presence and absence of dasatinib. Figure modified from (Braun et al., 2023).

Next, the optimal conditions for dasatinib treatment of PBMCs were investigated. Therefore, cells were incubated with increasing concentrations of dasatinib ranging from 0.39 nM up to 100 nM and subsequently transduced with constant vector amounts of 2.5×10^{10} particles. Three days post treatment and transduction, cells were analyzed by flow cytometry, revealing a dose dependent response towards dasatinib. The lowest dasatinib concentration of 0.39 nM was not sufficient to enhance transduction, while concentrations starting at 6.35 nM dasatinib led to a 2-fold increase. A plateau was reached at ≥ 50 nM dasatinib, determining the maximal increase of 3-fold for the applied particle number (Figure 10A).

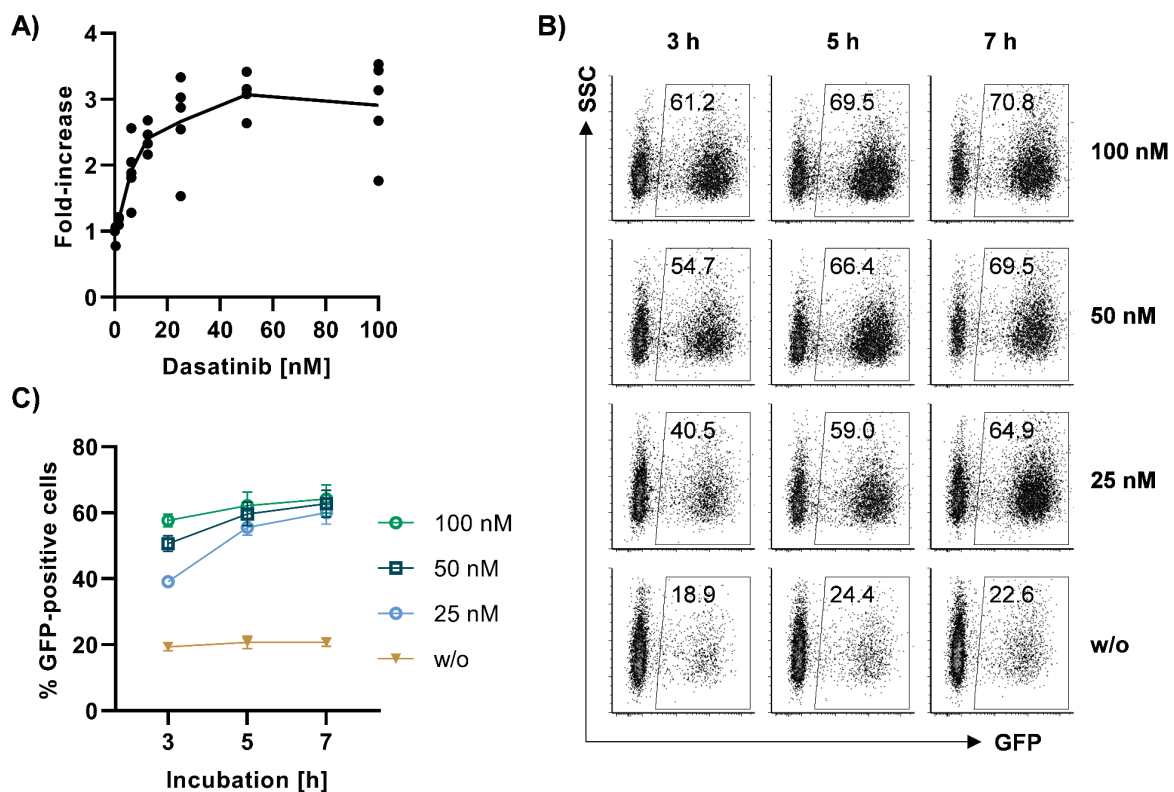


Figure 10: Dasatinib increases the transduction of CD3-LV in a time- and dose-dependent manner.

Fully activated human PBMCs were incubated with increasing concentrations of dasatinib during incubation with 2.5×10^{10} CD3-LV particles for three to seven hours. GFP expression was measured after three days by flow cytometry. **(A)** Fold-increase in GFP expression after five hour treatment with increasing concentrations of 0.39-100 nM dasatinib is shown for four to five donors. **(B)** Representative dot plots show GFP expression, three days post transduction. **(C)** The percentages of GFP⁺ cells after treatment for three, five or seven hours with different dasatinib concentrations, are shown as superimposed symbols connected by line. Data is shown as mean \pm standard error of the mean (SEM) derived from three donors. Figure modified from (Braun et al., 2023).

To evaluate the optimal incubation time of cells in presence of dasatinib, medium was refreshed and dasatinib removed after three, five or seven hours of treatment. GFP expression was analyzed after three days by flow cytometry (Figure 10B). When

treated for three hours with 50 nM dasatinib, transduction increased from 20% to 50%, and further to above 60% GFP expression when treatment was prolonged to five hours. Longer treatment of seven hours increased GFP expression only slightly to 62%. While the short incubation time of three hours showed a difference between the applied concentrations of 25 nM and 50 nM dasatinib, the longer treatment of seven hours, such as the higher dasatinib concentration of 100 nM, did not further increase GFP expression (Figure 10C). Thus, the treatment of activated PBMCs with 50 nM dasatinib for five hours was chosen to be the optimal condition for transduction enhancement with CD3-LV.

Dasatinib significantly enhanced CD3-LV-mediated gene transfer, increasing the viral titers with the strongest enhancing effect when applied during transduction with low particle numbers. The effect of dasatinib, was time- and dose-dependent and optimal conditions were determined to be the treatment with 50 nM containing medium for five hours during transduction.

2.1.2 Dasatinib's effect on viability and proliferation

As dasatinib is known to interfere with T cell activity, it was important to verify that the determined treatment conditions had no negative impact on cell viability and proliferation.

Therefore, viability of PBMCs after treatment with increasing amounts of dasatinib for five hours and transduction with CD3-LV transferring the reporter gene *gfp* or a therapeutically relevant gene encoding for a CD19.CAR was evaluated after three days. None of the treatment conditions applied compromised cell viability and, with exceptions, maintained cell viability above 80% (Figure 11A). Also, viability of transduced cells was transgene independent over all dasatinib concentrations, being slightly lower compared to untransduced cells. To investigate proliferation, activated PBMCs were labelled with the fluorescent dye CellTrace® Violet (CTV) prior to treatment with 50 nM dasatinib and transduction with CD3-LV or VSV-LV. Proliferation can be determined by loss of CTV in dividing cells measured via flow cytometry. The cells were analyzed prior to treatment, after one and after three days, revealing no difference in proliferative capacity of dasatinib treated (+dasat.) compared to untreated cells (Figure 11B). After three days, all cells had proliferated, as indicated by a decrease in CTV fluorescence intensity by two orders of magnitude.

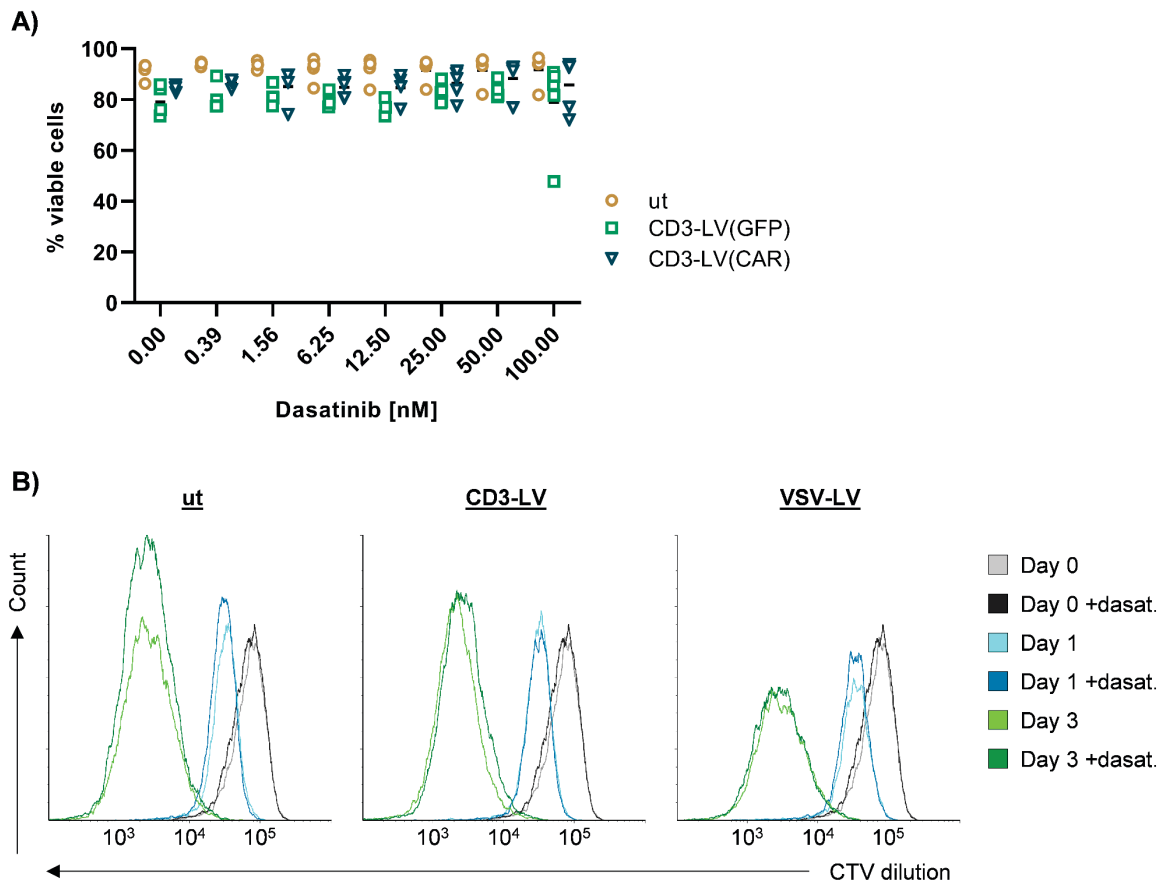


Figure 11: Dasatinib does not interfere with T cell viability or proliferation.

(A) Activated PBMCs were incubated with increasing concentrations of dasatinib for seven hours during transduction with CD3-LV delivering a GFP or CD19.CAR. Viability was measured three days post transduction and individual values in combination with the mean from four to five donors are shown. **(B)** Activated PBMCs were first labeled with CellTraceViolet (CTV) and then exposed to CD3-LV, VSV-LV, or left untransduced (ut). CTV dilution was measured by flow cytometry and histograms show fluorescence intensity of CTV from day zero to day three after transduction in presence (+dasat.) or absence of dasatinib. Figure modified from (Braun et al., 2023).

Taken together, the determined conditions of PBMC treatment with 50 nM dasatinib for five hours had no effect on cell viability and proliferative capacity, confirming the feasibility of the identified conditions.

2.1.3 Synergistic effect of dasatinib and vectofusin-1

The commonly used transduction enhancer vectofusin-1 (VF-1), has proven to be effective in enhancing transduction of the paramyxovirus pseudotyped targeted LVs CD4-, CD8- and CD3-LV by facilitating vector-to-cell interaction, while inhibiting the pH-dependent cell entry of the rhabdovirus pseudotyped VSV-LV (Frank et al., 2020; Jamali et al., 2019).

To evaluate the effect of VF-1 together with dasatinib, the transduction efficiency of CD3-LV and VSV-LV was next tested in presence of VF-1, dasatinib or the combination of both. VF-1 was applied as previously described (Jamali et al., 2019). When using VF-1 as transduction enhancer for CD3-LV on PBMCs, transgene expression increased from below 5% to 20%. Interestingly, dasatinib was a more potent enhancer for CD3-LV transduction, increasing GFP expression to 30%. The combination of VF-1 and dasatinib further boosted gene delivery, resulting in 69% GFP expression (Figure 12A). In line with previous data, VF-1 strongly inhibited gene delivery by VSV-LV (Figure 12B). The inhibitory effect of VF-1 on VSV-LV gene transfer was independent of the presence of dasatinib and the combination of both decreased transgene expression to 2%. Dasatinib itself had no effect on the pH-dependent cell entry of VSV-LV, leaving transgene expression unchanged at 53% (Figure 12B).

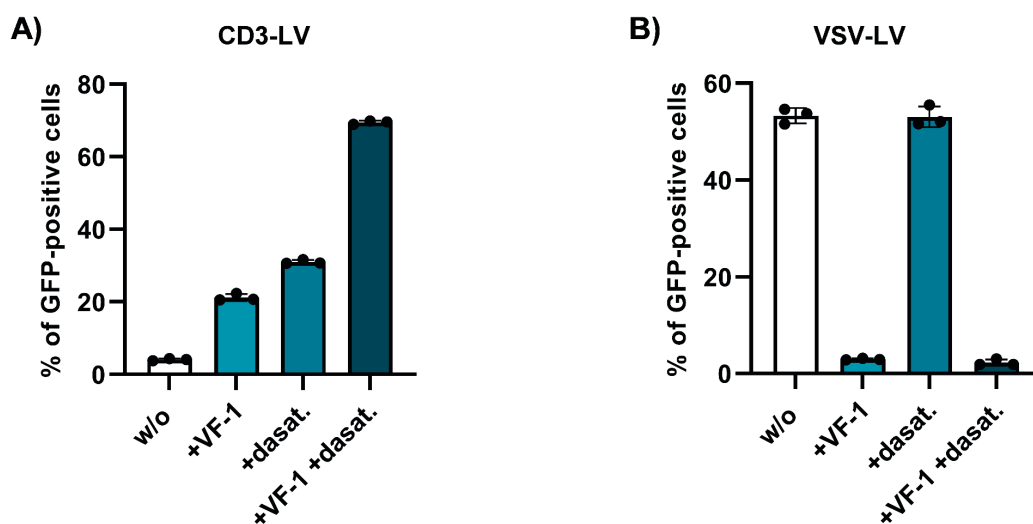


Figure 12: Dasatinib and vectofusin-1 have a synergistic effect on CD3-LV-mediated gene delivery.

Activated PBMCs were transduced with 2×10^{10} particles CD3-LV (A) or 8×10^8 particles VSV-LV (B) without transduction enhancers (w/o), in presence of vectofusin-1 (VF-1), in presence of 100 nM dasatinib or in presence of 100 nM dasatinib in combination with VF-1. GFP expression was determined three days post transduction and values are shown as mean \pm SD determined from technical triplicates of one donor. Figure modified from (Braun et al., 2023).

The combination of dasatinib with the transduction enhancer VF-1, resulted in an additive enhancing effect for CD3-LV, while it did not change the inhibitory effect of VF-1 on VSV-LV transduction.

2.1.4 Transduction of non-activated human T cells

A unique characteristic of the CD3-LV is its agonistic function, conferred by the TR66 scFv displayed on the vector surface. This allows activation and improves transduction of non-activated human T cells by CD3-LV (Frank et al., 2020).

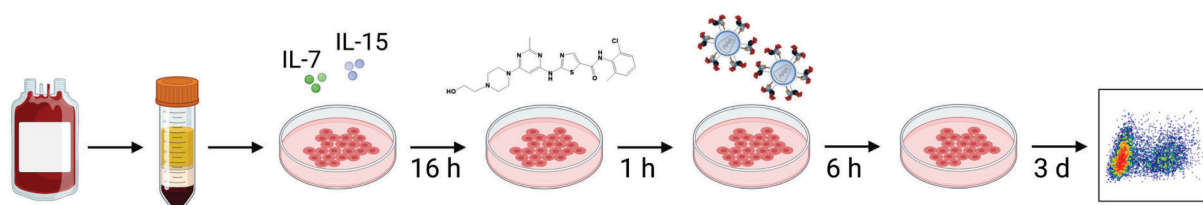


Figure 13: Experimental setup for transduction of non-activated PBMCs in presence of dasatinib. Human PBMCs were isolated from whole blood and cultured in medium containing IL-7 and IL-15 for 16 hours. The next day, cells were treated with dasatinib and subsequently incubated with LVs. The medium was refreshed after six hours and transgene expression was analyzed three days post transduction.

To assess if dasatinib also enhanced gene delivery to non-activated cells, PBMCs were freshly isolated from blood of healthy donors and incubated in IL-7 and IL-15 containing medium in the absence of activating antibodies, overnight. Subsequently, cytokine-only stimulated cells were incubated with LV in presence or absence of dasatinib or dasatinib and VF-1 for seven hours. Cells were further cultivated in cytokine-containing medium and transgene expression was analyzed after three days by flow cytometry (Figure 13). All vectors were able to transduce non-activated cells at low levels of 1-2%. Incubation with dasatinib increased transgene delivery by CD3-LV to 8%, while it led to only slightly higher transduction levels of 2.7% and 3.7% for CD8- and VSV-LV-mediated gene transfer (Figure 14A). In combination with VF-1, CD3-LV mediated gene transfer was increased to 10%, again demonstrating the combinability of dasatinib and VF-1 on enhancing CD3-LV gene transfer (Figure 14B).

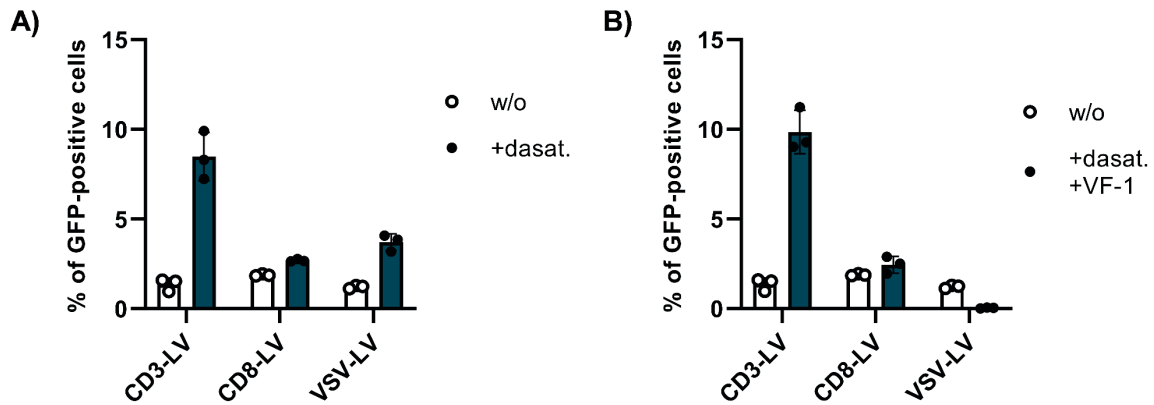


Figure 14: Dasatinib increases CD3-LV gene transfer to cytokine-only stimulated cells.

Freshly isolated human PBMCs were incubated in medium containing IL-7 and IL-15 overnight. The next day, cells were incubated with CD3-, CD8- or VSV-LV in presence (+dasat.) or absence (w/o) of 100 nM dasatinib (A) or in presence or absence of 100 nM dasatinib in combination with VF-1 (B) for seven hours. Three days post transduction, GFP expression was determined by flow cytometry and is shown as mean \pm SD from technical triplicates of one biological replicate.

The second approach to evaluate the effect of dasatinib on the transduction of non-activated T cells was performed in whole blood. In this *in vivo*-like setup, whole blood from a healthy donor was used for transduction, enabling the presence of all components present in blood, such as erythrocytes, thrombocytes and plasma proteins.

Freshly sampled human whole blood was pretreated with 100 nM dasatinib one hour prior to addition of vector particles and further incubated for four hours at 37°C under constant shaking at 120 rpm. Subsequently, PBMCs were isolated from whole blood by density centrifugation and cells were further cultivated in medium supplemented with IL-7 and IL-15 for five to six days, prior to analysis by flow cytometry (Figure 15A). CD3-LV transduced 0.5% of the T cells in blood remaining selective for CD3⁺ T cells (Figure 15B). When dasatinib was spiked into blood prior to CD3-LV addition, transduction of CD3⁺ T cells in whole blood increased by 4-fold on average (Figure 15C). In contrast, VSV-LV showed lower transduction rates compared to CD3-LV into both CD3⁺ and CD3⁻ cells of 0.1-0.4%, independent of dasatinib exposure (Figure 15B).

Overall, the transduction enhancing activity of dasatinib for CD3-LV transduction was confirmed for non-activated T cells, outperforming VSV-LV transduction, and was unaffected by the components and cells present in blood.

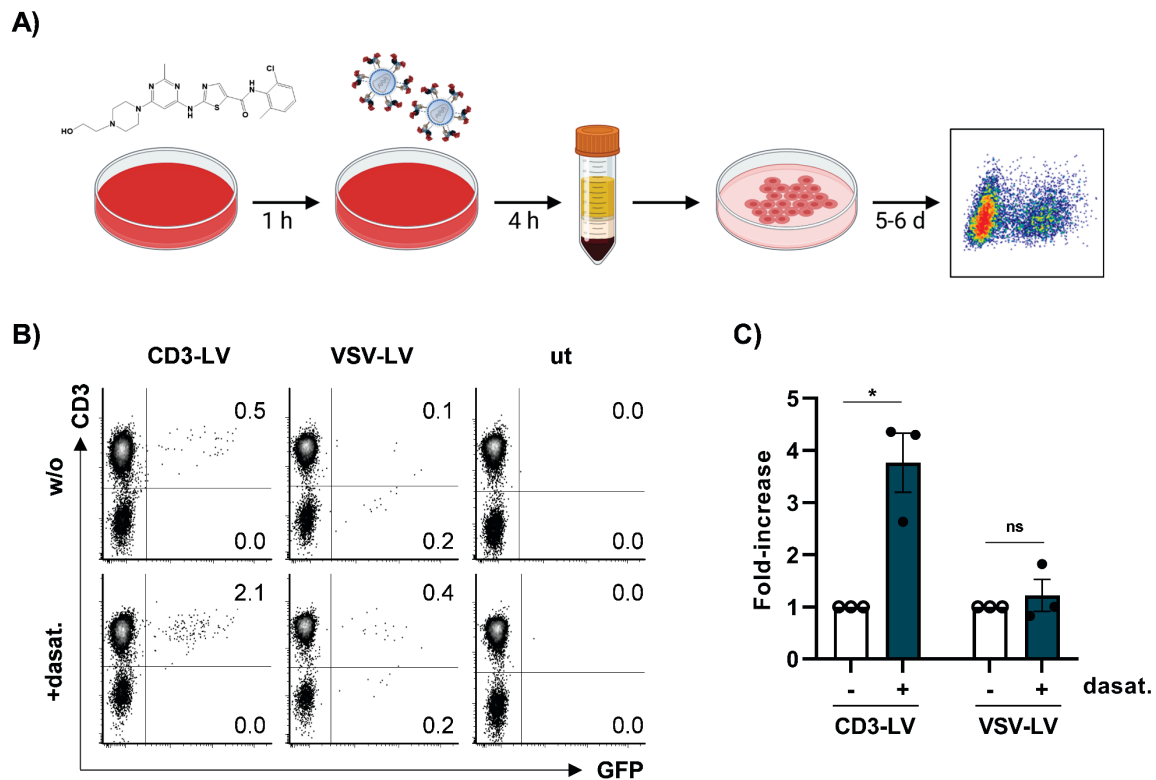


Figure 15: Dasatinib increases CD3-LV gene transfer to T cells in whole blood.

Whole blood was taken from healthy donors and incubated with 100 nM dasatinib (+dasat.) or without (w/o) one hour before adding 8.5×10^{10} particles CD3-LV or 3×10^{10} particles VSV-LV. Blood was further incubated for four hours under constant shaking at 120 rpm before PBMCs were isolated via density centrifugation. PBMCs were cultivated in medium supplemented with IL-7/15 for five to six days. **(A)** Experimental design. **(B)** Representative dot plots show GFP expression in CD3⁺ and CD3⁻ viable cells six days after transduction. **(C)** Fold-increase in GFP expression, five to six days post transduction, is shown as mean ± SEM of three donors. Ns: non-significant; * $p < .05$, by ratio paired t-test. Figure modified from (Braun et al., 2023).

2.1.5 Dasatinib enhances *in vivo* transduction in some mice

Based on a study by (Mestermann et al., 2019) in which dasatinib was used as on/off switch for CAR T cell regulation *in vivo*, we evaluated the transduction enhancing effect of dasatinib *in vivo*.

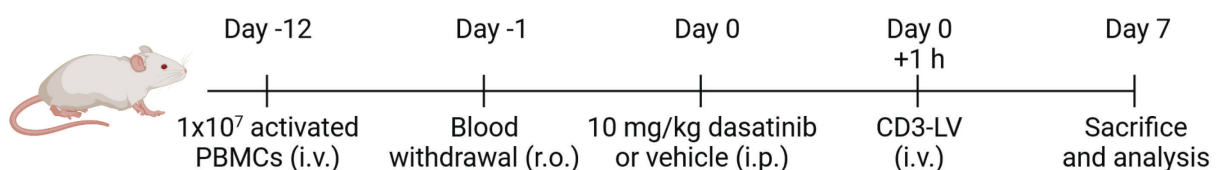


Figure 16: Experimental design for *in vivo* CD3-LV transduction in presence of dasatinib.

Immunodeficient NSG mice were intravenously (i.v.) injected with 1×10^7 fully activated human PBMCs and blood was taken retroorbitally (r.o.) eleven days later to determine the level of humanization. The next day, mice were intraperitoneally (i.p.) injected with 10 mg/kg dasatinib or vehicle one hour before i.v. injection of CD3-LV. Mice were sacrificed seven days after vector administration.

Therefore immunodeficient NSG mice were transplanted with 1×10^7 fully activated human PBMCs (Figure 16). After eleven days of engraftment, mice were bled retroorbitally (r.o.) for analysis prior to treatment. The next day, mice were injected intraperitoneally (i.p.) with 10 mg/kg dasatinib or vehicle, one hour before intravenous (i.v.) injection of CD3-LV. Seven days post dasatinib and vector treatment, mice were sacrificed and cells from blood, spleen and bone marrow were analyzed for GFP expression by flow cytometry and transgene integration by quantitative polymerase chain reaction (qPCR).

After sacrifice, human cells were firstly identified by staining for human CD45⁺ cells. Cells isolated from organs of mice treated with or without dasatinib showed an even distribution of CD45⁺ cells of around 60% in blood (Figure 17A), 80% in spleen (Figure 17B) and 5-8% in bone marrow (Figure 17C).

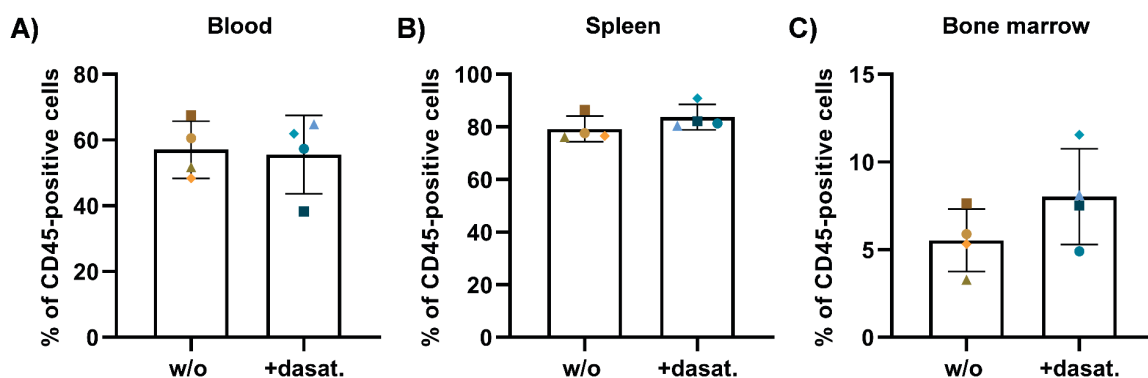


Figure 17: Humanization of NSG mice.

NSG mice were injected with human PBMCs. Twelve days later, they were treated with dasatinib or vehicle and then injected with CD3-LV. Seven days after vector administration mice were sacrificed. Cells were isolated from blood (A), spleen (B) and bone marrow (C) and analyzed for the amount of human CD45-positive cells of all viable cells, comparing mice treated with dasatinib (+dasat.) or without (w/o). Bar diagrams show mean \pm SD of CD45-positive cells determined from four individual mice depicted with distinct symbols and colors.

After pre-gating on human cells, the level of transduced cells was determined and revealed GFP expression in all mice (Figure 18). Each animal's results are labeled with unique symbols and colors to track samples from one animal throughout the organs analyzed. Expression levels in blood ranged from 0.7-4.2%, averaging at 2% in mice treated with dasatinib and at 1.2% in mice treated with vehicle (Figure 18A). The increase in the average transduction level in the dasatinib treated group can mainly be traced back to a single mouse treated with dasatinib (depicted as blue circle ●). Very similar transduction levels of 0.5-4% were observed in cells isolated from spleen and

bone marrow (Figure 18B, C). Successful transduction and transgene integration were verified by determining the vector copy number (VCN) in the genome of the isolated cells. QPCR revealed VCN from 0.01 to 0.09 reflecting the results determined by flow cytometry for the individual samples (Figure 18A-C).

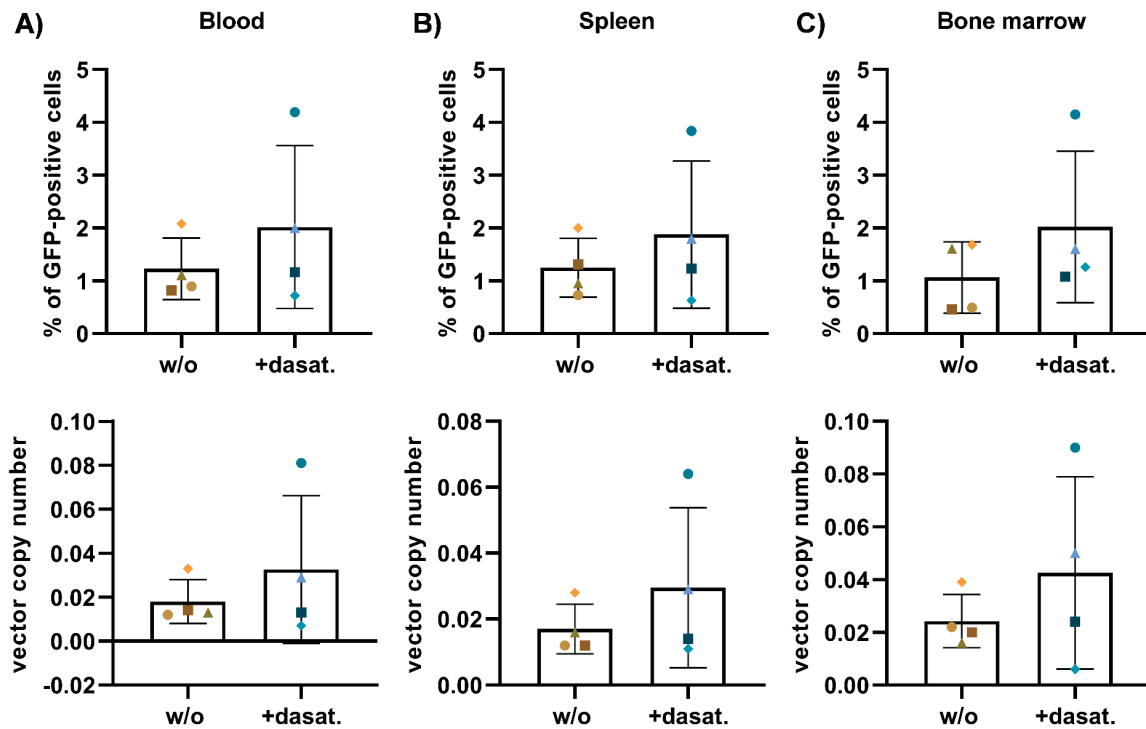


Figure 18: *In vivo* transgene delivery by CD3-LV in presence or absence of dasatinib.

Seven days after vector administration mice were sacrificed. Cells were isolated from the blood (A), the spleen (B) and the bone marrow (C) and analyzed for GFP expression in viable CD45⁺ cells by flow cytometry and vector copy number (VCN) by qPCR, comparing mice treated with dasatinib (+dasat.) or without (w/o). Bar diagrams show mean \pm SD determined from four individual mice per group, depicted with distinct symbols and colors.

Not only was transgene delivery with CD3-LV successful in transducing human T cells *in vivo* (Figure 19A) but also in transducing both the CD4⁺ and CD8⁺ T cell subsets, with CD8⁺ T cells defined as CD4⁻ (Figure 19B). When taking the mice with the highest transduction level of each group as an example, 1.9% of the transduced cells in the blood of the vehicle treated mouse were CD4⁺ cells and 0.2% CD8⁺ cells, respectively 3.8% were CD4⁺ cells and 0.4% were CD8⁺ cells in the dasatinib treated mouse (Figure 19B). Most importantly, transduction with CD3-LV was highly selective for human CD3⁺ cells when taking into account all viable cells (not pre-gated on human CD45⁺), showing no detectable GFP expression in CD3⁻ cells in mice treated with vehicle or dasatinib (Figure 19C).

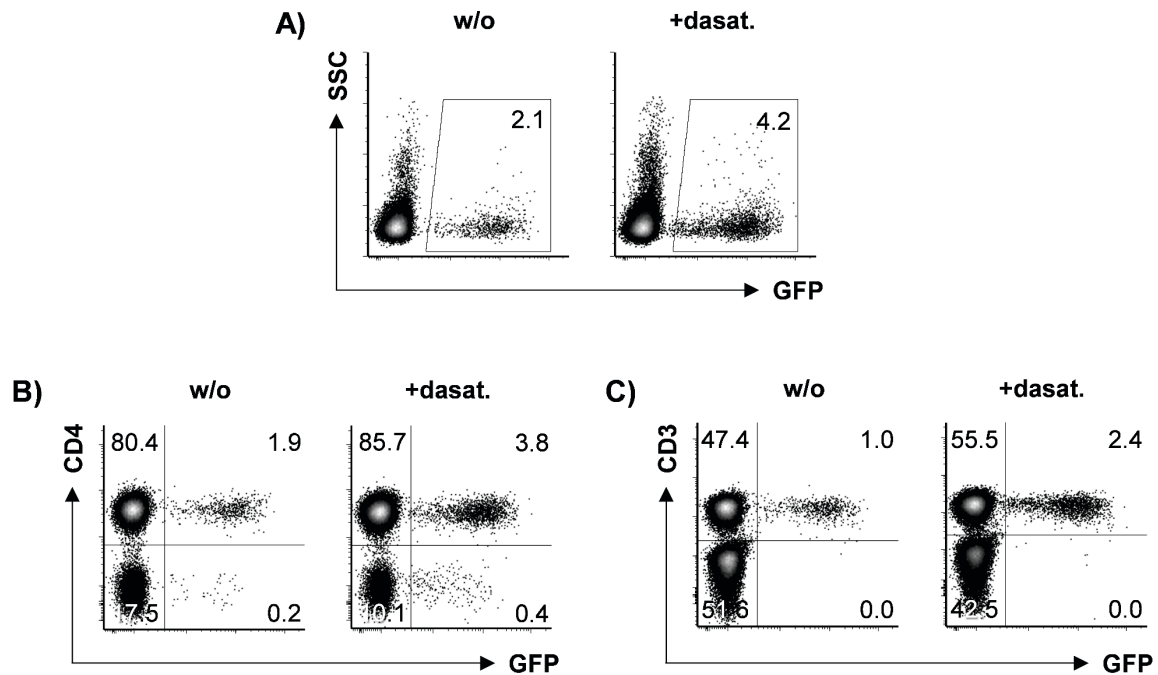




Figure 19: Selectivity of *in vivo* transduction by CD3-LV in presence or absence of dasatinib.

Seven days after vector administration mice were sacrificed and cells were isolated from the blood and analyzed for GFP expression. Dot plots of GFP expression in CD45⁺ viable cells (**A**), in CD4⁺ and CD4⁻ viable CD45⁺ cells (**B**) and in CD3⁺ of all viable cells (**C**), shown from one representative mouse treated with vehicle (w/o; orange check ) and one treated with dasatinib (dasat.; blue circle )

Taken together, CD3-LV transduced human T cells *in vivo*, being highly selective for human CD3⁺ cells. The administration of dasatinib increased transduction in some mice and did not compromise the selectivity of CD3-LV.

In conclusion, dasatinib enhanced CD3-LV directed gene transfer in a dose- and time-dependent manner and could be combined with the transduction enhancer VF-1. In addition to enhancing the gene delivery to activated PBMCs, dasatinib also increased GFP expression in non-activated T cells in culture or directly in whole blood. Administration of dasatinib during *in vivo* gene delivery increased transduction in some mice and maintained the vector's selectivity for CD3⁺ cells.

2.2 Mechanism of transduction enhancement by dasatinib

The results of the previous chapter have demonstrated the enhancing effect of dasatinib on CD3-LV transduction. To better understand the mechanism behind the enhancement, requirements for successful transduction with CD3-LV, such as the effect of dasatinib on the T cell, were further investigated. At first, the CD3-LV cell entry

was evaluated, as the effect of transduction enhancers often depends on the entry mechanism of the different viral vectors used. Receptor-targeted LVs pseudotyped with paramyxoviral glycoproteins (NiV-LV and MV-LV) undergo pH-independent cell membrane fusion, triggered by the target-receptor (Frank & Buchholz, 2018). The VSV-G glycoprotein, on the other hand, is dependent on endocytosis of the LDL receptor for cell entry and inhibition of endocytosis can therefore decrease transduction of VSV-LV. Anyhow, the receptor targeted by the LVs needs to be accessible which was next analyzed. This is of special importance when targeting the CD3 receptor, as triggering the CD3:TCR complex leads to activation and downregulation of the complex (Frank et al., 2020; Schade et al., 2008). Therefore, it was investigated whether the inhibition of kinases by dasatinib, might prevent receptor downregulation and improve CD3-LV transduction. At last, the effect of other tyrosine kinase inhibitors (TKIs) on the transduction with targeted LVs was investigated, to confirm the specific inhibition of dasatinib which causes enhanced transduction.

2.2.1 CD3-LV transduction is endocytosis independent

Since CD3-LV cell entry is pH-independent, inhibition of endocytosis may positively effect CD3-LV-mediated transduction by preventing endocytosis of the target receptor or reducing degradation of the vector particles due to acidification of the endosome.

Here, the V-ATPase inhibitor bafilomycin A1 (BfIA1) was used to inhibit endocytosis during transduction. Therefore, PBMCs were incubated for one hour with 0-20 nM BfIA1 before adding the vector particles, and medium was changed four hours after vector addition. After four days, transduction efficiency of CD3-LV was unaltered upon treatment with BfIA1 independent of the concentration applied (Figure 20). In line with previous publications, VSV-LV transduction efficiency was significantly decreased following BfIA1-treatment in a dose-dependent manner. Exposure of cells to 20 nM BfIA1 during VSV-LV transduction reduced transgene expression to 0.2-fold that of BfIA1 untreated condition (Figure 20).

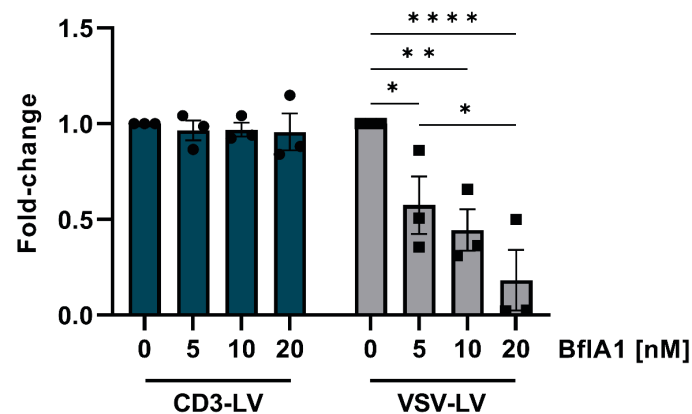


Figure 20: Effect of endocytosis inhibitor BflA1 on CD3- and VSV-LV transduction.

Activated human PBMCs were incubated with 0-20 nM bafilomycin A1 (BflA1) for five hours during transduction with CD3-LV or VSV-LV. Three days post treatment, fold-change in transduction compared with transduction in absence (0 nM) of BflA1 was determined and is shown for three donors as mean \pm SEM. * $p < .05$, ** $p < .01$, **** $p < .0001$ by two-way ANOVA followed by Tukey's multiple comparisons test. Figure modified from (Braun et al., 2023).

Though recent findings have shown a slight increase of CD3-LV-mediated transduction on cell lines (Frank et al., 2020), no beneficial outcome was observed on primary cells. Therefore it was concluded, that the low transduction efficiency of CD3-LV in absence of enhancers was not due to endocytosis of the receptor or vector particles, and that prevention of endocytosis was not the key to enhance CD3-LV transgene delivery to primary cells.

2.2.2 Dasatinib exclusively enhances CD3-LV gene transfer

In the previous chapter, dasatinib has proven to be an efficient CD3-LV enhancer, while it had no effect on VSV-LV transduction. To obtain better insights into the mechanism of CD3-LV transduction enhancement, the effect of dasatinib on other receptor targeted LVs pseudotyped with paramyxoviral glycoproteins, namely CD4- and CD8 LV, was evaluated.

Activated PBMCs were incubated with 100 nM dasatinib one hour prior to addition of T cell receptor-targeted LVs or VSV-LV. After three days, transgene expression was determined by flow cytometry. As expected, dasatinib increased transgene expression following CD3-LV transduction from 10% to 46% and had no effect on the transduction efficiency of VSV-LV which remained unchanged at 74% (Figure 21). Cells transduced with CD8-LV reached expression levels of around 23% independent of dasatinib exposure. CD4-LV transduced cells showed a slight increase upon dasatinib

incubation from 14% to 21% GFP expression on average, while values varied widely among donors.

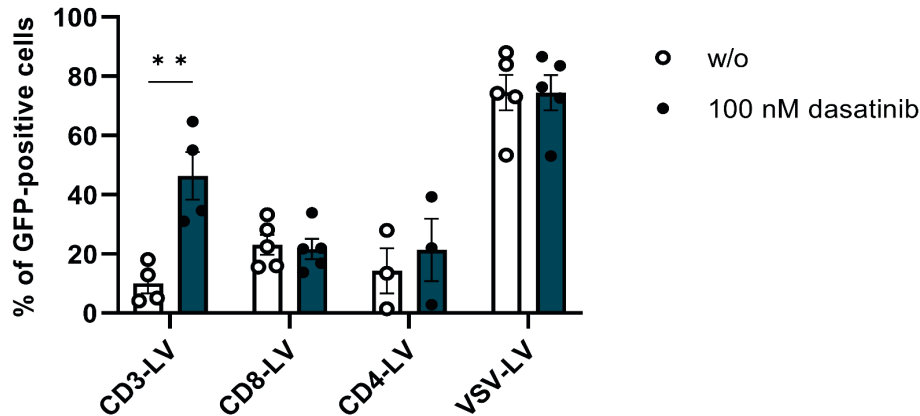


Figure 21: Effect of dasatinib on receptor-targeted LVs.

Fully activated PBMCs were incubated with 100 nM dasatinib or without (w/o) for seven hours during transduction with CD3-, CD8-, CD4- or VSV-LV. Amount of GFP-positive cells was determined after three days and is shown as mean \pm SEM determined from three to five donors. ** $p < .01$, by paired t-test.

In summary, dasatinib was not able to enhance transduction of other paramyxoviral glycoprotein pseudotyped LVs. In fact, these results indicated that transduction enhancement by dasatinib was rather specific for the molecular properties of the target receptor CD3 than for the entry pathway.

2.2.3 Dasatinib prevents CD3-LV induced T cell activation

As the employed CD3-LV contains a scFv derived from TR66 directed against the CD3 ϵ domain of the CD3 receptor, which is associated with the T cell receptor, the vector itself has the ability to activate resting T cells. This unique feature of the CD3-targeted LVs was demonstrated by upregulation of the high affinity alpha chain of the interleukin-2 (IL-2) receptor, CD25, in non-activated primary cells upon incubation with the vector particles (Frank et al., 2020). In turn, dasatinib is known to prevent T cell activation upon CD3:TCR engagement by inhibiting Lck phosphorylation (Schade et al., 2008). Here, dasatinib's effect on the agonistic activity of CD3-LV was assessed.

Freshly isolated human PBMCs were cultured in medium containing IL-7 and IL-15, overnight. The cells were then incubated with 100 nM dasatinib one hour prior to addition of LV or activating antibody cocktail (α CD3/ α CD28). Four days after treatment,

activation of the cells was determined by the level of CD25 expression. Incubation of non-activated cells with α CD3/ α CD28 or CD3-LV increased the CD25 expression level to above 80%, compared to background expression of 20% (Figure 22). The presence of dasatinib during exposure to activating antibodies decreased the expression of the activation marker, causing only slight upregulation to 54%. Following CD3-LV incubation in presence of dasatinib, CD25 expression remained close to background levels at an average of 31%. As expected, VSV-LV and CD8-LV, which have no agonistic activity, caused no upregulation of the activation marker, maintaining CD25 expression at a background level of 20%, independent of dasatinib treatment (Figure 22).

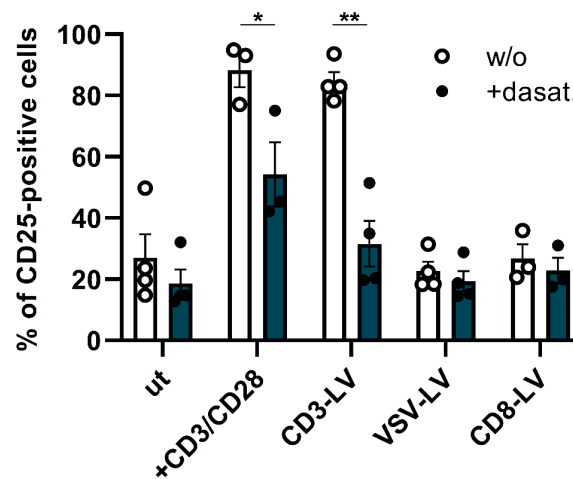


Figure 22: Dasatinib prevents CD25 upregulation.

PBMCs were cultured in IL-7/15 supplemented medium overnight. The following day, cells were exposed to activating antibodies α CD3/ α CD28, CD3-LV, VSV-LV, CD8-LV or remained untreated (ut), in presence or absence of 100 nM dasatinib for seven hours. Expression of CD25 was determined four days after transduction and is shown as mean \pm SEM of three to four donors, of which one was measured in technical triplicates. * $p < .05$, ** $p < .01$, by paired t test. Figure modified from (Braun et al., 2023).

In conclusion, CD3-LV triggered T cell activation in cytokine-stimulated cells which was prevented in presence of dasatinib. Thus, it needed to be determined how dasatinib-induced inhibition of T cell activation during incubation with CD3-LV could enhance transduction.

2.2.4 Dasatinib increases CD3 receptor availability and improves vector particle binding

T cell activation is known to induce downregulation of the TCR in complex with the CD3 receptor to prevent over-activation of the cell (Escors et al., 2011). The agonistic CD3-LVs have shown to cause downregulation of the CD3:TCR complex. As just described, dasatinib is capable of preventing CD3-LVs agonistic activity while increasing transgene delivery. Hence it was investigated, whether preventing CD3-LV induced T cell activation affects CD3 receptor availability and vector particle binding to the cell.

At first, PBMCs treated with dasatinib and incubated with CD3-LV were analyzed for CD3 receptor density, after three days. Cells incubated with CD3-LV in absence of dasatinib showed significantly lower CD3 surface levels compared to dasatinib treated cells (Figure 23A). While the MFI of CD3 for the 50 nM and 100 nM dasatinib treated cells was above 1440-1800, CD3 cell surface detection for untreated cells averaged at 685. Collectively, dasatinib increased CD3 receptor availability upon CD3-LV incubation, which was still detectable three days after treatment.

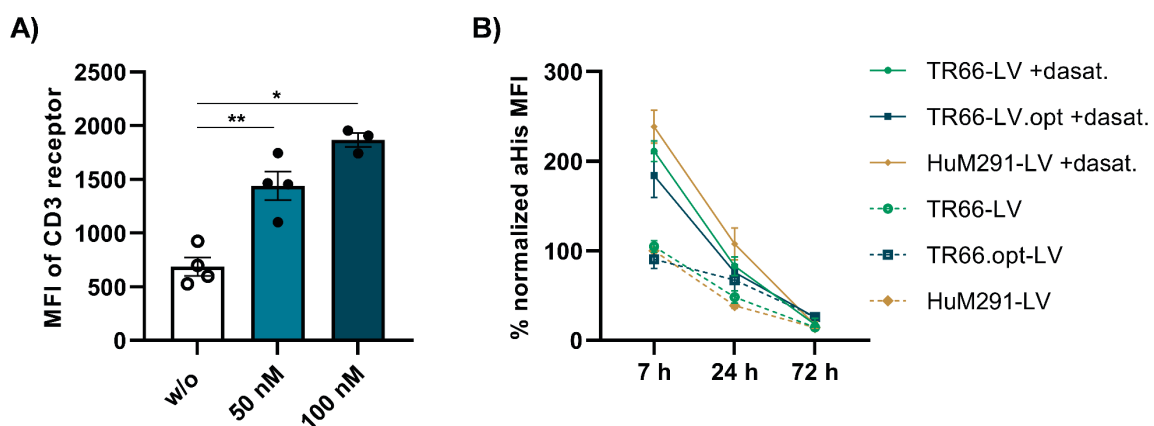


Figure 23: Dasatinib increases CD3 receptor availability for CD3-LV binding.

(A) Mean fluorescence intensity (MFI) of the CD3 receptor was determined three days after CD3-LV transduction in presence of 50 nM, 100 nM or in absence of dasatinib. Each value represents the average value derived from one particular vector stock tested on one to three donors. Values are shown as mean \pm SEM. * $p < .05$, ** $p < .01$, by repeated measure one-way ANOVA followed by Tukey's multiple comparison test. **(B)** Activated PBMCs were incubated with 100 nM dasatinib or without dasatinib for seven hours during transduction with CD3-LVs. MFI of anti-His staining was measured seven hours, 24 hours and 72 hours after dasatinib addition, allowing the detection of CD3-LVs bound to the cells. Results are shown in a timeline, normalized to seven hours HuM291-LV, in which filled symbols and lines represent the binding of LVs to cells treated with dasatinib (+dasat.), and blank dots connected by dashed lines indicate binding of LVs to cells in absence of dasatinib. Data are mean \pm SEM of three donors measured in technical duplicates. Figure modified from (Braun et al., 2023).

The next step was to investigate how the increased receptor availability affects particle binding. Therefore, activated PBMCs were incubated with three different CD3-targeted vector particles in presence or absence of 100 nM dasatinib. The CD3-LVs varied in their displayed scFv being either derived from TR66 (TR66-LV), a modified version of TR66 (TR66.opt-LV) or a scFv derived from an alternative CD3-specific antibody HuM291 (HuM291-LV) (Frank et al., 2020). After seven, 24 and 72 hours, vector particles bound to cells were detected by flow cytometry using an antibody recognizing the His-tag attached to the binding glycoprotein of LVs and normalized to the values determined after seven hours with HuM291-LV. The results were normalized due to large differences of MFI levels between the separate measurements (Figure 24). All three CD3-LVs were present at a substantially higher level on cells treated with dasatinib during vector incubation (Figure 23B). This was most pronounced seven hours after start of incubation, when the level of CD3-LVs bound to the cells was twice as high for the dasatinib-treated cells compared to the untreated cells. Increased particle binding upon dasatinib treatment remained detectable for 24 hours, but was no longer present after 72 hours. In conclusion, preventing CD3-LV induced T cell activation by the kinase inhibitor dasatinib, increased CD3 receptor availability on the target cells. This increased receptor availability allowed more CD3-LV particles to bind to the cell, presumably increasing vector particle uptake and therefore enhancing transgene delivery.

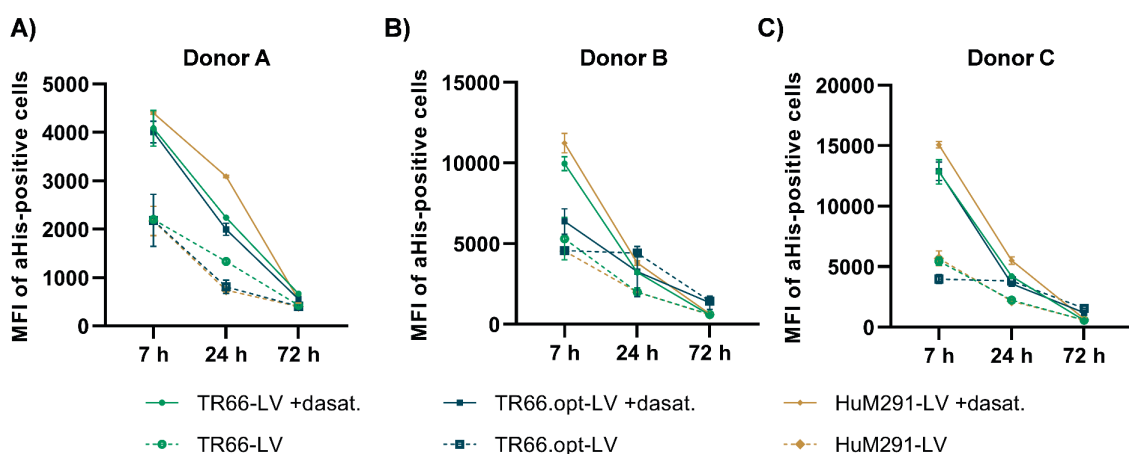


Figure 24: Dasatinib increases CD3-LV binding to T cells.

Activated PBMCs were incubated with 100 nM dasatinib or without dasatinib for seven hours during transduction with CD3-LVs. Timelines show MFI of anti-His staining from three donors (A-C) over 72 hours after incubation with dasatinib. Filled symbols and lines show the binding of LVs to cells treated with dasatinib (+dasat.), blank dots connected by dashed lines show binding of LVs to cells in absence of dasatinib. Mean \pm SD of one donor measured in technical duplicates. Figure modified from (Braun et al., 2023).

2.2.5 The effect of tyrosine kinase inhibitors on LV gene delivery

Dasatinib is a member of the Src/Abl tyrosine kinase inhibitor (TKI) family, able to inhibit Lck tyrosine kinase, an upstream kinase in the T cell activation cascade. It is described to block phosphorylation of Lck upon T cell stimulation, thereby preventing TCR downregulation and T cell activation (Lissina et al., 2009; Schade et al., 2008). To lastly confirm, that the transduction enhancing effect of dasatinib is due to inhibition of the Lck tyrosine kinase, other TKIs were tested for their activities on targeted LV-mediated transduction. Therefore, imatinib which targets Abl, c-Kit and PDGFR, the Src/Abl inhibitor bosutinib, and the TKI and cell cycle arrest inducer genistein were tested.

Activated PBMCs were incubated with 50 nM dasatinib, 1 μ M bosutinib, 1 μ M imatinib, 30 μ M genistein or in absence of TKIs one hour prior to addition of CD3-, CD8- or VSV-LV. Medium was changed to remove the TKIs four hours after adding the vector particles and transgene expression, such as cell viability of the cells was determined after three days by flow cytometry. While treatment with dasatinib led to a 6-fold increase in transduction with CD3-LV, imatinib, which inhibits Abl phosphorylation but not Lck at this concentration (Seggewiss et al., 2005; Shah et al., 2004), did not lead to an increase in transduction with targeted vector (Figure 18A). Bosutinib, on the other hand, is a dual Src/Abl kinase inhibitor, which acts as a Src inhibitor interfering with Lck showing similar inhibition profiles as dasatinib (Puttini et al., 2006; Remsing Rix et al., 2009). The treatment with 1 μ M bosutinib during transduction with CD3-LV induced an increase in transgene expression of 3-fold (Figure 25A). At last genistein was tested, which has been described to increase VSV-LV induced transduction by 2-fold at 30 μ M due to G2 cell cycle arrest, facilitating lentiviral gene transfer and replication (Zhang 2006). In our case, the treatment of cells with 30 μ M genistein showed no effect on transduction for any of the three LVs. Cell viability after treatment with the different TKI and LVs, was generally unaffected and remained above 80% under nearly all conditions (Figure 25B). In some cases, viability dropped to below 60%, mainly when cells were treated with genistein.

These results emphasize, that the increase in transduction in presence of dasatinib was caused by inhibition of the Src kinase Lck rather than Abl or other tyrosine kinases.

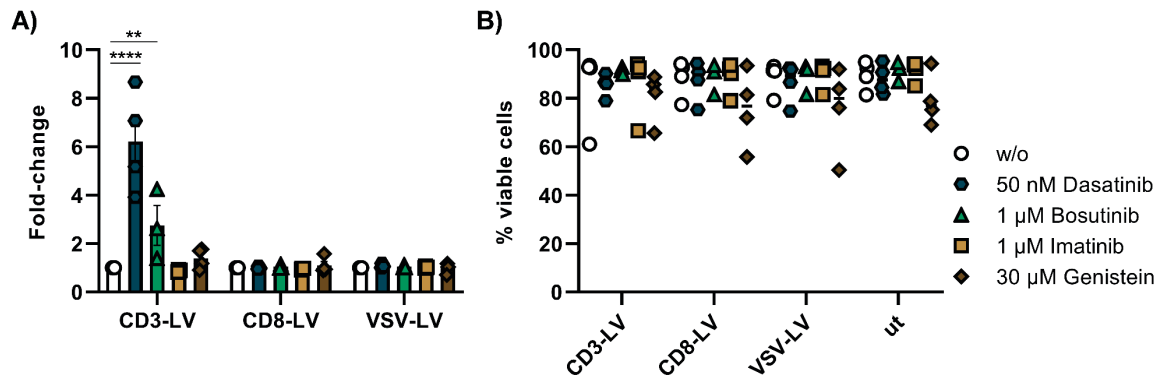


Figure 25: Effect of various tyrosine kinase inhibitors on lentiviral gene delivery.

Activated PBMCs were incubated in tyrosine kinase inhibitor (TKI)-containing medium, namely 50 nM dasatinib, 1 μM bosutinib, 1 μM imatinib or 30 μM genistein for five hours during transduction with CD3-, CD8-, VSV-LV or remained untransduced. **(A)** Bar diagrams show fold-increase in GFP expression upon treatment with the inhibitors, indicated with distinct symbols and colors, three days post transduction as mean \pm SEM of three to four biological replicates. $**P < .01$, $****P < .0001$ by two-way ANOVA following Dunnett's multiple comparison test. **(B)** Scatter plot shows the viability of three to four biological replicates three days after treatment, with the mean value per condition indicated.

Overall, CD3-LV transduction and thus transduction enhancement in presence of dasatinib, was shown to be independent of endocytosis. In fact, dasatinib prevented CD3-LV induced T cell activation, following CD3:TCR downregulation, by inhibiting the tyrosine kinase Lck. This led to an increase in CD3 receptor availability and allowed more vector particles to bind and transduce the target cell, making the transduction enhancing effect of dasatinib exclusive for CD3-LV.

2.3 Generation of CAR T cells in presence of dasatinib

The previous chapters demonstrated the use of dasatinib as transduction enhancer for the delivery of the reporter gene *gfp*, as a proof of concept. Next, the effect of dasatinib was tested on the generation of therapeutically relevant CAR T cells. Therefore, a second generation CAR directed against the tumor antigen CD19, composed of a scFv derived from the monoclonal FMC63 antibody with a myc-tag, a CD28 co-stimulatory domain and CD3 ζ intracellular signaling domain was used (Figure 26). The effect of dasatinib on CAR gene delivery was evaluated and the CD19.CAR T cells were characterized regarding their cytotoxic activity, exhaustion, phenotype, and cytokine secretion. Therefore, the difference between CD3-LV generated CAR T cells in presence or absence of dasatinib was investigated and later on compared to

conventionally generated CAR T cells, produced by transduction with VSV-LV in presence or absence of dasatinib.



Figure 26: Schematic representation of the CD19.CAR construct.

Second-generation CD19.CAR encoded on the lentiviral transfer plasmid pSEW-mycCD19.CAR(28z). SFFV: spleen focus forming virus, myc: myc-tag, TMD: transmembrane domain, ICD: intracellular domain.

2.3.1 Dasatinib enhances CD3-targeted CD19.CAR gene delivery in a time- and dose-dependent manner

At first, the functionality of dasatinib on enhancing CAR gene delivery was verified by transduction of primary human PBMCs with CD3-LVs carrying the CD19.CAR (CD3-LV(CD19.CAR)). The functional titers of the CD3-LV stocks in presence of dasatinib and the optimal conditions for enhancing CAR gene delivery were determined.

Fully activated PBMCs were incubated with 50 nM dasatinib one hour before and four hours after adding CD3-LV(CD19.CAR). CAR expression was measured three days post transduction by staining and detecting the myc-tag via flow cytometry. Dasatinib increased the CAR expression level from 8% to 45% on average (Figure 27A, B). The combination of VF-1 and dasatinib during vector incubation, generated up to 70% CAR T cells and 50% on average, compared to 20% CAR expression when VF-1 was used alone as transduction enhancer (Figure 27C). Functional titers of CD3-LV delivering the CD19.CAR were determined by incubation of a serial dilution of vector particles on activated PBMCs in presence or absence of dasatinib. Flow cytometry measurement three days after vector incubation revealed titers of up to 2×10^7 T.U./mL in presence of dasatinib, corresponding to a 9-fold increase compared to titration of vector particles alone (Figure 27D).

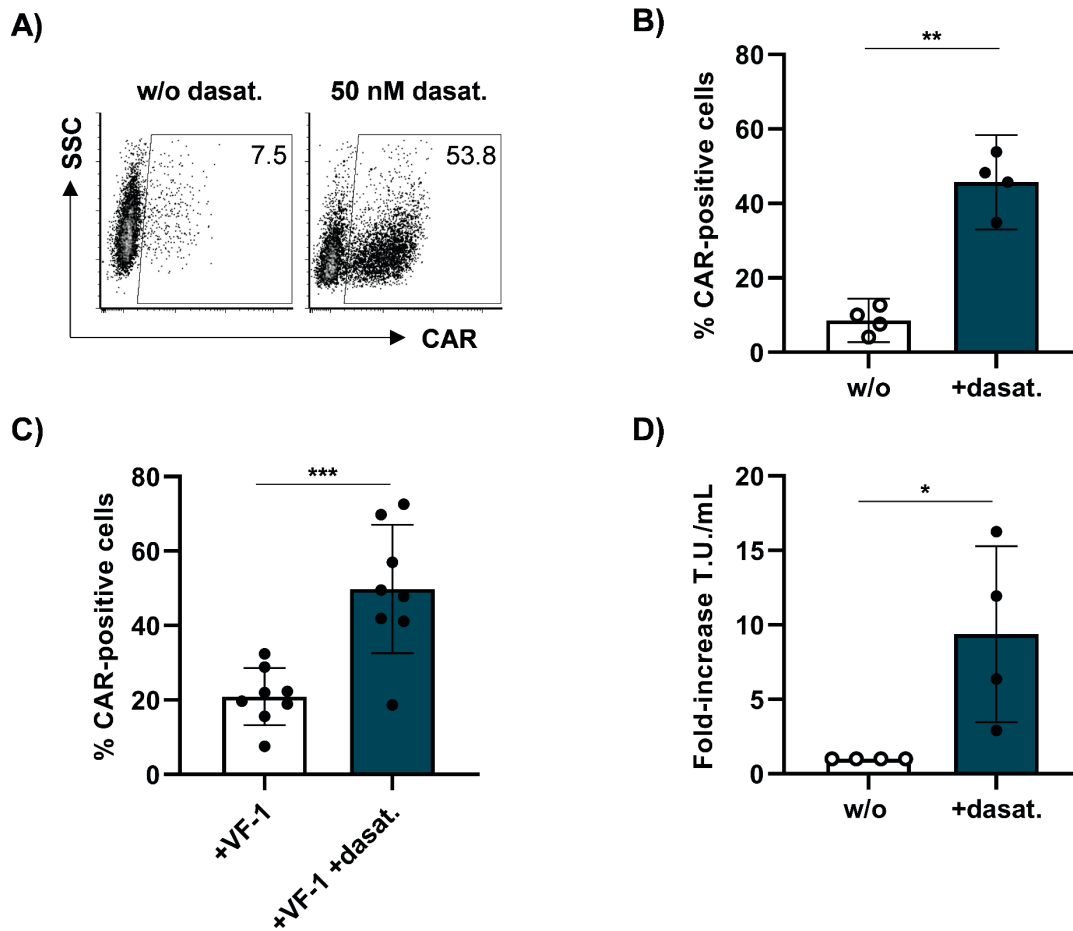


Figure 27: Dasatinib enhances CD3-targeted CD19.CAR gene transfer.

Activated PBMCs were incubated in 50 nM dasatinib-containing medium or without dasatinib for five hours during transduction with CD3-LV(CD19.CAR). CD19.CAR expression was determined three days post transduction by flow cytometry detecting the myc-tag. **(A)** Representative dot plots showing CAR expression of PBMCs in presence or absence of dasatinib. **(B)** Scatter bar diagrams show the percent of CAR⁺ cells after transduction without (w/o) or in presence of dasatinib (+dasat.) as mean \pm 95% CI of four donors. ** $p < .01$ by paired t-test. **(C)** CAR-expression of PBMCs three days after CD3-LV transduction in presence of VF-1 or VF-1 in combination with dasatinib is shown as mean \pm SD of eight biological replicates. *** $p < .001$, by paired t-test. **(D)** Scatter bar diagrams summarize the fold-increase in T.U./mL three days post transduction with a serial dilution of vector, comparing transduction in presence and absence of dasatinib. Data are shown as mean \pm SD of four vector stocks tested on one to four donors. * $p < .05$, by ratio paired t-test. Figure modified from (Braun et al., 2023).

The optimal concentration and incubation time of dasatinib were also assessed for CAR gene delivery. Therefore, PBMCs were treated with 25 nM, 50 nM, 100 nM or without dasatinib for three, five or seven hours during incubation with CD3-LV(CD19.CAR). Transgene expression was evaluated three days after vector incubation and showed the highest CAR expression of 26.6% upon treatment with 50 nM dasatinib for five hours (Figure 28A). Examining all treatment conditions revealed that cells incubated with 100 nM dasatinib for three hours showed a higher CAR expression of 22.6% compared to the cells treated with 25 nM or 50 nM dasatinib

(Figure 28A, B). However, CAR expression in cells treated with 50 nM or 100 nM dasatinib peaked after five hours of treatment, reaching similar CAR expression levels of around 25%. Therefore, incubation with 50 nM dasatinib for five hours was shown to be the optimal condition for enhancing CD19.CAR gene delivery by CD3-LV.

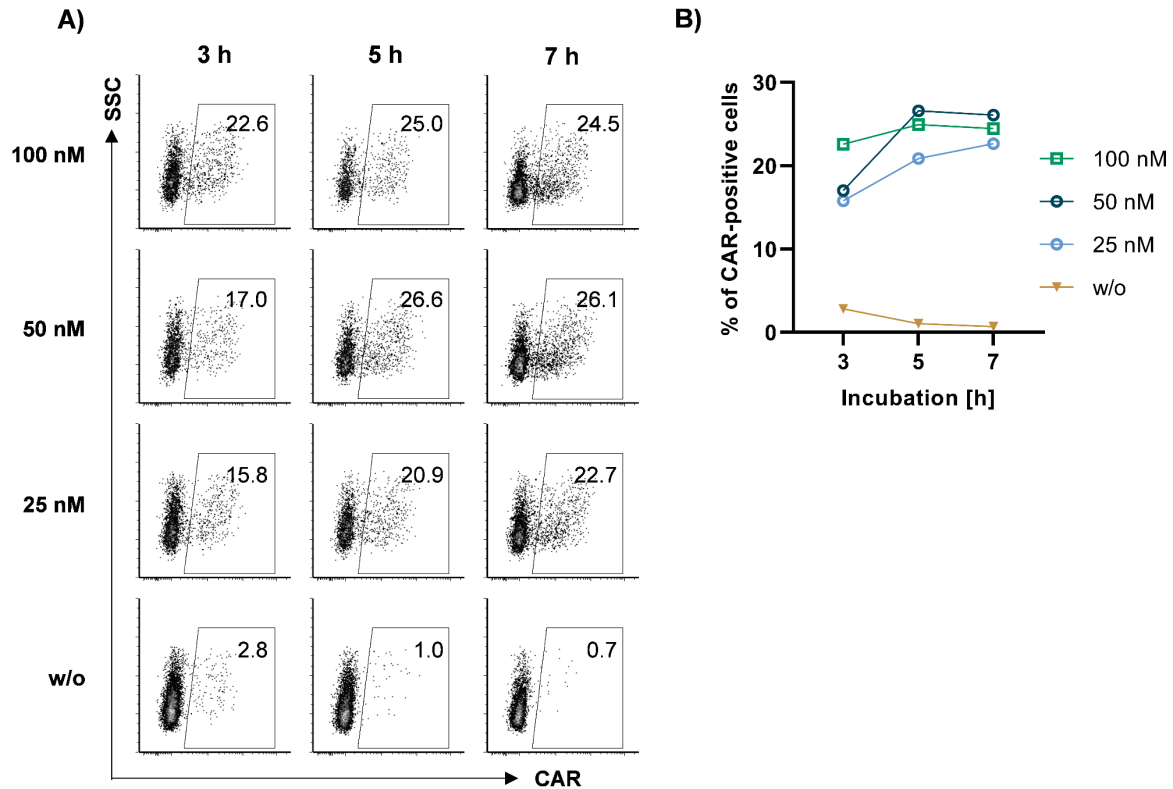


Figure 28: Dasatinib increases CD3-targeted CD19.CAR gene transfer in a time- and dose-dependent manner.

Activated PBMCs were incubated in medium without dasatinib or containing 25 nM, 50 nM or 100 nM dasatinib for three, five or seven hours during transduction. **(A)** Representative dot plots show CAR expression on day three post transduction. **(B)** Superimposed symbols connected by line show CAR expression after the different dasatinib treatments, three days post transduction. Data is derived from one biological donor. Figure modified from (Braun et al., 2023).

As demonstrated for reporter gene delivery, dasatinib also increased CAR gene transfer, using the same optimal conditions as previously determined. Also, further enhancement in CAR expression could be achieved when dasatinib was combined with VF-1 treatment. The effect of dasatinib was therefore transgene independent and could likely be applied for the delivery of various therapeutic genes.

2.3.2 Dasatinib enhances CAR expression in a co-culture with tumor cells, allowing long-term killing activity

Because CD3-LV has the advantage of selectively transducing CD3⁺ T cells, it has the potential to direct CAR gene delivery to the cell of interest while preventing transduction of non-target cells, such as tumor cells. To combine this ability of CD3-LV with the use of dasatinib as transduction enhancer, it was necessary to demonstrate that dasatinib does not interfere with the generation and functionality of CAR T cells when directly exposed to tumor cells. For this purpose, T cells were incubated with dasatinib and CD3-LV and shortly thereafter mixed with tumor cells. The generation and functionality of CAR T cells were monitored over time.

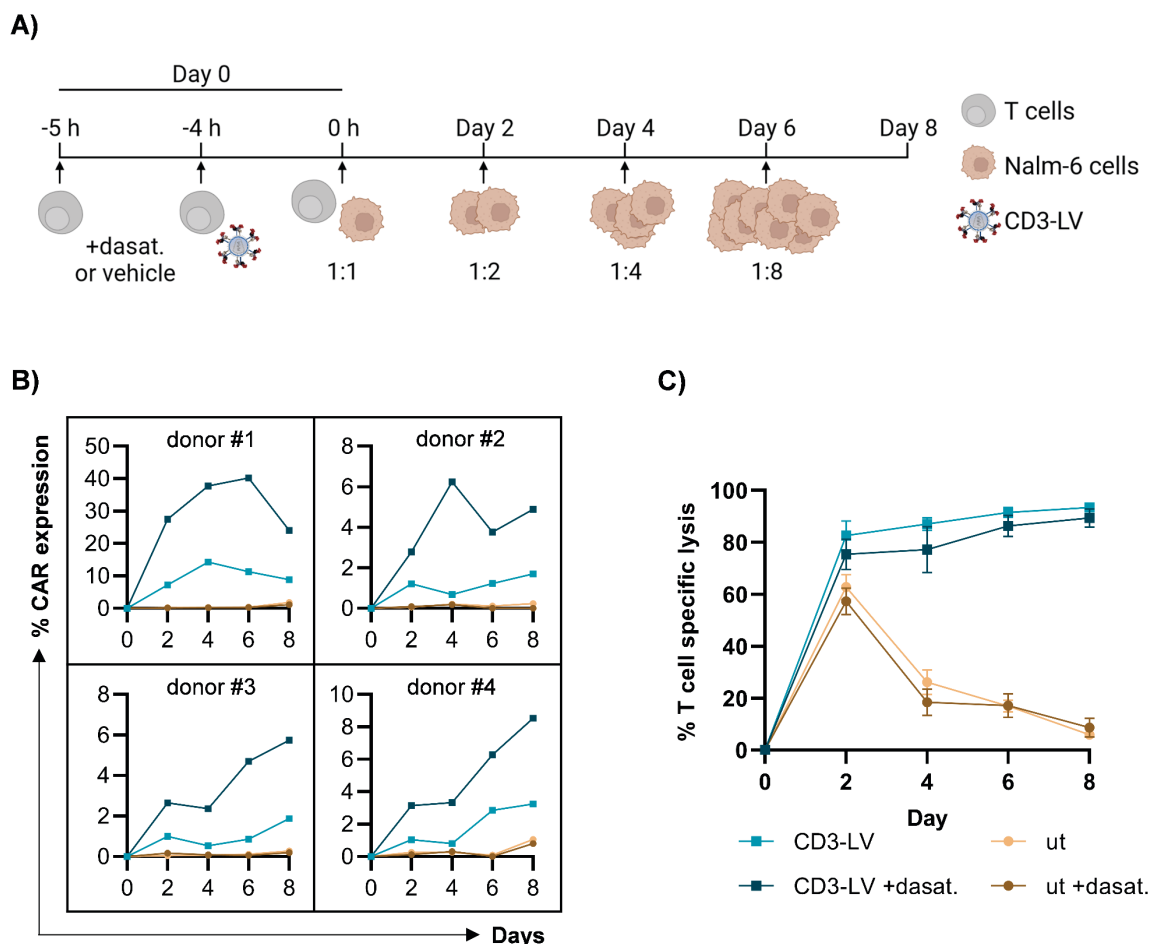


Figure 29: Long-term tumor killing mediated by transduction with CD3-LV.

Activated PBMCs were treated with 50 nM dasatinib-containing medium (+dasat.) or medium without dasatinib for five hours during incubation with CD3-LV prior to the addition of CTV-labeled Nalm-6 cells to achieve a 1:1 ratio of T cells to tumor cells. **(A)** Experimental design. **(B)** Percent of CAR⁺ cells over the time of the killing assay is shown in separate plots for each donor. **(C)** The percent T cell specific lysis of the tumor cells is shown over time. Data represent mean \pm SEM values of four donors, of which one was measured in technical triplicates. Figure modified from (Braun et al., 2023).

Fully activated PBMCs were incubated with dasatinib or vehicle in cytokine-free medium followed by addition of CD3-LV or left untreated. After the start of incubation, CTV-labeled CD19⁺ Nalm-6 cells were supplemented to the T cell culture in a 1:1 ratio. Increasing numbers of fresh tumor cells were added to the culture every other day, re-challenging the T cells four times (Figure 29A). Cell viability and CAR expression were measured by flow cytometry every other day. In all conditions incubated with CD3-LV, CAR T cells became detectable in the presence of tumor cells as early as two days after start of the assay, with increased CAR expression in cells treated with dasatinib (Figure 29B). While CAR T cell numbers varied widely between donors, donor #1 reached 28% CAR expression after two days, rising to 40% on day six after treatment with dasatinib. Without dasatinib incubation, donor #1 reached 7% CAR expression on day two and a maximum of 14% CAR expression on day four. Donor #3 and #4, on the other hand, showed a constant increase in CAR expression up to day eight after start of the assay, with CAR expression around 6-8% when treated with dasatinib and remaining below 3% without dasatinib. PBMCs that were not incubated with the vector particles showed no CAR expression (Figure 29B). When investigating tumor cell elimination, the untransduced cells treated with (ut +dasat.) or without (ut) dasatinib were not able to control the tumor upon repetitive stimulation, showing T cell specific tumor cell lysis of 60% on day two, which rapidly decreased after second stimulation, reaching less than 10% tumor cell lysis at the end of the assay (Figure 29C). In contrast, CD3-LV transduced cells efficiently lysed increasing numbers of tumor cells, independent of dasatinib treatment. No difference in target cell reduction was observed throughout the co-culture, with nearly complete tumor cell lysis of 90% achieved by the end of the assay (Figure 29C).

This assay showed that CAR T cells were generated in presence of tumor cells at elevated levels when pre-treated with dasatinib. CAR T cells efficiently killed increasing amounts of tumor cells, even when CAR T cell levels were low. Since CAR T cells were generated during the course of this assay and numbers varied greatly between donors, no conclusions about dose-efficacy correlations could be drawn from this assay.

2.3.3 Dasatinib mediates generation of functional and less exhausted CAR T cells

Having shown that dasatinib enhances the generation of CAR T cells by CD3-LV and that the CAR T cells are able to eliminate increasing numbers of tumor cells, further characteristics of the cells were to be investigated.

In several studies the use of less differentiated and less exhausted CAR T cells have been described to be advantageous in tumor cell elimination and persistence. This can be achieved by using less differentiated T cells as source for CAR T cell generation (Meyran et al., 2023; Sabatino et al., 2016) or by switching CAR T cells off, allowing them to restore their functionality. With the ability of dasatinib to switch off CAR T cells, tonic signaling was diminished resulting in memory-like CAR T cells with improved antitumor efficacy (Weber et al., 2021; H. Zhang et al., 2021). Combined with the new findings that dasatinib can inhibit CD3-LV induced T cell activation, the question arose whether the presence of dasatinib during vector incubation could affect the fate of CAR T cells.

At first, CAR T cells generated by transduction with CD3-LV in presence or absence of dasatinib were assessed, followed by a comparison to conventional CAR T cells, generated by transduction with VSV-LV. Therefore, cytotoxic activity in regard to dose efficacy correlations such as characteristic of the generated CAR T cell based on exhaustion, phenotype and cytokine secretion were evaluated.

2.3.3.1 Comparing CD3-LV generated CAR T cells with and without dasatinib

Dasatinib has been described as on/off switch for CAR T cells at the time of treatment (Mestermann et al., 2019; Weber et al., 2019) and to restore functionality by inhibiting tonic signaling (Weber et al., 2021; H. Zhang et al., 2021). Therefore, it was investigated whether the short treatment of the cells with dasatinib during vector incubation compromised killing efficacy or had an effect on T cell exhaustion and phenotype of the mature CAR T cells, three days post treatment. The cytotoxic activity of the CAR T cells was determined in a four hour and 24 hour killing assay with CD19⁺ Nalm-6 cells (Figure 30).

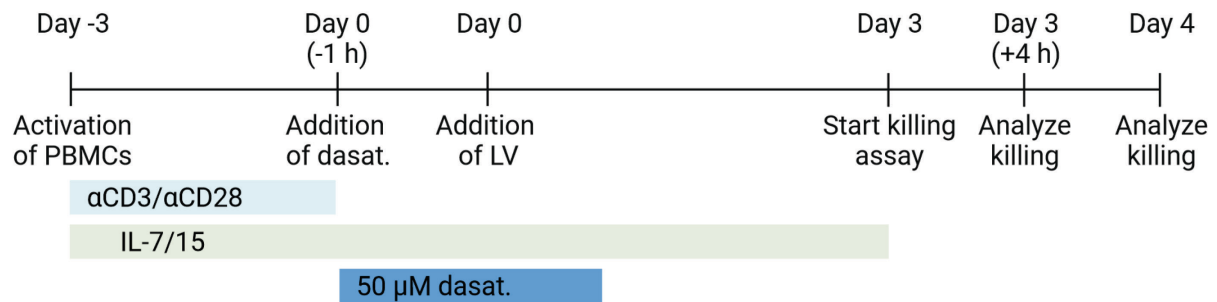


Figure 30: Experimental setup for CD19.CAR T cell generation in presence of dasatinib.

PBMCs were activated for three days, followed by transduction with LV delivering the CD19.CAR in presence or absence of dasatinib. Cells were cultured for three days before analyzing the cells and testing their activity in a killing assay.

Three days after treatment with dasatinib and transduction with CD3-LV, cells were analyzed by flow cytometry to determine the CAR T cell level. To start the assay, 5×10^3 CAR T cells, supplemented with untransduced T cells to achieve the same number of T cells in all conditions, were co-cultured with 1×10^4 CTV-labeled Nalm-6 cells (0.5:1 E:T ratio), in cytokine-free medium. To evaluate background killing independent from the CAR activity, untransduced T cells were co-cultured with the tumor cells, at the same cell density. The co-culture was abrogated after four hours or 24 hours and cells were analyzed by flow cytometry.

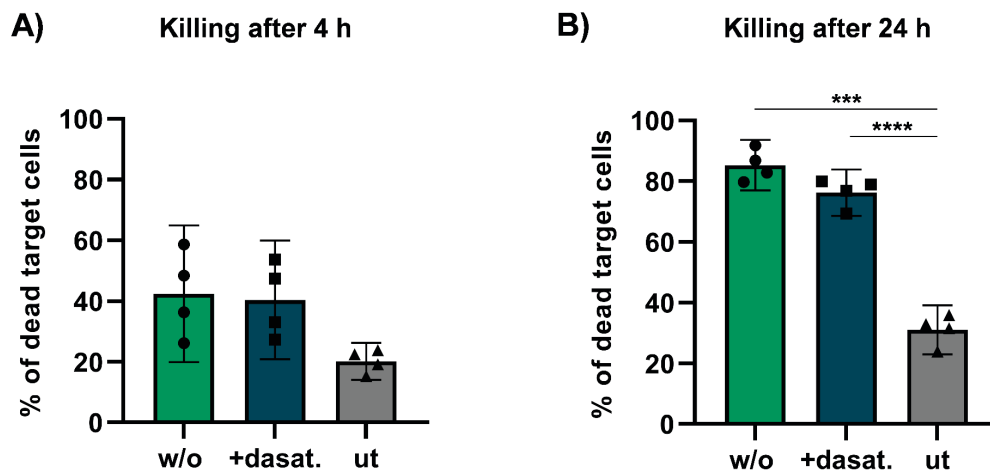


Figure 31: Dasatinib does not compromise CAR T cell activity.

CAR T cells were generated by transduction with CD3-LV in presence or in absence of 50 nM dasatinib. Three days post transduction, untransduced T cells (ut), CAR T cells transduced in absence (w/o) or in presence of dasatinib (+dasat.) were co-cultured with CTV-labeled Nalm-6 cells at an effector to target ratio of 0.5:1. The percentage of dead CTV-labeled target cells was assessed by flow cytometry after four hours (4 h) (A) and 24 hours (24 h) (B). Bar diagrams show killing as mean \pm 95% CI derived from four donors measured in technical triplicates. * $p < .05$, *** $p < .001$, by repeated measure one-way ANOVA followed by Tukey's multiple comparison test. Figure modified from (Braun et al., 2023).

When monitoring Nalm-6 cell viability after four hours of co-culture, both conditions containing CAR T cells (w/o and +dasat.) showed slightly higher tumor cell killing of 40% on average, compared to the untransduced cells (ut) which eliminated 20% of the tumor cells (Figure 31A). After 24 hours of co-culture, CAR T cells generated in presence or absence of dasatinib were able to lyse 75-85% of the tumor cells, with no significant difference in killing activity, while untransduced cells eliminated only 30% of the tumor cells (Figure 31B).

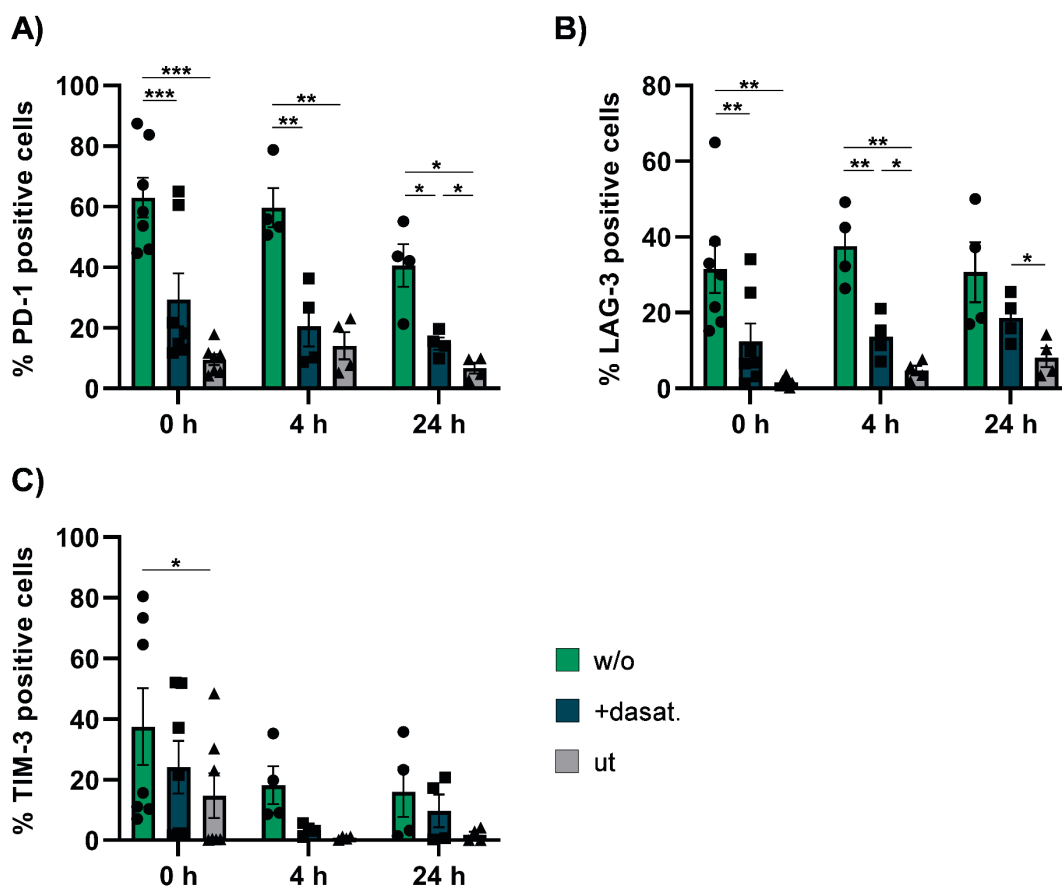


Figure 32: Dasatinib mediates the generation of less exhausted CAR T cells.

Three days post transduction, CAR T cells generated in presence or in absence of 50 nM dasatinib were analyzed for the expression of exhaustion markers PD-1 (A), LAG-3 (B) and TIM-3 (C) before killing (0 h), after four hours and after 24 hours of killing. Data are shown as mean \pm SEM of four to seven donors. * $p < .05$, ** $p < .01$, *** $p < .001$, by repeated measure one-way ANOVA followed by Tukey's multiple comparison test. Figure modified from (Braun et al., 2023).

Next, the effect of short-term exposure to dasatinib on T cell exhaustion and T cell phenotype was investigated before killing, as well as four hours and 24 hours after killing (Figure 32). Expression of the exhaustion markers LAG-3, TIM-3 and PD-1 was overall lower in cells transduced in presence of dasatinib compared to without. In detail, PD-1 expression (Figure 32A) was significantly higher for CAR T cells not exposed to

dasatinib at all three time points (0 h, 4 h, and 24 h), as was LAG-3 expression (Figure 32B) before (0 h) and after four hours of killing. Before killing, PD-1 expression levels of cells transduced in presence of dasatinib were reduced from above 60% to 30%, respectively LAG-3 levels were reduced from 30% to 10% (Figure 32A, B). Likewise, TIM-3 expression was elevated in CD3-LV transduced cells, at all time points (Figure 25C).

Additionally, the amount of LAG-3/TIM-3 double positive cells was significantly higher for cells transduced in absence of dasatinib after four hours of killing, reaching 12% compared to 2% when treated with dasatinib, and was also elevated at the other time points (Figure 33). Overall, transduction with CD3-LV induced an upregulation of exhaustion markers compared to untransduced cells, which was reduced in the presence of dasatinib.

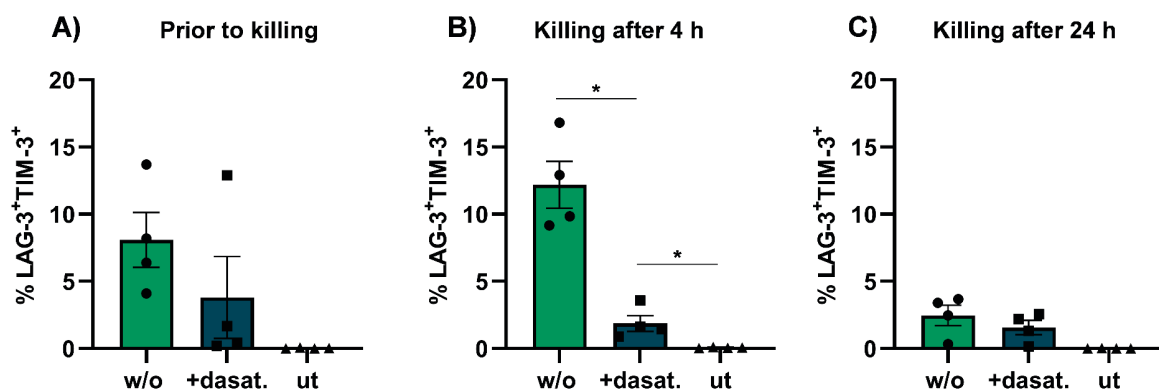


Figure 33: Dasatinib reduces coincident expression of LAG-3 and TIM-3.

Three days post transduction in presence or absence of dasatinib, the level of LAG-3⁺TIM-3⁺ cells was determined prior to killing (A), after four hours of killing (B) and after 24 hours of killing (C). Data is shown as mean \pm SEM of four donors. * $p < .05$, by repeated measure one-way ANOVA followed by Tukey's multiple comparison test. Figure modified from (Braun et al., 2023).

When investigating the T cell phenotypes, the short exposure to dasatinib during LV incubation led to a tendency for the cells to remain less differentiated (Figure 34). While untransduced cells showed the highest proportion of around 10% naïve cells (T_N) at all times, incubation with dasatinib during transduction increased the proportion of naïve cells, from 1% up to 5%. When comparing the CD3-LV incubated cells, the presence of dasatinib increased the central memory T cells (T_{CM}) and decreased the amount of effector memory T cells (T_{EM}), prior to and after four hours of killing (Figure 34A, B).

Overall, the short incubation of dasatinib during incubation with CD3-LV did not compromise the killing efficacy of the arising CAR T cells. However, it decreased the

expression of exhaustion markers before and after killing, and showed a tendency towards a less differentiated phenotype.

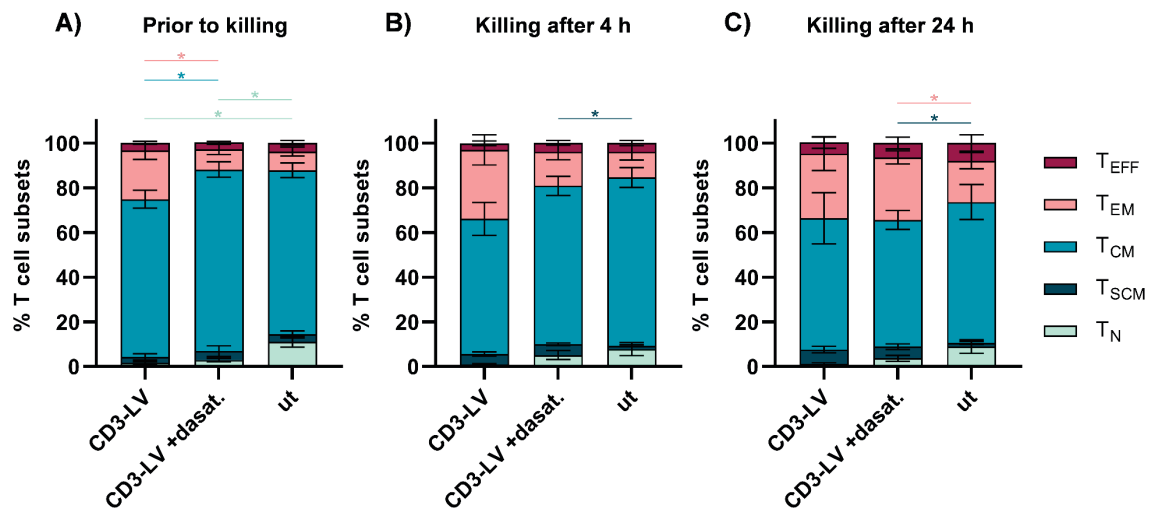


Figure 34: Dasatinib influences the T cell phenotype of CD3-LV transduced cells.

Three days post transduction in presence or absence of dasatinib, T cell phenotypes were assessed by measuring the expression of CD62L, CD45RA and CD45RO by flow cytometry and used to define the percentage of effector (T_{EFF}), effector memory (T_{EM}), central memory (T_{CM}), stem cell memory (T_{SCM}) and naïve (T_N) cells. The percentage of T cell subsets are shown prior to killing (A), after four hours of killing (B) and after 24 hours of killing (C). Data are shown as mean ± SEM of four to six donors. *p < .05, by repeated measure one-way ANOVA followed by Tukey's multiple comparison test. Figure modified from (Braun et al., 2023).

2.3.3.2 Comparing CD3-LV to VSV-LV generated CAR T cells with and without dasatinib

As not only dasatinib can have an impact on the characteristics of the CAR T cells, but also the vector used to target and genetically modify the cells, CAR T cells generated by VSV-LV were compared to CAR T cells generated by CD3-LV in presence or absence of dasatinib.

Activated PBMCs were transduced with CD3-LV(CD19.CAR) or VSV-LV(CD19.CAR) in presence or absence of 50 nM dasatinib. Three days post vector incubation, 50% of the cells transduced with VSV-LV were CAR-positive independent of dasatinib treatment (Figure 35A). Without dasatinib, 27% of the cells transduced with CD3-LV were CAR-positive which was increased to 60% in presence of dasatinib. The CAR T cells were then subjected to a killing assay and further characterized as described in section 2.3.3.1. After four hours of co-culture with CTV-labeled Nalm-6 cells, CD3-LV- and VSV-LV-transduced T cells lysed around 30%

of the tumor cells compared to 12% T cell specific lysis of untransduced T cells (Figure 35B). Extended cultivation for 24 hours, showed significantly higher T cell specific tumor lysis of up to 80% in the transduced T cell conditions compared to 27% for untransduced cells (Figure 35C). No difference in killing efficiency was observed between dasatinib treated conditions or CAR T cells generated with CD3-LV versus VSV-LV.

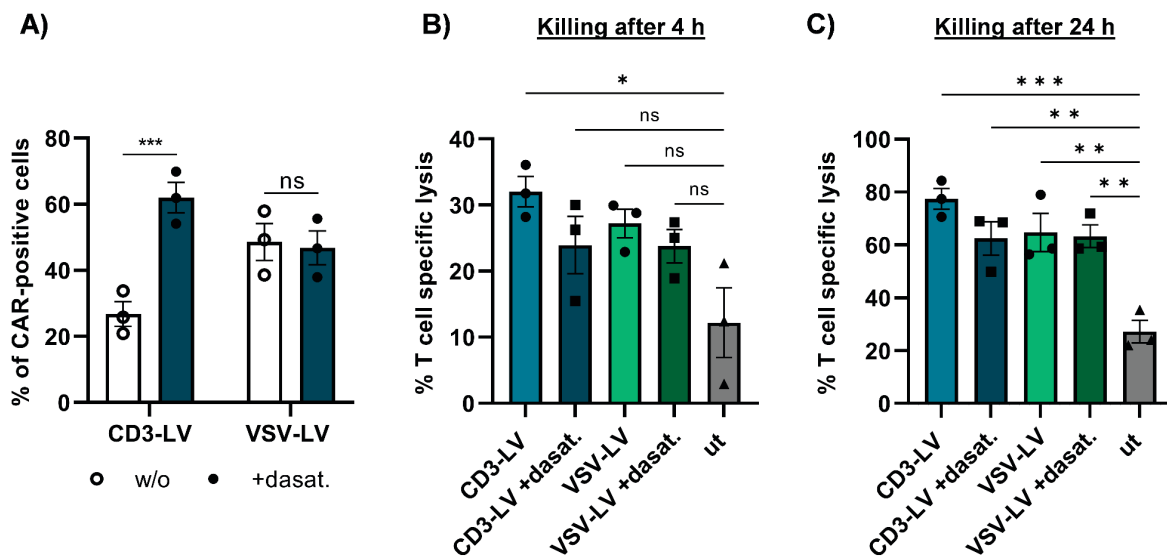


Figure 35: Effect of dasatinib on CAR T cells generated with CD3-LV compared to VSV-LV.

Activated PBMCs were cultivated in 50 nM dasatinib-containing medium or in medium without dasatinib for five hours during transduction with CD3-LV or VSV-LV delivering a CD19.CAR. **(A)** The amount of CAR-positive cells three days post transduction is shown as mean \pm SD of three donors. *** $p < .001$ by paired t-test. **(B, C)** CAR T cells were subsequently co-cultured with CTV-labeled Nalm-6 cells for four hours **(B)** and 24 hours **(C)** before T cell specific lysis was determined. Data is shown as mean \pm SEM of three donors. Ns, non-significant; * $p < .05$, ** $p < .01$, *** $p < .001$, by ordinary one-way ANOVA followed by Tukey's multiple comparison test.

Next, the expression of exhaustion markers was measured before, four hours and 24 hours after killing. At all time points, the exhaustion markers were highest for cells transduced with CD3-LV in absence of dasatinib (Figure 36). Treatment with dasatinib during incubation with CD3-LV reduced the expression of exhaustion markers, reaching lower levels compared to VSV-LV transduced cells in absence of dasatinib. The treatment with dasatinib during VSV-LV incubation, also showed an effect on expression of exhaustion markers, reaching similar levels as cells transduced with CD3-LV in presence of dasatinib. In the case of LAG-3, the expression in CD3-LV transduced cells reached 40% compared to 12% when treated with dasatinib, after four hours of killing (Figure 36A). VSV-LV transduction alone caused 20% LAG-3

expression after four hours of killing and decreased to 12% when treated with dasatinib. The effect of dasatinib was even more pronounced when focusing on LAG-3/TIM-3 double positive cells (Figure 36D). After four hours of killing, 23% of CD3-LV transduced cells were LAG-3/TIM-3 double positive compared with 7% of VSV-LV transduced cells. In presence of dasatinib, only 3% of CD3-LV and VSV-LV transduced cells were LAG-3/TIM-3 double positive.

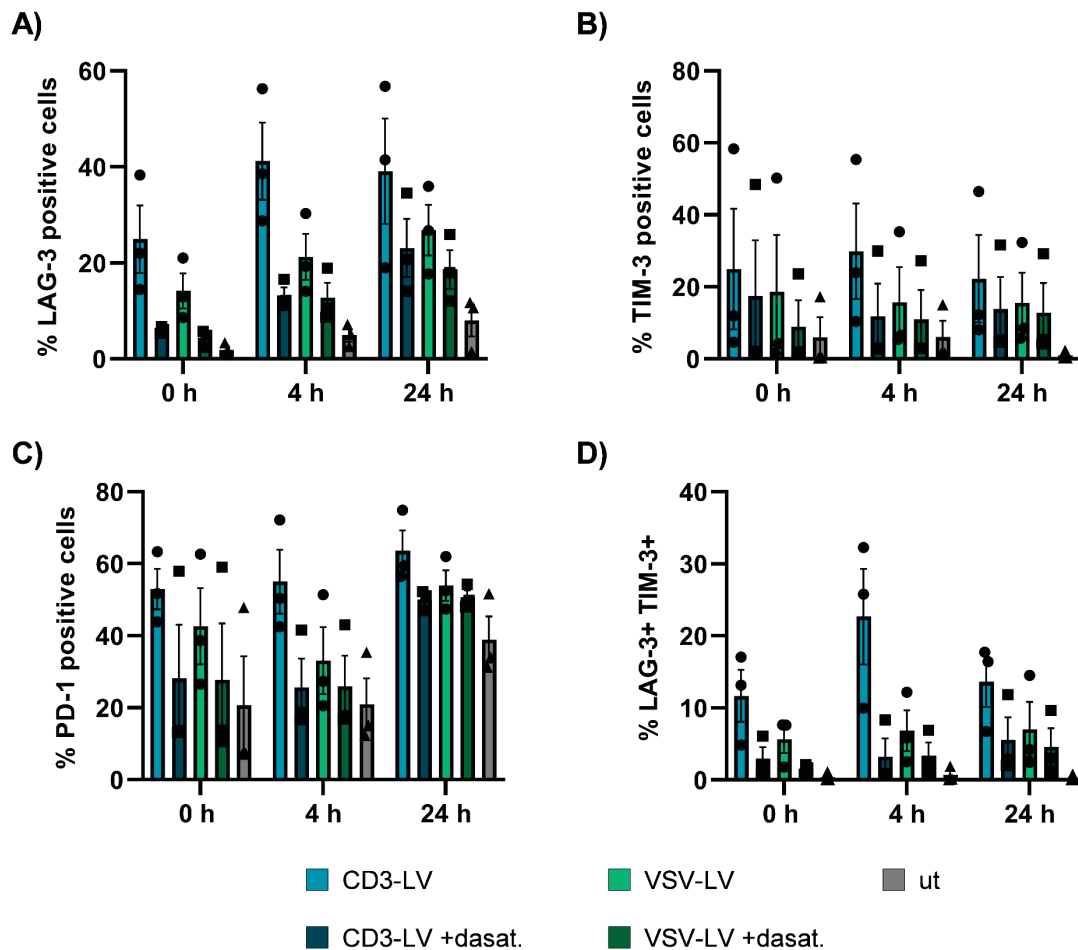


Figure 36: Dasatinib reduces the expression of exhaustion markers.

Three days post transduction with CD3- or VSV-LV, CAR T cells generated in presence or in absence of 50 nM dasatinib and untransduced cells were analyzed for the expression of exhaustion markers LAG-3 (A), TIM-3 (B), PD-1 (C) and coincident expression of LAG-3 and TIM-3 (D) before killing (0 h), after four hours, and after 24 hours of killing. Data are shown as mean \pm SEM of three donors.

When evaluating the T cell phenotype, the treatment with dasatinib during vector incubation led to slight changes in the phenotype for CD3-LV and for VSV-LV transduced cells (Figure 37). Treatment with dasatinib increased the amount of T_N cells and reduced the amount of T_{EM} cells in the CD3-LV transduced group, from 1% to 8% for T_N and from 27% to 5% for T_{EM} , and slightly in the VSV-LV transduced group, from

8% to 11% for T_N and from 12% to 5% for T_{EM} , after four hours of killing (Figure 37B). Upon dasatinib treatment, CD3-LV incubated cells resembled the phenotype of VSV-LV incubated cells.

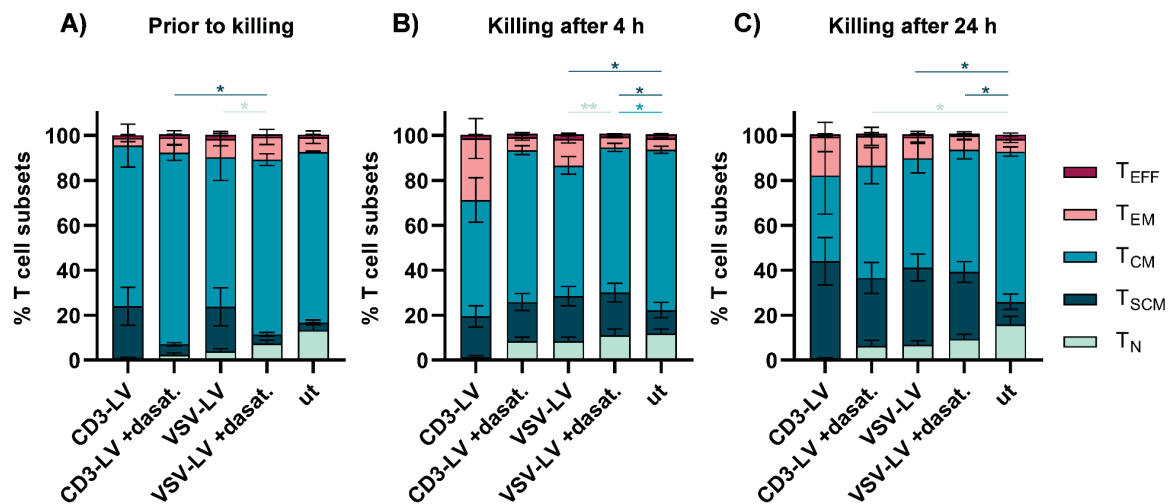


Figure 37: Dasatinib and LV transduction affect the T cell phenotype.

Three days post transduction with CD3- or VSV-LV in presence or absence of dasatinib, T cell phenotypes were assessed prior to killing (A), after four hours of killing (B), and after 24 hours of killing (C). Data are shown as mean \pm SEM of three donors. * $p < .05$, ** $p < .01$, by repeated measure one-way ANOVA followed by Tukey's multiple comparison test.

Taken together, the treatment with dasatinib during transduction with CD3-LV or VSV-LV did not affect the killing efficacy, showing similar killing activity for all CAR T cell conditions. However, dasatinib treatment reduced the expression of exhaustion markers in CD3-LV transduced cells to levels lower than those of VSV-LV transduced cells, inducing a similar phenotype for CD3-LV and VSV-LV transduced cells.

2.3.3.3 Cytokine secretion after CD19.CAR T cell killing assay

As no difference in killing activity between dasatinib treated and untreated CAR T cells was observed, cytokine secretion upon tumor cell encounter was assessed, to ultimately determine the effects of dasatinib on the CAR T cells.

Therefore, human cytokines secreted in the culture media after a 24 hour killing assay of CAR T cells, generated by CD3-LV or VSV-LV in presence or absence of dasatinib, or untransduced cells were measured using a bead-based multi-analysis kit. The determined cytokine levels revealed an effect of dasatinib on the cytokine

secretion of cytotoxic CAR T cells. Pro-inflammatory cytokines were elevated in all transduced CAR T cell conditions compared to untransduced cells, with the highest levels secreted by CD3-LV transduced T cells (Figure 38). Treatment with dasatinib during transduction reduced secretion of cytokines by CD3-LV transduced cells to levels lower than for VSV-LV transduced cells. Treatment with dasatinib during VSV-LV transduction also reduced cytokine secretion to levels similar to CD3-LV transduced cells in presence of dasatinib. Interestingly, GM-CSF reached similar levels of 20-30 pg/mL for transduced as well as untransduced cells, which were reduced to 10 pg/mL for CD3- and VSV-LV transduced cells in presence of dasatinib. When focusing on the difference between CD3-LV +dasat. and VSV-LV w/o, all five pro-inflammatory cytokines were secreted at slightly lower levels by CD3-LV transduced T cells treated with dasatinib compared to VSV-LV transduced cells.

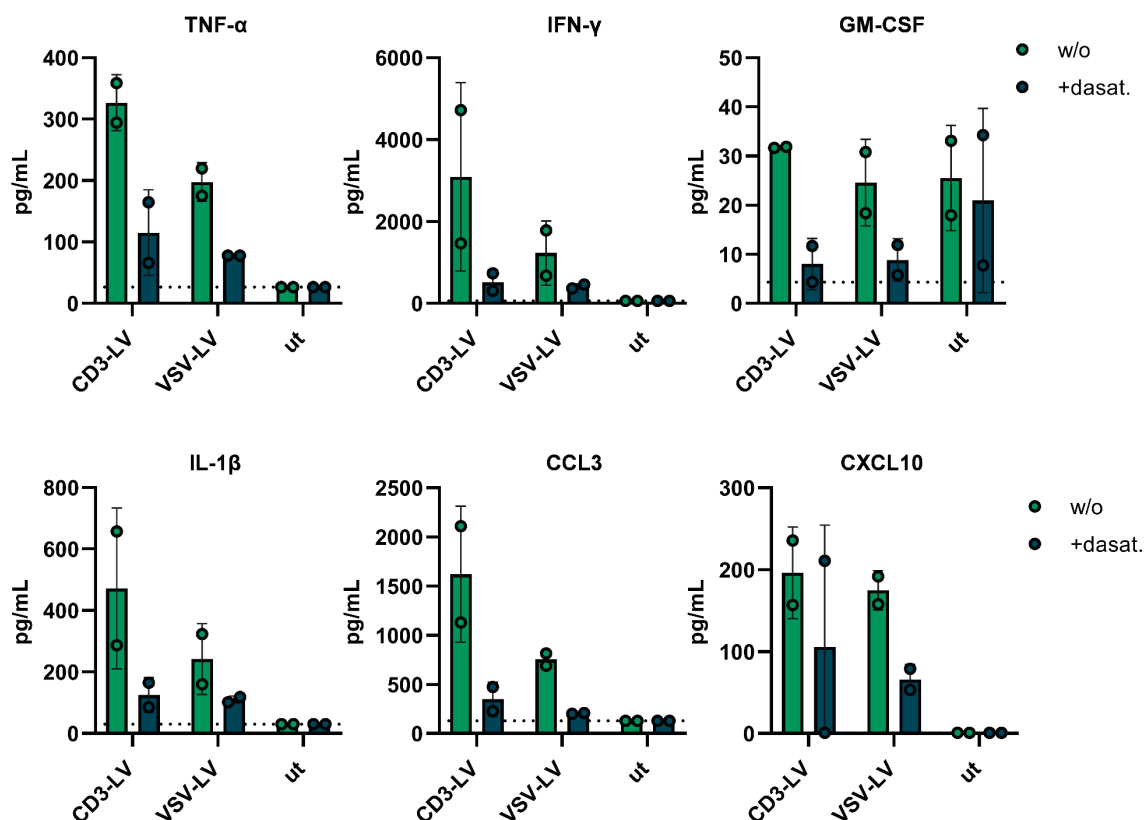


Figure 38: Cytokine secretion after a 24 hour killing assay.

Supernatants were harvested after a 24 hour cytotoxic assay and human cytokines secreted by cells transduced with CD3-LV, VSV-LV or untransduced in presence or absence of dasatinib, were measured using a bead-based multi-analysis kit. Each data point represents the mean of one donor, pooled from technical triplicates after killing, and measured in technical duplicates. Values are shown as mean \pm SD.

Overall, the presence of dasatinib during transduction led to reduced secretion of T cell associated pro-inflammatory cytokines during the process of tumor cell elimination by CAR T cells. Although less pronounced than for CD3-LV, dasatinib also reduced cytokine secretion of cells transduced with VSV-LV, giving the assumption, that dasatinib not only inhibits the agnostic property of CD3-LV during transduction but might in general reduce activation induced by stimulation through transduction.

In conclusion, dasatinib allowed the generation of higher numbers of CAR T cells that efficiently killed increasing numbers of tumor cells with equal killing activity compared to untreated cells. The incubation with dasatinib during transduction reduced the expression of exhaustion markers three days post transduction and upon tumor cell elimination. Additionally, dasatinib reduced the secretion of pro-inflammatory cytokines, without reducing the killing activity. This was not only the case when comparing CD3-LV transduced CAR T cells, but also when comparing CD3-LV transduced CAR T cells in presence of dasatinib to conventionally generated VSV-LV transduced CAR T cells. In presence of dasatinib, CD3-LV was able to transduce a high number of T cells, generating less exhausted, slightly less differentiated CAR T cells that secrete lower levels of pro-inflammatory cytokines while being equally functional compared to conventionally generated CAR T cells.

2.4 Urolithin A promotes the expansion of CAR T_{SCM} cells

CAR T cells have shown great success in eliminating tumor cells but poor expansion and persistence have led to relapse and tumor progression in several patients. Therefore, CAR T cells with high proliferative capacity and long-term survival are thought to further improve clinical outcome. These features have recently been described for T_{SCM} cells (Arcangeli et al., 2022; Meyran et al., 2023). T_{SCM} cells are minimally differentiated cells that share several markers with naïve T cells but are distinct in the expression of CD62L⁺CD45RA⁺CD45RO⁺. They have extreme longevity, the ability to self-renew and the potential for immune reconstitution, equipping them with potent antitumor immunity (Gattinoni et al., 2017). Previous results have shown that UA has immunomodulatory effects on cells by promoting mitophagy (D'Amico et al., 2021; Toney et al., 2021) and that mitochondrial accumulation is associated with exhaustion and dysfunction of T cells (Yu et al., 2020). Based thereupon the effect of

UA on the expansion of human T_{SCM} cells and more precisely on human CAR T cells was investigated.

2.4.1 Urolithin A facilitates generation of CD19.CAR T_{SCM} cells

To firstly evaluate the potential of UA to induce CAR T_{SCM} cells, fully activated PBMCs were incubated with VSV-LV(CD19.CAR) for five hours before changing the medium to medium supplemented with 25 μ M UA, DMSO or without anything (w/o) (Figure 39). Cells were cultured in the supplemented medium until day three post transduction, when cells were analyzed for CAR expression and the proportion of T_{SCM} by flow cytometry and subsequently used in a killing assay.

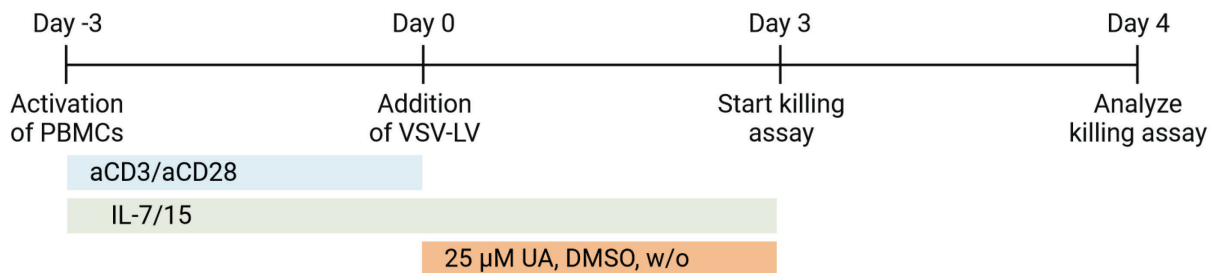


Figure 39: Experimental setup for CD19.CAR T cell generation in presence of UA.

PBMCs were activated for three days, followed by transduction with VSV-LV delivering the CD19.CAR. Cells were further expanded in 25 μ M UA-containing medium, DMSO-containing medium or normal medium (w/o), for three days before analyzing the cells and testing their activity in a killing assay.

The treatment with 25 μ M UA did not compromise gene delivery into PBMCs, neither did the presence of DMSO, showing CAR levels of 40-50% in all conditions (Figure 40A). After having determined the CAR T cell levels, the ability to eliminate tumor cells was evaluated. Therefore, the killing assay was performed as described in section 2.3.3.1 by incubating T cells with CTV-labeled Nalm-6 cells at a 0.5:1 effector to target ratio, in T cell medium without cytokines for 24 hours. Nalm-6 cell viability was determined 24 hours after start of the co-culture and showed CAR T cell specific tumor cell elimination in all conditions. UA treated CAR T cells eliminated 50% of the tumor cells, while CAR T cells exposed to DMSO or only medium (w/o) killed 60% of the tumor cells (Figure 40B). The respective untransduced cells eliminated around 20% of the tumor cells. Overall, the treatment with UA or DMSO, did not affect the ability of either CAR T cells (transduced) or T cells (untransduced) to eliminate tumor cells.

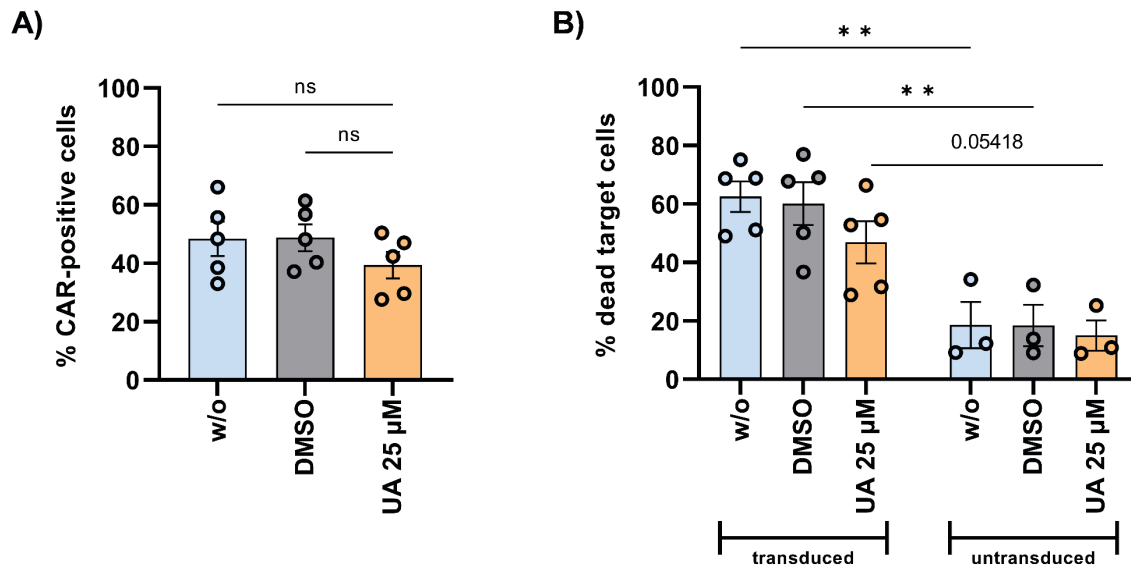


Figure 40: UA does not affect CAR gene delivery or CAR T cell activity.

Activated PBMCs were cultured in medium containing 25 μM UA, DMSO or without (w/o) for three days after transduction with VSV-LV(CD19.CAR). **(A)** On day three post transduction, the level of CAR T cells was determined. Data is shown as mean ± SEM of five donors. Ns: non-significant, by RM one-way ANOVA followed by Tukey's multiple comparison test. **(B)** The CAR T cells were assessed for their killing activity in a co-cultured with CTV-labeled Nalm-6 cells at a 0.5:1 effector to target ratio. After 24 hours of co-culture, the percentage of dead target cells was measured and is shown as mean ± SEM of three to five donors. **p < .01, by two-way ANOVA followed by Tukey's multiple comparison test. Figure modified from (Denk et al., 2022).

The proportion of T_{SCM} after transduction and treatment with UA, prior to killing, was determined by staining for CD62L⁺CD45RA⁺CD45RO⁺ expressing cells. All T cell subsets, regardless of CAR expression, showed an increase in the amount of T_{SCM} cells when treated with UA (Figure 41). Analysis of the T_{SCM} cell proportion on viable T cells, showed that 50% of the cells treated with UA were T_{SCM} cells compared to 7% when treated with DMSO or without (Figure 41A). When examining the proportion of T_{SCM} cells in the CD4⁺ and CD8⁺ T cell subtypes separately, CD4⁺ cells treated with UA showed an increase of T_{SCM} cells from 4% to 40% (Figure 41B), while CD8⁺ T cells showed an overall higher background level of 15% T_{SCM} cells in the control conditions (DMSO and w/o), which was increased to 65% upon UA treatment (Figure 41C). The proportion of CAR⁺ T_{SCM} cells was increased from 5% to 50% when treated with UA (Figure 41D), which was also the case for CD4⁺CAR⁺ cells (Figure 41E). Slightly higher levels were reached in CD8⁺CAR⁺ T cells, showing an increase from 11% to 63% (Figure 41F). Collectively, the treatment with UA increased the level of T_{SCM} cells in all T cell subtypes to a similar extend. These results showed that the effect of UA on

human T cells was not exclusive for one T cell subtype nor influenced by the transduction and CAR expression of the cell.

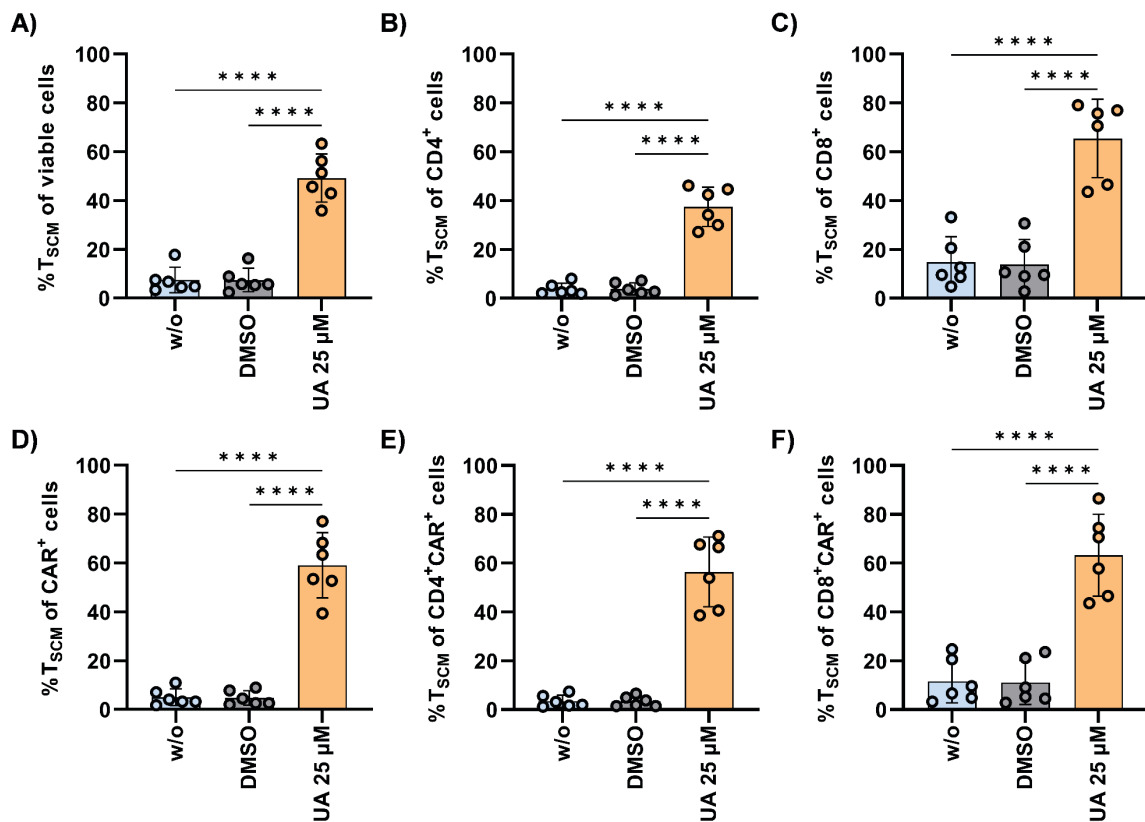


Figure 41: UA facilitates the expansion of T_{SCM} in CD4⁺, CD8⁺ and CAR⁺ T cells.

Activated PBMCs were cultured in medium containing 25 μM UA, DMSO or without (w/o) for three days after transduction with VSV-LV(CD19.CAR). After three days, the amount of T_{SCM} cells was determined by staining for CD62L⁺CD45RA⁺CD45RO⁺ cells of viable cells (A), of viable CD4⁺ cells (B), of viable CD8⁺ cells (C), of viable CAR⁺ cells (D), of viable CD4⁺CAR⁺ cells (E) and of viable CD8⁺CAR⁺ cells (F). Data is shown as mean ± SD of six donors. ****p < .0001, by ordinary one-way ANOVA followed by Tukey's multiple comparison test.

In conclusion, treatment with UA did not affect T cell transduction, while it enhanced the expansion of human T_{SCM} and CAR T_{SCM} cells, regardless of the T cell subtype. This effect was caused by UA and not by the vehicle DMSO, therefore the DMSO condition was left out in further experiments. The shift in CAR T cell phenotype did not impair CAR T cell activity and efficient tumor cell elimination was observed for all CAR T cell conditions.

2.4.2 Urolithin A facilitates the generation of CEA.CAR T_{SCM} cells and can be combined with dasatinib

CAR T cell therapy faces a significant challenge in achieving an antitumor response within the solid tumor microenvironment, often leading to CAR T cell exhaustion. Enhancing CAR T cell functionality against solid tumors has become a topic of great interest. Therefore, the effect of UA on CAR T cells directed towards the solid tumor associated carcinoembryonic antigen (CEA) differentially expressed in colorectal cancer (CRC) thus frequently used as biomarker, was investigated. The second generation CEA.CAR construct composed of a CEA-specific scFv derived from the BW431/26 anti-CEA antibody (Bosslet et al., 1988) linked by an IgG1 hinge domain to the CD28 transmembrane domain followed by the intracellular CD28 costimulatory domain and CD3 ζ signaling domain, was used (Figure 42). For CAR detection, a truncated LNGFR (dLNGFR) reporter protein connected to the CEA.CAR was expressed under the same SFFV-promotor. During translation, dLNGFR is cleaved at the P2A site and separately presented on the cell surface.



Figure 42: Schematic representation of the CEA.CAR construct.

Second-generation CEA.CAR encoded on the lentiviral transfer plasmid pSEW-CEA.CAR(28z)-P2A-dLNGFR. SFFV: spleen focus forming virus, TMD: transmembrane domain, ICD: intracellular domain.

For the generation of CEA.CAR T cells, the conventional LV gene delivery approach with VSV-LV was pursued as was the transduction with the T cell targeted CD3-LV in presence and absence of dasatinib. This approach was chosen in order to further demonstrate the feasibility of CD3-LV in combination with dasatinib to have the same potential with improved characteristics compared to VSV-LV.

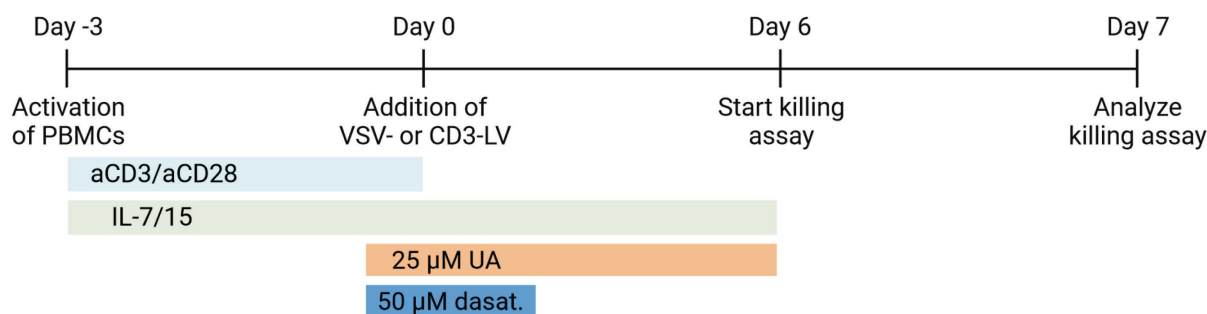


Figure 43: Experimental design of CEA.CAR T cell generation in presence of UA and dasatinib. PBMCs were activated for three days, followed by incubation in dasat., UA or dasat. and UA supplemented medium one hour before transduction with CD3-LV or VSV-LV delivering the CEA.CAR. Medium was changed after four hours and cells were further expanded in 25 μM UA-containing medium or unsupplemented medium, for six days before analyzing the cells by flow cytometry and testing their activity in a killing assay.

To test the effect of UA on CEA.CAR gene delivery and CAR T cell cytotoxicity, activated PBMCs were incubated in medium supplemented with 25 μM UA, 50 nM dasatinib, 25 μM UA and 50 nM dasatinib or unsupplemented, one hour prior to incubation with CD3-LV or VSV-LV (Figure 43). The medium was removed four hours after vector addition and refreshed with medium supplemented with or without UA, respectively. Six days after transduction and further cultivation with or without UA, cells were analyzed for CAR expression by staining for LNGFR⁺ cells. Cultivation in presence of UA did not affect LNGFR expression in any of the three transduction conditions (Figure 44A). Transduction with CD3-LV led to 12% LNGFR expression which was increased to 40% in presence of dasatinib, while VSV-LV transduction resulted in 50% LNGFR⁺ cells, all independent of UA treatment. UA had no effect on gene delivery or LNGFR expression, while dasatinib increased transduction of CD3-LV reaching similar levels to those obtained with VSV-LV.

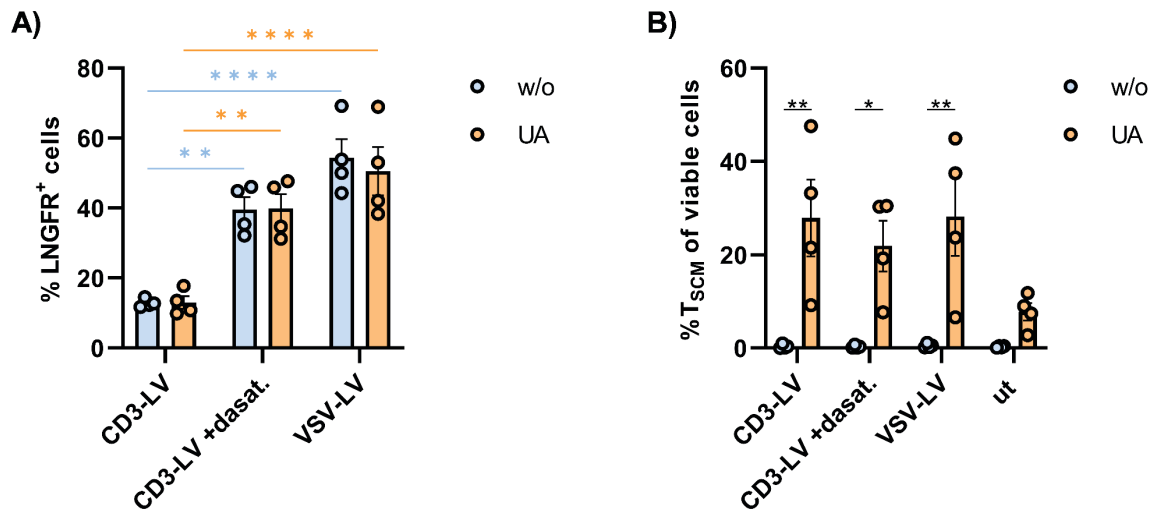


Figure 44: Combination of UA and dasatinib during CEA.CAR gene delivery.

Activated PBMCs were incubated in 25 μ M UA-supplemented or unsupplemented medium (w/o), optionally in presence of dasatinib, one hour prior to addition of CD3- or VSV-LV. Four hours after vector addition, the medium was changed and the cells were further cultured in UA supplemented or unsupplemented medium. **(A)** Six days post transduction, the amount of CAR T cells was determined by staining for the reporter protein LNGFR. Data is shown as mean \pm SEM of four donors. ** $p < .01$, **** $p < .0001$, by two-way ANOVA followed by Tukey's multiple comparison test. **(B)** The frequency of T_{SCM} of viable cells was determined for the different transduction and cultivation conditions, six days after transduction. Data is shown as mean \pm SEM of four donors. * $p < .05$, ** $p < .01$, by ordinary one-way ANOVA followed by Sidak's multiple comparison test.

The proportion of T_{SCM} of viable T cells six days post transduction was significantly increased to 20-30% for all transduced conditions cultured in presence of UA, compared to less than 1% when cultured in the absence of UA (Figure 44B). In cells that never encountered LVs (ut), the proportion of T_{SCM} was increased from less than 1% in absence of UA to 8% in presence of UA.

Having shown that in all gene delivery conditions, the treatment with UA caused a similar expansion of T_{SCM} CAR T cells, these CAR T cells were used in a 24 hour killing assay. Therefore, the adherent tumor cell line LS174T expressing CEA was labeled with CTV and seeded at 3×10^4 cells/well one day before starting the killing assay. Subsequently, 1×10^4 CEA.CAR T cells were added to the wells and co-cultured for 24 hours, in cytokine-free medium. Tumor cell killing was evaluated by flow cytometry 24 hours after the start of the co-culture.

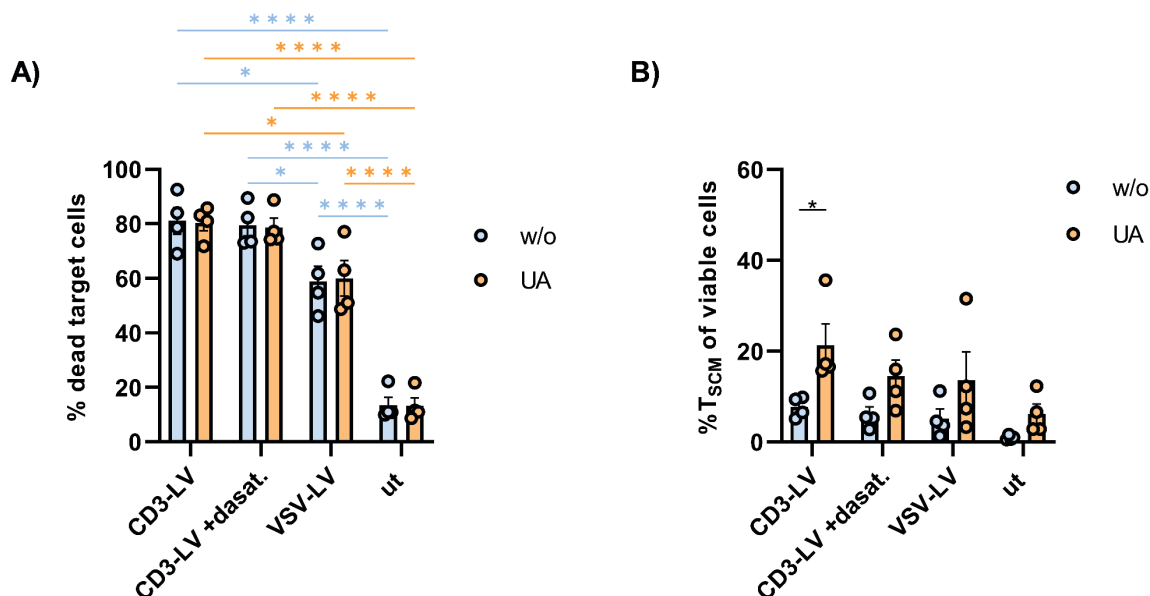


Figure 45: Potent killing activity of UA treated CEA.CAR T cells.

After six days of cultivation in medium containing UA or without, untransduced or CEA.CAR T cells were co-cultured with CTV-labeled LS174T cells and killing activity was assessed. **(A)** After 24 hours of co-culture the percentage of dead LS174T cells was determined and is shown as mean \pm SEM of four donors. * $p < .05$, ** $p < .01$, *** $p < .001$, **** $p < .0001$, by two-way ANOVA followed by Tukey's multiple comparison test. **(B)** The frequency of T_{SCM} of viable cells was determined after 24 hours of co-culture with tumor cells. Data is shown as mean \pm SEM of four donors. * $p < .05$, by ordinary one-way ANOVA followed by Sidak's multiple comparison test.

CEA.CAR T cells generated by CD3-LV in presence or absence of dasatinib eliminated 80% of the tumor cells, while VSV-LV-generated CEA.CAR T cells eliminated 60% (Figure 45A). Untransduced T cells only lysed 15% of the tumor cells. For the transduced conditions, the amount of T_{SCM} cells after a 24 hour co-culture with tumor cells was slightly reduced to 20% (Figure 45B) compared to before encountering the tumor cells (Figure 44B), but was still increased compared to cells not treated with UA, which reached around 5% (Figure 45B). The levels of T_{SCM} cells in untransduced cells resembled those observed before exposure to tumor cells and were slightly higher when cells had been treated with UA. Overall, the treatment with UA causing a shift in phenotype again had no impact on tumor cell elimination by CEA.CAR T cells or untransduced T cells.

Apart from only investigating the shift in the proportion of T_{SCM} cells, the complete phenotype of the differently treated T cells was analyzed. Prior to killing and without UA treatment, untransduced cells showed the highest proportion of T_N cells at 26%, while there were no other major differences in T cell phenotype observed between the other conditions (Figure 46).

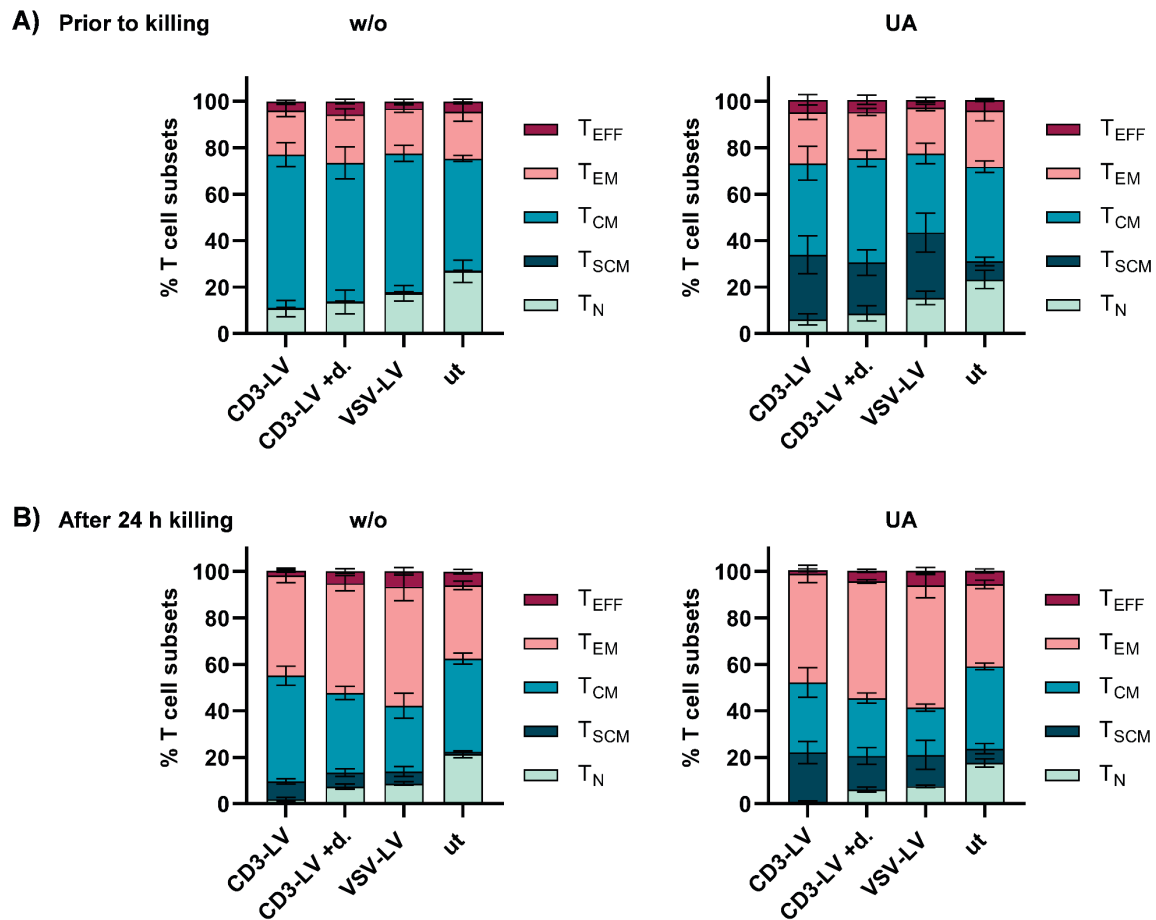


Figure 46: Effect of UA on T cell phenotype.

Six days post transduction and continuous cultivation in presence or absence of UA, the T cell phenotype of viable cells was assessed prior to killing (A) and after 24 hours of killing (B). Data are shown as mean \pm SEM of for donors.

Treatment with UA increased the proportion of T_{SCM} cells in all conditions, as described above, mainly by reducing the amount of T_{CM} and slightly the amount of T_N cells (Figure 46A). Upon killing, the amount of T_{SCM} of UA treated cells was slightly reduced and mainly shifted towards T_{EM} cells, for which the level increased from 20% to 50%, but still showed higher levels compared to cells not treated with UA (Figure 46B). The shift towards more T_{EM} cells was also visible for cells not treated with UA and mainly induced by a lower amount of T_{CM} cells from around 60% to around 30%. Overall, the proportion of T_N cells was reduced upon killing in all conditions, while there was a slight effect visible for dasatinib treated cells which showed a higher level of T_N cells of 7% after killing compared to 2% in CD3-LV transduced cells in absence of dasatinib.

At last, cytokine secretion during killing was evaluated. The supernatant of the killing assay after a 24 hour co-culture was collected and used to determine the levels of

human cytokines secreted by the cells. The cytokine secretion of UA treated cells compared to untreated cells, showed no considerable difference in any of the conditions (Figure 47).

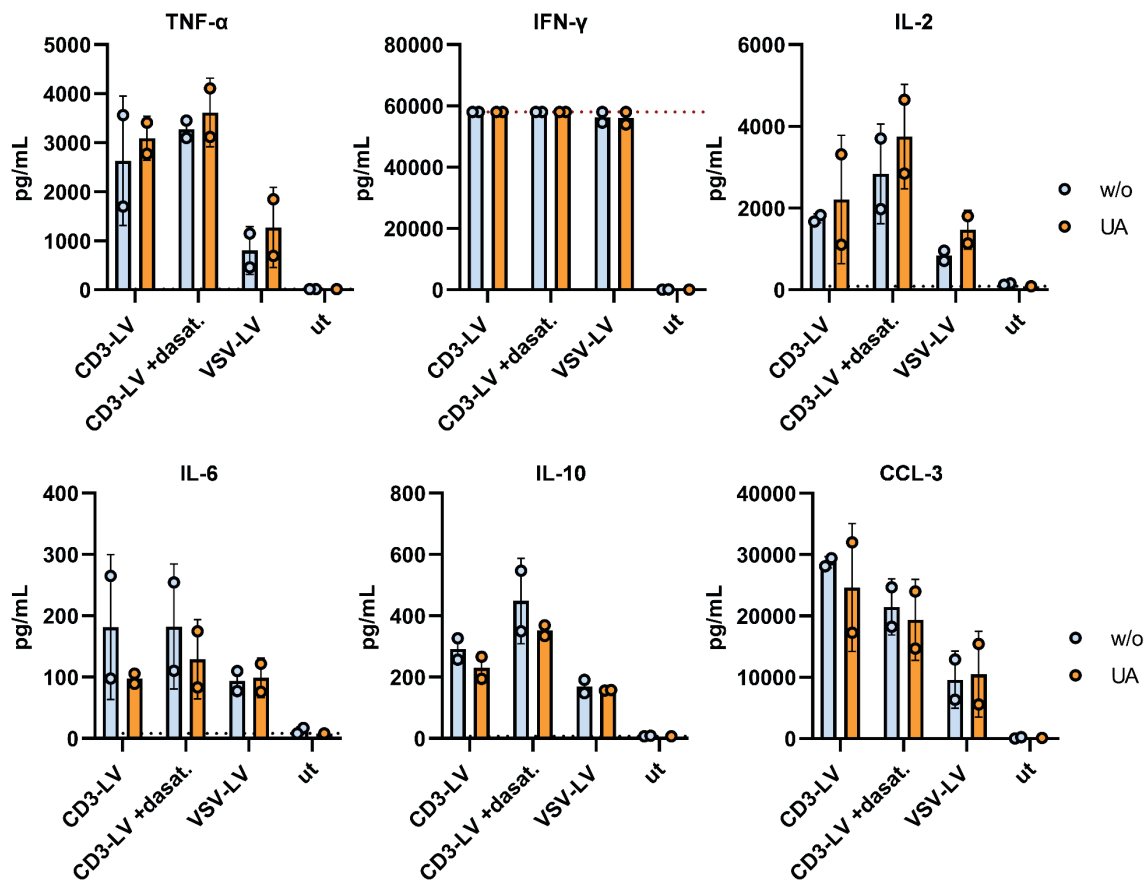


Figure 47: Cytokine secretion of UA treated cells after a 24 hour killing assay.

Supernatants were harvested after a 24 hour cytotoxic assay with cells transduced with CD3-LV, CD3-LV+dasat, VSV-LV or untransduced cells, previously cultured for six days in presence or absence of UA. Secreted human cytokines were measured using a bead-based multi-analysis kit. Each data point represents the mean of one donor, pooled from technical triplicates after killing, and measured in technical duplicates. Values are shown as mean \pm SD.

While untransduced cells secreted nearly no pro-inflammatory cytokines, cells transduced with CD3-LV or VSV LV showed an increase in CAR T cell associated pro-inflammatory cytokines TNF- α , IFN- γ , IL-2 and CCL3. TNF- α reached around 3000 pg/mL for CD3-LV and 1000 pg/mL for VSV-LV transduced cells, the levels of IFN- γ secreted by all transduced cells exceeded the upper limit of the assay (58 ng/mL), IL-2 reached 2000-4000pg/mL for CD3 LV and around 1000 pg/mL for VSV-LV transduced cells and CCL3 was elevated to 20-30 ng/mL for CD3-LV and 10 ng/mL for VSV-LV transduced cells. The anti-inflammatory cytokine IL-10 was also elevated after the co-culture reaching around 200 pg/mL for CD3-LV and VSV-LV

transduced cells and slightly higher levels of around 400 pg/mL for CD3-LV transduced cells in presence of dasatinib. Besides, the clinical CRS-relevant cytokine IL-6 was secreted by all transduced cells at levels around 100 pg/mL and up to 200 pg/mL for CD3-LV transduced cells.

The high cytokine release by the transduced cells was consistent with the cytotoxic activity seen in the killing assay (Figure 45A) as were the unaltered cytokine levels between UA treated and untreated cells (Figure 47). The slightly elevated cytokine levels in the CD3-LV transduced conditions could have been triggered by the transduction with the agonistic CD3-LV generating more active CAR T cells which is also in line with the slightly better killing efficiency by CD3-LV transduced cells.

In conclusion, the presented results show that small molecules can be combined to further refine CAR T cells. While dasatinib can enhance transgene delivery by CD3-LV, achieving CAR T cell levels as high as those achieved with VSV-LV, UA promotes the expansion of the desired T_{SCM} phenotype in CAR T cells. The combination of dasatinib and UA during the transduction of human PBMCs with CD3-LV allows the targeted generation of an increased number of CAR T cells along with the expansion of CAR T_{SCM} cells that, despite the shift in phenotype, can efficiently kill tumor cells, secreting high levels of pro-inflammatory cytokines.

3 Discussion

Several approaches to improve CAR T cell manufacturing and CAR T cell efficacy are being investigated. Here, the use of the small molecules dasatinib and UA combined with T cell-targeted gene transfer using CD3-LV was proposed to refine the generation of CAR T cells. The following section will discuss the mechanism of dasatinib as transduction enhancer for CD3-LV and the importance of target receptor availability. Furthermore, the advantage of using CD3-LV and the selection of a favorable T cell subset and phenotype for CAR T cell generation will be discussed. Thereby, the expansion of CAR T_{SCM} cells by cultivation in presence of UA will be discussed as a simple approach to enrich T_{SCM} cells. Concluding, the feasibility of combining small molecules such as dasatinib and UA with CAR T cell therapy will be evaluate.

3.1 A novel class of transduction enhancers

3.1.1 Dasatinib as transduction enhancer

The use of targeted vectors is thought to improve gene delivery and add an additional safety step in the manufacturing of CAR T cells. Targeted LVs directed towards CD4⁺ and CD8⁺ T cells are highly selective in transducing the corresponding T cell subpopulation *in vitro* and *in vivo* (Agarwal et al., 2020; Pfeiffer et al., 2018). More recently, LVs targeting the CD3 receptor, expressed on CD4⁺ as well as CD8⁺ T cells, were shown to mediate selective transduction in both T cell subsets while simultaneously activating the cells, causing downregulation of the CD3:TCR complex (Frank et al., 2020).

However, transduction efficiency of these targeted vectors, in particular CD3-LV, lagged behind that of the commonly used VSV-LV and therefore limited clinical application. To overcome this problem, transduction enhancers can be used. Commonly used transduction enhancers interact with the vector to form a complex, aggregate or conjugate to facilitate vector-to-cell contact. Therefore, substances including cationic polymers, lipids or peptides, such as vectofusin-1 (VF-1), polybrene, retronectin or Lentiboost, are most frequently used (Hanenberg et al., 1996; Höfig et al., 2012; Kaygisiz & Synatschke, 2020; Vermeer et al., 2017). Their modes of actions

range from neutralization of charge repulsion, permeabilization of the cell membrane to nanofibrill-mediated cell contact. However, many of these substances are associated with laborious synthesis, limited efficacy, and cellular toxicity (Delville et al., 2018; Fenard et al., 2013). Small molecules, which interfere with cellular processes, such as gene transcription, cell entry mechanisms or DNA replication have also been tested. As such, the cytostatic drugs etoposide, camptothecin, taxol, and aphidicolin have been investigated, in the hope of combining transduction-promoting properties with therapeutic effects (Groschel & Bushman, 2005; Kaygisiz & Synatschke, 2020). Instead, their high cytotoxicity caused by DNA damage ruled out their use as transduction enhancers (Kaygisiz & Synatschke, 2020).

The small molecule dasatinib is a member of the Src/Abl tyrosine kinase inhibitor (TKI) family and approved for the treatment of Philadelphia chromosome-positive chronic myeloid leukemia and acute lymphoblastic leukemia (Maiti et al., 2020). Dasatinib inhibits the constitutively active Bcr-Abl kinase and has improved therapeutic potential over imatinib by binding to multiple states of the kinase in its active and inactive form (Tokarski et al., 2006). Due to its less stringent binding requirements, dasatinib potently inhibits imatinib-resistant Bcr-Abl mutants. Functioning as a Src tyrosine kinase inhibitor, dasatinib inhibits Lck, an important upstream kinase in the T cell activation cascade. Blocking Lck prevents the phosphorylation of the CD3 receptor signaling domains and subsequently the recruitment and activation of ZAP-70. Therefore, dasatinib prevents signal transduction through the TCR and T cell activation-induced downregulation of the CD3:TCR complex (Lissina et al., 2009; Schade et al., 2008). Stimulation-induced downmodulation of the CD3:TCR complex has been observed upon T cell incubation with CD3-LV and has been associated with the reduced transduction efficiency compared to other targeted LVs (Frank et al., 2020).

In this work, dasatinib was used for the first time during transduction of T cells with targeted LVs and evaluated for the enhancement of transduction. The presence of dasatinib did indeed increase CD3-LV mediated gene transfer to activated PBMCs by 3- to 10-fold, in a concentration- and time-dependent manner (Section 2.1.1 and 2.3.1). The maximal enhancing effect was reached when incubating the cells for five hours with 50 nM dasatinib. This is consistent with the observed suppression of protein tyrosine phosphorylation initiated at a dasatinib concentration of 10 nM, reaching complete inhibition at 100 nM (Schade et al., 2008). The incubation time is important,

given that dasatinib inhibits TCR signaling and thus cell proliferation, at concentrations starting at 10 nM (Schade et al., 2008). Incubation of cells with dasatinib for five hours had no effect on viability or proliferation (Section 2.1.2), as the interaction between dasatinib and Lck is reversible and T cell function can be rapidly and completely restored (Mestermann et al., 2019; Tokarski et al., 2006). This explains the transduction enhancing effect of dasatinib also on non-activated T cells (Section 2.1.4), given that inhibition can be rapidly restored, allowing efficient T cell signaling, cell proliferation and transgene expression.

Since commonly used transduction enhancers act receptor independently, they can promote unwanted vector-to-cell interaction. This has been described for VF-1, which mediated receptor-independent binding of targeted LVs to target receptor-negative cells, but importantly not their transduction (Jamali et al., 2019). Other transduction enhancers that facilitate complex formation or reduce membrane microviscosity might also cause unwanted vector-to-cell interaction increasing the risk of off-target transduction. Therefore, it is important to verify selectivity of targeted LVs upon treatment with transduction enhancers.

The sustained selectivity in the presence of dasatinib towards CD3⁺ T cells was demonstrated in a whole blood transduction assay and in an *in vivo* experiment (Section 2.1.4 and 2.1.5). In both setups, CD3-LV exclusively transduced CD3⁺ cells and showed no detectable transgene expression in CD3⁻ T cells, also in presence of dasatinib. Administration of dasatinib to mice prior to CD3-LV injection did not affect the vector's specificity and resulted in transgene expression in both CD4⁺ and CD8⁺ T cells (Section 2.1.5).

With the exception of one mouse in the dasatinib-treated group showing slightly increased GFP expression of 4%, the induced transgene expression levels in dasatinib-treated mice were around 1-2% and comparable to those observed in untreated mice. These results are insufficient to make a profound conclusion on a potential transduction enhancing effect of dasatinib *in vivo*. Although the mouse model was based on a study by Mestermann *et al.* in which mice were intraperitoneally (i.p.) injected with dasatinib to control the activity of CAR T cells (Mestermann et al., 2019), several limitations may have interfered with a conclusive outcome of the present study. In particular, the actual serum level of dasatinib in the blood of the mice was not determined, and therefore a sufficient dasatinib concentration at the time of CD3-LV injection (required threshold ≥ 40 nM (Mestermann et al., 2019)) could not be ensured.

Pharmacokinetics of dasatinib in mice have been evaluated upon intravenous (i.v.) or oral (p.o.) administration, revealing a half-life between one and two hours and oral bioavailability varying from 14% to 51% (Kamath et al., 2008; Luo et al., 2006). Anyhow, based on the study by Mestermann *et al.*, i.p. injection of 10 mg/kg dasatinib every six hours demonstrated full blockade of T cell function (Mestermann et al., 2019). Another limitation of our study is the relatively small group size of four mice per group. Since only one mouse in the dasatinib-treated group showed higher transgene expression, it cannot be excluded that this was due to an outlier.

Overall, this is the first description of dasatinib as transduction enhancer in general, and in particular for the gene delivery by CD3-LVs. In this work, conditions for optimal transduction enhancement with dasatinib were established by treating T cells with 50 nM of dasatinib for five hours during vector incubation. Dasatinib can enhance gene delivery to activated T cells, non-activated T cells in culture and resting T cells in whole blood, and may need further validation to support its function *in vivo*.

3.1.2 The importance of receptor availability and particle binding for successful transduction

Most transduction enhancers act by facilitating vector-to-cell interaction receptor independently and vary in efficiency depending on the entry mechanism of the vector. This is the case for VF-1, which is effective in enhancing transduction for the paramyxovirus glycoprotein-pseudotyped LVs, such as CD4-, CD8-, and CD3-LV, while it inhibits the pH-dependent cell entry of VSV-LV. Receptor-targeted LVs pseudotyped with paramyxoviral glycoproteins undergo pH-independent cell membrane fusion, while VSV-G-pseudotyped LVs depend on endocytosis of the LDL receptor for cell entry (Frank & Buchholz, 2018). Blocking endocytosis using bafilomycin A1 (BflA1) prevented VSV-LV transduction, while it did not affect CD3-LV-mediated transduction (Section 2.2.1). In the case of dasatinib, VSV-LV and paramyxovirus glycoprotein-pseudotyped LVs targeting the CD4 or CD8 receptor were not affected by dasatinib, whereas transduction with CD3-LV was significantly increased (Section 2.2.2). This suggests that the mode of action of dasatinib differs from that of commonly used transduction enhancers and is specific to the molecular properties of the CD3 receptor. A particular property of the CD3:TCR complex is the downregulation of the receptor complex upon stimulation and CD3 crosslinking

(Salvatore Valitutti & Lanzavecchia, 1997). The CD3 receptor in complex with the TCR is continuously trafficking between plasma membrane and endosomal compartments, undergoing rapid cycles of endocytosis and recycling, and upon stimulation, CD3:TCR surface expression is decreased (Alcover et al., 2018). CD3:TCR downmodulation is described as having the dual effect of contributing to signal transduction by bringing the domains into close proximity (José et al., 2000) and terminating the cellular response to prevent overstimulation (Escors et al., 2011).

Several mechanisms have been proposed and are thought of working together, inducing CD3:TCR downmodulation (Chakraborty & Weiss, 2014; Escors et al., 2011). The mechanism of serial TCR-triggering states that a single ligand can trigger multiple TCR complexes, resulting in their downregulation and prompt degradation in the lysosome (S. Valitutti et al., 1995; Salvatore Valitutti & Lanzavecchia, 1997; van der Donk et al., 2021). Co-modulation, on the other hand, describes the downmodulation of engaged and non-engaged TCRs by preventing recycling back to the cell surface rather than promoting internalization (José et al., 2000; Liu et al., 2000). The model of extrinsic signaling suggests the participation of at least one extrinsic signal such as PD-L1 co-stimulation to further promote CD3:TCR downmodulation (Escors et al., 2011; Karwacz et al., 2011). An integrative model combining these three mechanisms most likely regulates CD3:TCR signal transduction and downmodulation (Escors et al., 2011).

While ligand-induced TCR downregulation involves multiple internalization mechanisms, including endocytic and phagocytic pathways, they all rely on the phosphorylation of the intracellular CD3 signaling domains, controlled by the tyrosine kinase Lck (Alcover et al., 2018; van der Donk et al., 2021). Inhibiting phosphorylation of these residues with dasatinib has shown to increase the presence of the receptor on the cell surface, reduce the degradation of the complex and block T cell activation (Lissina et al., 2009; Schade et al., 2008; van der Donk et al., 2021). CD3-LVs have shown to trigger CD3:TCR downmodulation and induce T cell activation (Frank et al., 2020).

In this work, the presence of dasatinib prevented CD3-LV-induced T cell activation (Section 2.2.3) and increased the availability of the CD3 receptor (Section 2.2.4). The increased availability of the CD3:TCR complex on the cell surface, allowed 2-fold more vector particles to bind to the cells and remain bound longer (Section 2.2.4). These results are consistent with the concepts of serial triggering and co-modulation. In

presence of dasatinib, blocking the downmodulation of triggered receptors prolonged binding of the vector particles to the cell surface, and preventing co-modulation causing downmodulation of non-engaged receptors increased the amount of particles detected on the cell surface.

BflA1, which inhibits endocytosis by preventing acidification of the endosome (Nishi & Forgac, 2002), was shown to block degradation of the CD3:TCR complex, but did not prevent CD3:TCR downregulation, as was the case with the Abl inhibitor imatinib (van der Donk et al., 2021). Both BflA1 and imatinib were unable to increase CD3-LV transduction in this work (Section 2.2.1 and 2.2.5). Only bosutinib, a Lck inhibitor with an inhibition profile similar to that of dasatinib (Puttini et al., 2006; Remsing Rix et al., 2009), increased CD3-LV-mediated transduction, but not that of CD8-LV or VSV-LV (Section 2.2.5). This further supports the fact that transduction enhancement of CD3-LV by dasatinib is based on blocking CD3:TCR downregulation and increasing the receptor availability rather than preventing endocytosis or inhibiting other kinases.

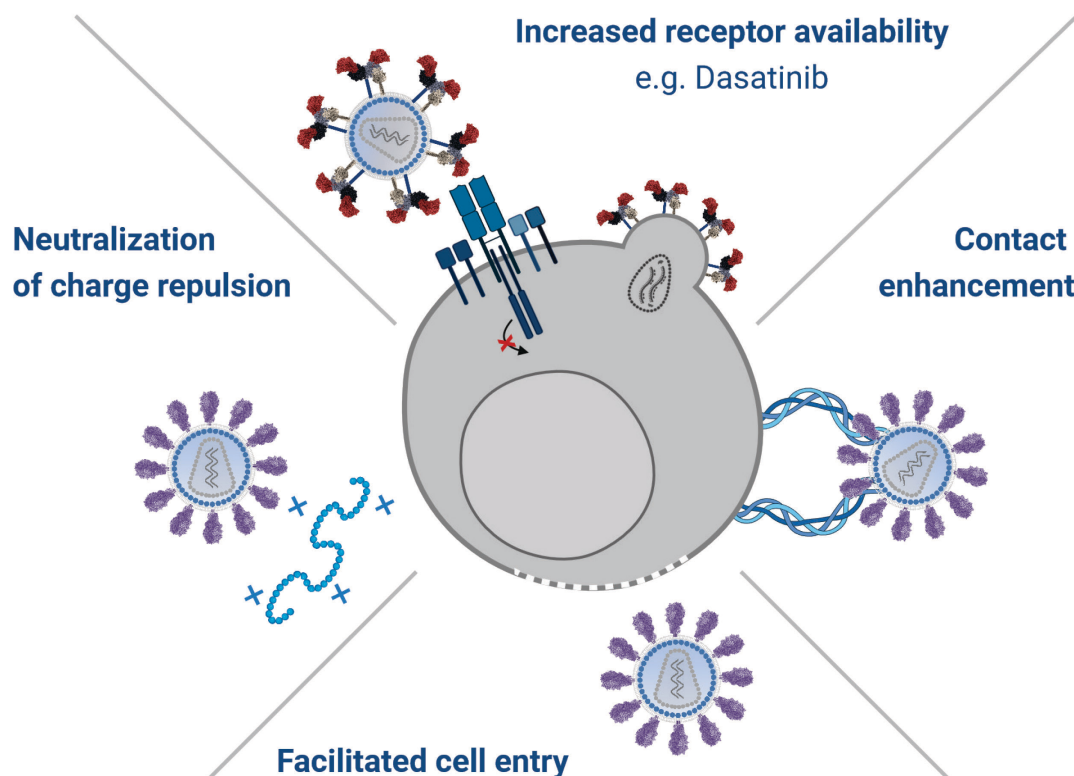


Figure 48: Dasatinib as a new transduction enhancer.

As a member of a new class of transduction enhancers, dasatinib enhances transduction by interacting with intracellular mechanisms, in this case inhibition of Lck, preventing CD3:TCR downregulation, and thereby increasing the target receptor availability. Other transduction enhancers commonly function by facilitating vector-to-cell interaction outside of the cell.

The main finding of this thesis was that dasatinib differs from conventional transduction enhancers as it does not facilitate vector-to-cell interaction receptor independently, but increases the availability of the targeted receptor by a cell intrinsic mechanism (Figure 48). This describes a new class of small molecule transduction enhancers that enhance transduction by intracellularly modifying the cell surface expression of targeted receptors, for example by inhibiting kinases.

A close interaction between the CD3-LV and the target receptor is required to overcome the resistance of the two membranes and trigger membrane fusion (Harrison, 2015). The increased target receptor availability and thus particle binding upon dasatinib treatment clearly helps to achieve successful membrane fusion. Moreover, it may also help to evade restriction factors (RFs). As the LVs used here derived from HIV-1, they are susceptible to innate immune responses through pattern recognition receptors (PRRs) and intrinsic antiviral restriction factors (Borsotti et al., 2016; Kajaste-Rudnitski & Naldini, 2015). PRRs and RFs induce antiviral defense mechanisms that target selective steps of the retroviral life cycle including viral entry, reverse transcription, nuclear transport, integration and transgene expression (Borsotti et al., 2016; Kajaste-Rudnitski & Naldini, 2015). Activation of PRRs, such as Toll-like receptors (TLRs), by virus-derived nucleic acids induces an innate immune response, resulting in the activation of signal transduction pathways that lead to the production of cytokines, chemokines, and antiviral type I interferons (IFNs) that prevent viral transduction (Coroadinha, 2023; Kajaste-Rudnitski & Naldini, 2015). Since many PRRs reside in endosomal or lysosomal compartments, LVs capable of directly fusing with the plasma membrane may partially evade detection (Kajaste-Rudnitski & Naldini, 2015).

However, intrinsic antiviral RFs can also recognize viral nucleic acids and proteins, and act directly to abrogate transduction (Coroadinha, 2023). These RFs include IFITMs, which localize to the plasma membrane or to the membranes of endosomes and lysosomes, where they inhibit viral entry by disrupting fusion between viral and cellular membranes (Hornick et al., 2016; Zhao et al., 2018). IFITM-1 localizes to the plasma membrane and is effective in restricting viruses that enter the cytoplasm by direct fusion with the cell membrane (Zhao et al., 2018). This has recently been described to have a major impact on T cell-targeted LV transduction. Using single-cell transcriptomics, (Charitidis et al., 2023) demonstrated that antiviral factors are

upregulated in those T cells that, upon encountering LVs, do not convert to CAR T cells. Transduction with CD4 and CD8 receptor-targeted LVs, which undergo direct fusion with the cell membrane, was significantly increased when IFITM-1 was downregulated by rapamycin (Charitidis et al., 2023).

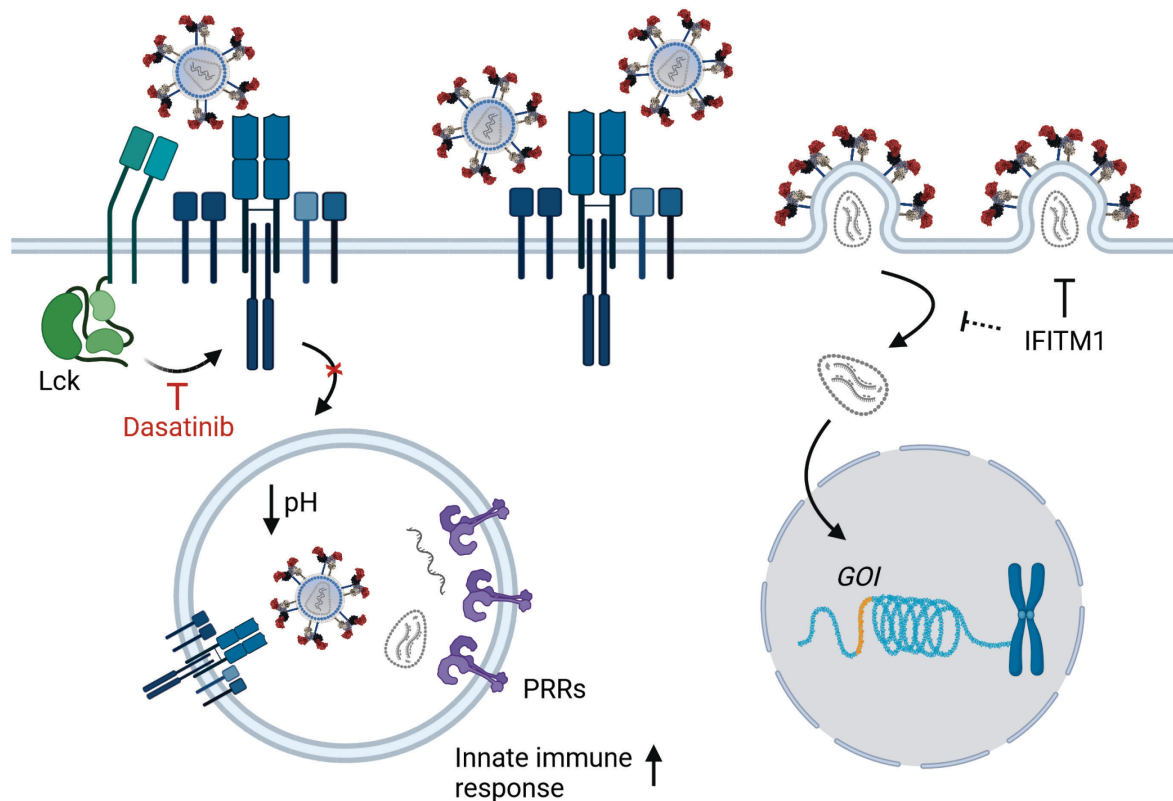


Figure 49: Evasion of cellular restriction mechanisms in presence of dasatinib.

The inhibition of Lck by dasatinib blocks phosphorylation of ITAMs and thereby CD3:TCR downregulation. This prevents endocytosis of vector particles together with the receptor complex and subsequent detection by pattern recognition receptors (PRRs) in the endosome, which activates the innate immune response. Instead, the attachment of more vector particles to the cell surface, allows more particles to fuse with the cell membrane, potentially evading restriction factors (dashed line), such as IFITM-1, and enabling integration of the gene of interest (GOI) into the genome.

Because of these host-vector interactions, effective transduction with LVs requires a high vector dose and prolonged *ex vivo* cultivation (Kajaste-Rudnitski & Naldini, 2015; Petrillo et al., 2018). The application of a high viral particle load over a prolonged period of time may overwhelm the cell's innate regulatory mechanisms and allow evasion of RFs to some extent. Dasatinib increased the amount of particles that bound to and thus were able to fuse with the cell (Section 2.2.4), helping outcompete limiting factors that may inhibit successful transduction. By preventing early downregulation of the CD3:TCR complex in presence of dasatinib, CD3-LVs that might be endocytosed

with the receptor complex and recognized by PRRs, can instead bind to a greater number of available target receptors on the cell surface, helping to overcome other RFs (Figure 49). The immunomodulatory effects of dasatinib might additionally reduce PRRs-induced innate immune response upon encountering LVs, inhibiting downstream signaling and the secretion of inflammatory cytokines. This would also explain the reduced secretion of inflammatory cytokines of CAR T cells generated in presence of dasatinib, independent of VSV- or CD3-LV transduction (Section 2.3.3).

This work highlights the importance of target receptor availability for successful transduction with CD3-LV. The inhibition of CD3:TCR downregulation by dasatinib, allows more CD3-LV particles to bind to and fuse with the cell, helping to evade RFs that limit successful transduction.

3.2 Towards better CAR T cells

3.2.1 Improved CAR T cell manufacturing using CD3-LV with dasatinib

As the demand for CAR T cell therapies increases, there is a growing need to improve manufacturing platforms. The current challenges of CAR T cell manufacturing cannot be solved with a single approach, but addressing the different steps could collectively contribute to its overall improvements in terms of speed, quality, and safety.

For genetic modification of the T cells, four of the six authorized CAR T cell products use VSV-LV as gene delivery tool, due to its high stability and good transduction efficiency (Irving et al., 2021). VSV-LV utilizes the LDL receptor, which is ubiquitously expressed on nearly all cells, including B cells, but is present only at low levels on resting T cells (Amirache et al., 2014; Finkelshtein et al., 2013). Therefore, transduction is preceded by extensive T cell isolation and proper T cell activation to ensure efficient and exclusive T cell transduction (Vormittag et al., 2018). Transduction of a single leukemic cell has been shown to cause CAR T cell resistance, followed by relapse and death of the patient, upon transduction of a single leukemic cell (Ruella et al., 2018). Though this does not occur frequently, the remaining risk along with extensive isolation and activation procedures can be omitted with the use of T cell-targeted vectors. The use of T cell-targeted LVs for the clinical generation of CAR T cells has been limited by the rather low transduction efficiencies. This thesis provides a new method to enhance transduction efficiency for CAR T cell generation using T cell-targeted LVs.

The use of dasatinib during CD3-LV incubation with the cells overcomes the low transduction efficiency, allowing the generation of 45% CD19.CAR T cells on average (Section 2.3.1). Transduction with CD3-LV in presence of dasatinib was highly selective for T cells, providing an additional level of safety during CAR T cell generation. In combination with the commercially available transduction enhancer VF-1, transduction with CD3-LV generated up to 75% CAR T cells, comparable to levels achieved with VSV-LV (Section 2.3.1).

An additional limitation is the long manufacturing time together with the manufacturing process itself, which accelerates differentiation, exhaustion and senescence of the cells (Abou-El-Enein et al., 2021; Ghassemi et al., 2018; Watanabe et al., 2022). During transduction, the properties of the applied vectors, in this case CD3-LV, which stimulates and activates the cells by binding to the CD3:TCR complex, influence differentiation and exhaustion of the cells. Alone the exposure of the cells to LVs have shown to alter gene expression profiles even when the cell is not transduced, upregulating among others apoptosis- and exhaustion-related genes, regardless of the receptor targeted (Charitidis, 2023; Charitidis et al., 2023).

Although dasatinib was solely present for five hours during incubation of the cells with vector, it nevertheless reduced the expression of exhaustion markers and altered the T cell phenotypes (Section 2.3.3.1). Dasatinib not only prevented receptor-induced stimulation during its incubation time with the cells, in the case of CD3-LV, but also partially prevented exhaustion induced by the exposure of the cells to LVs (VSV- or CD3-LV) (Section 2.3.3.2). This is evidenced by the reduced expression of exhaustion markers and reduced secretion of inflammatory cytokines by CD3- and VSV-LV generated CAR T cells, not only after cultivation, but also after tumor cell killing (Section 2.3.3.2 and 2.3.3.3). Thus, in addition to preventing TCR-induced stimulation, dasatinib may also limit signaling pathways induced by the cell's innate immune system upon contact with HIV-1-derived viral vectors.

Others have used dasatinib in the context of CAR T cells for different purposes. It was employed to regulate CAR T cell activity and function, by inhibiting the phosphorylation of the CD3 ζ signaling domain of the CAR construct (Mestermann et al., 2019). The presence of dasatinib was shown to inhibit cytolytic activity, cytokine secretion and proliferation, and was therefore proposed as an on/off switch for

CAR T cells (Mestermann et al., 2019; Weber et al., 2021). When using dasatinib as an on/off switch, it can help counteract the development of CRS upon CAR T cell infusion (Mestermann et al., 2019). Also, the induction of rest from tonic CAR signaling by dasatinib was shown to reverse exhaustion and induce transcriptional reprogramming of differentiated CAR T cells, significantly improving CAR T cell fitness (Weber et al., 2021). Likewise, dasatinib was used to prevent fratricide during manufacturing of CAR T cells directed towards T cell antigens, which improved effector function *in vitro* and *in vivo* (Hebbar et al., 2022). The use of dasatinib as transduction enhancer during the production of CAR T cells can be easily combined with its further use as pharmacological control. The implementation of CD3-LV in combination with dasatinib would provide an additional level of safety, yield high levels of CAR T cells and reduce transduction-induced exhaustion of the product.

In summary, this thesis shows that dasatinib enhances CAR gene delivery by CD3-LV and achieves similar CAR T cell levels as with VSV-LV, thus reducing the barriers to clinical translation.

3.2.2 CAR T cell subset and phenotype

The quality and composition of the CAR T cell product strongly influence the function and therapeutic efficacy. Therefore, much research is devoted to determining the optimal CAR T cell composition in terms of T cell subset and phenotype (Sommermeyer et al., 2016; Turtle et al., 2016).

Initially, CD8⁺ CAR T cells were thought to be the favorable T cell subset for CAR T cell generation, due to their effector functions and cytotoxic capabilities, while CD4⁺ CAR T cells were thought to solely confer helper functions. More recently, CD4⁺ CAR T cells were described to have direct cytotoxic activity, capable of mediating antitumor response (Agarwal et al., 2020). When combining both, a defined composition of CD4⁺ and CD8⁺ CAR T cells exhibited superior antitumor activity compared to CD4⁺ or CD8⁺ CAR T cells alone. The synergy between CD4⁺ and CD8⁺ CAR T cells enhanced efficacy in mouse models (Sommermeyer et al., 2016) and clinical trials (Turtle et al., 2016). These findings support CD3-LV as CAR gene delivery vector because it allows the generation of both CD4⁺ and CD8⁺ CAR T cells, while remaining exclusive to CD3⁺ T cells.

Great initial response rates of CAR T cells are often hampered by limited engraftment and reduced persistence of the cells, associated with a highly differentiated and exhausted T cell phenotype (Fraiatta et al., 2018). This is even more critical in the treatment of solid tumors, where successful infiltration and sustained antitumor activity in an immunosuppressive environment are required (Jung et al., 2023; Tantaló et al., 2021). The use of ideal T cell phenotypes for clinical applications is thought to overcome current limitations of inefficient T cell engraftment, reduced persistence, and insufficient immune attack in adoptive T cell transfer (Gattinoni et al., 2012; Gattinoni et al., 2017). Originally, T_{EFF} cells were considered to have the optimal phenotype for CAR T cell therapy, due to their high effector function and killing capacity (Tantaló et al., 2021). Instead, the poor expansion and persistence of T_{EFF} cells prevents long-term antitumor activity, and less differentiated T cells have been shown to be superior in tumor suppression (Fraiatta et al., 2018). A phenotype with the ability to self-renew and persist, traffic to and penetrate the site of disease and exert cytotoxic function while resisting exhaustion, would be ideal and is reflected by T_{SCM} cells. T_{SCM} cells are minimally differentiated cells with stem-like attributes and the ability to self-renew and differentiate into T_{CM}, T_{EM} and T_{EFF} cells (Gattinoni et al., 2012; Gattinoni et al., 2011). A clinical trial revealed that the amount of CAR T_{SCM} cells positively correlates with the *in vivo* expansion and clinical response of the CAR T cells (Biasco et al., 2021; Xu et al., 2014).

However, the clinical exploitation of T_{SCM} cells has been hindered by the lack of manufacturing protocols (Tantaló et al., 2021). By developing a clinical-grade production of CAR T_{SCM} cells, (Sabatino et al., 2016) were able to demonstrate the enhanced metabolic fitness of CAR T_{SCM} cells, with superior and more durable antitumor responses compared to conventional CAR T cells. Given the high therapeutic potential of T_{SCM} cells, various methods have been employed to enhance their abundance. The cultivation of sorted naïve T cells in medium containing IL-7/15 instead of IL-2 enriched the amount of T_{N/SCM} cells from 30% to 60% (Cieri et al., 2013). Further procedures based on cell sorting, enrichment, and epigenetic reprogramming resulted in high frequencies of CAR T_{SCM} cells with superior antitumor activity upon repeated exposure, increased proliferation *in vivo*, and less tendency to induce CRS, but added a costly and time-consuming step to the manufacturing process (Arcangeli et al., 2022; Arcangeli et al., 2020; Jung et al., 2023; Meyran et al., 2023).

Mitochondrial dynamics alter T cell phenotype and function (Buck et al., 2016), and reduced mitophagy activity in tumor-infiltrating lymphocytes has shown to cause terminal exhaustion of the cells (Yu et al., 2020). The natural metabolite of elagitannins, urolithin A (UA), induces mitophagy *in vivo*, slowing the progression of aging-related diseases and having immunomodulatory effects (D'Amico et al., 2021; Toney et al., 2021). Recent results have shown that UA can enhance antitumor immunity and the efficacy of adoptive T cell transfer in distinct mouse models by promoting T_{SCM} cell expansion (Denk et al., 2022). When applied to human T cells, UA also increased the frequencies of human T_{SCM} cells as determined by cell surface expression. Induction of mitophagy by UA was shown to drive T cell differentiation into T_{SCM} cell subsets, linking mitochondrial dynamics and adaptive immunity. Despite these previous findings, it was surprising to see how much UA affects CAR T cell phenotypes.

The application of UA during the generation of CAR T cells promoted the expansion of the T_{SCM} phenotype by up to 10-fold, resulting in 20-60% T_{SCM} cells (Section 2.4.1 and 2.4.2), thus increasing the expansion to higher levels than previously observed with IL-7/15 cultivation alone (Cieri et al., 2013). Its use is simple. UA solely needed to be supplemented to the medium during cultivation and expansion of the CAR T cells. The presence of UA did not affect the generation of CAR T cells nor did the shift in phenotype influence the killing ability of CD19.CAR T cells or CEA.CAR T cells (Section 2.4.1 and 2.4.2). This method describes a readily applicable way of rapidly generating potent CAR T_{SCM} cells, bypassing common manufacturing challenges.

Thus, the finding of this thesis was that UA induces high levels of the favorable CAR T_{SCM} cells by solely incubating the cells in UA-containing medium.

3.3 Combining small molecules with CAR T cell therapy

Combining two or more therapeutic agents to treat one condition is known as combination therapy. In the CAR T cell field, combination therapy aims to improve the efficacy of CAR T cell therapy and overcome some of its limitations. Common combination therapies with CAR T cells are oncolytic viruses and immune checkpoint inhibitors. Oncolytic viruses can selectively infiltrate and infect tumor cells, acting as a vaccine by presenting tumor-associated antigens (TAA), or deliver therapeutic genes that are expressed to reinforce the cytotoxic activity of CAR T cells (Al-Haideri et al., 2022; Rezaei et al., 2022). The combination with immune checkpoint inhibitors can

sustain persistence and function of CAR T cells by blocking inhibitory signals and reactivating the exhausted immune response (Sterner & Sterner, 2021). These approaches are particularly useful in the immunosuppressive microenvironment of solid tumors and open new possibilities for more successful cancer treatment. In addition, immunomodulatory agents and metabolic inhibitors have been suggested to increase the proliferation, persistence, and cytokine secretion of CAR T cells, thereby helping the cells to adapt and efficiently function in the tumor microenvironment (Al-Haideri et al., 2022).

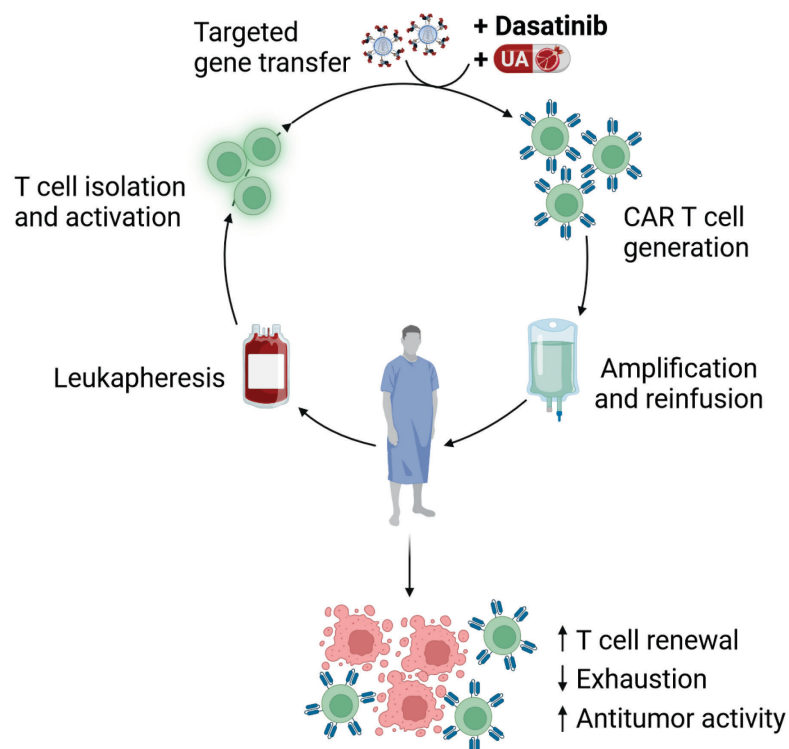


Figure 50: Small molecules for the refined generation of CAR T cells.

Proposed manufacturing of CAR T cells in which the genetic modification is performed using CD3-LV in the presence of dasatinib, to achieve selective and efficient transduction of T cells. Cells are cultivated in presence of urolithin A (UA), resulting in less exhausted CAR T cells with the ability to self-renew and maintain antitumor activity.

The approach proposed here, differs principally from the combination therapies described above in that dasatinib and UA are used during manufacturing. While most combination therapies promote the function of finalized CAR T cells in the microenvironment, dasatinib and UA are thought to create better CAR T cells to begin with. Transduction of PBMCs with CD3-LV in presence of dasatinib facilitated efficient and selective CAR gene transfer to T cells, generating high numbers of CAR T_{SCM} cells upon cultivation with UA (Section 2.4.2). Transduction in presence of dasatinib

mediated a slightly more naïve T cell phenotype before and after killing, while the additional cultivation with UA significantly increased the frequency of T_{SCM} cells that predominantly differentiated into T_{EM} cells upon tumor cell encounter and killing. The high proportion of T_{SCM} cells after UA treatment did not affect *in vitro* killing efficacy, nor did the transduction regimes used to generate the CAR T cells (Section 2.4.2). The superior antitumor activity described for CAR T_{SCM} cells is mainly based on increased proliferative capacity and persistence upon rechallenge *in vivo*, which awaits conformation here.

The implementation of dasatinib and UA in combination with CAR T cell therapy should be straightforward, as both molecules are safe and functional when administered orally in humans (Andreux et al., 2019; Kamath et al., 2008). The combination of these therapeutic molecules during the manufacturing of CAR T cells could make the process faster and safer, generating less exhausted CAR T cells with high antitumor activity and the ability to self-renew (Figure 50). In addition, this approach is well compatible with the further use of UA as immunomodulatory or dasatinib as pharmacological control after CAR T cell infusion. In the future, small molecules such as dasatinib and UA might be able to improve not only *ex vivo* manufacturing but also *in vivo* generation of CAR T cells using receptor-targeted vectors (Michels et al., 2022).

While the use of dasatinib and UA during the generation of CAR T cells using receptor-targeted LVs is unlikely to solve all the limitations of CAR T cell therapy, it represents a viable approach to facilitate gene delivery and the generation of a favorable CAR T cell phenotype, thereby further improving the therapeutic outcome.

4 Material and methods

4.1 Material

4.1.1 Chemicals and reagents

Name	Supplier
4Cell® Nutri-T medium	Sartorius
Acridine Orange/Propidium Iodide Stain	Logos biosystem
Ammoniumchloride (0.86%)	Paul-Ehrlich-Institut
Bosutinib	Selleckchem
Bafilomycin A1 (Bfla1)	Santa Cruz
BD PharmLyse™	BD Biosciences
Biguacid plus	Antiseptica
Bovine serum albumin (BSA)	Sigma-Aldrich
Dasatinib	Selleckchem
Dimethyl sulfoxide (DMSO), 99.9% p.a.	AppliChem GmbH
Dulbecco's Modified Eagle Medium (DMEM), high glucose	Biowest
Ethylenediaminetetraacetic acid (EDTA)	Paul-Ehrlich-Institut
Fetal bovine serum (FBS)	Sigma-Aldrich
Fc receptor (FcR) blocking reagent, human	Miltenyi Biotec
Formaldehyde	Sigma-Aldrich
Genistein	Selleckchem
H ₂ O, cell culture grade	Sigma-Aldrich
Histopaque®-1077	Sigma-Aldrich
Human IL-15, research grade	Miltenyi Biotec
Human IL-7, research grade or premium grade	Miltenyi Biotec
Imatinib	Selleckchem
Isoflurane CP	CP-Pharma
L-glutamine (200 mM)	Sigma-Aldrich
MACSQuant® Buffers (Running, Wash, Storage)	Miltenyi Biotec
N-2-hydroxyethylpiperazine-N'-2-ethanesulfonic acid (HEPES)	Sigma-Aldrich
Pancoll	PAN-Biotech

PBS, without (w/o) Mg ²⁺ /Ca ²⁺	Lonza, Paul-Ehrlich-Institut
Polyethylene glycol (PEG) 300	Sigma-Aldrich
Penicillin/streptomycin (P/S)	Paul-Ehrlich-Institut
Polyethyleneimine, branched, 25 kDa	Sigma-Aldrich
RPMI 1640 medium	Biowest
Sodium azide (NaN ₃) solution, 10%	Paul-Ehrlich-Institut
Sucrose	Sigma-Aldrich
Terralin®	Schülke & Mayr
Trypan blue	Sigma-Aldrich
Trypsin (Melnick, 2.5% solution)	Paul-Ehrlich-Institut
Tween™ 80	Sigma-Aldrich
UltraComp eBeads™ compensation beads	Thermo Fisher Scientific
Urolithin A	Tocris
Vectofusin-1	Miltenyi Biotec

4.1.2 Kits

Name	Supplier
CellTrace™ Violet Cell Proliferation Kit	Thermo Fisher Scientific
Customized LEGENDplex™ Multiplex Assay Kit	BioLegend
DNeasy® Blood and Tissue Kit	Qiagen
Fixable Viability Dye, eFluor™ 780	Thermo Fisher Scientific
LightCycler® 480 Probes Master, 2X	Roche

4.1.3 Buffers and solutions

Name	Formulation
Blocking solution	2% BSA in PBS
FACS fix buffer	1% formaldehyde in PBS
FACS wash buffer	2% FBS, 0.1% NaN ₃ in PBS
Sucrose solution	20% (w/v) sucrose in PBS
Transfection reagent	18 mM branched polyethyleneimine in H ₂ O
Trypsin/EDTA	0.25% trypsin, 1% EDTA in PBS

4.1.4 Cell culture media

Name	Formulation
DMEM complete	DMEM supplemented with 10% FBS, 2 mM L-glutamine
Cryopreservation medium	10% DMSO, 90% FBS
NutriT medium	4Cell® Nutri-T medium containing 0.4% penicillin/streptomycin
RPMI complete	RPMI 1640 supplemented with 10% FBS, 2 mM L-glutamine
T cell medium (TCM)	RPMI complete containing 25 nM HEPES, 0.4% penicillin/streptomycin

4.1.5 Cell lines

Name	Description	Source	Culturing medium
HEK-293T	Human embryonic kidney cell line, transformed to express the SV40 large T antigen	ATCC, CCL-11268	DMEM complete
Lenti-X-293T	HEK-293T cell clone selected for susceptibility towards transfection and efficient protein expression	Takara Bio Europe	DMEM complete
HEK-293T β 2M ^{-/-} CD47 ^{high}	HEK-293T knocked-out for β 2 microglobulin and overexpressing human CD47	(Milani et al., 2019)	DMEM complete
Jurkat E6.1 (JE6.1)	Human T lymphoblast cell line, clone E6.1; CD3 ⁺ CD4 ⁺ CD8 ⁻	ATCC, TIB-152	RPMI complete
LS174T	Epithelial cell line from a Duke's type B adenocarcinoma of the colon	DSMZ, ACC-759	DMEM complete
Molt4.8	Human T lymphoblast cell line, clone 4.8; CD3 ⁺ CD4 ^{dim} CD8 ⁺	A.Pfeiffer, PEI	RPMI complete
Nalm-6	Human adult acute lymphoblastic leukemia cell line	ATCC, CRL-3273	RPMI complete

4.1.6 Antibodies

Marker	Fluorophore	Clone	Dilution	Supplier
anti-CD3	PerCP	BW264/56	1:200	Miltenyi Biotec
anti-CD4	VioBlue	VIT4	1:200	Miltenyi Biotec
anti-CD4	APC	VIT4	1:100	Miltenyi Biotec
anti-CD4	PE-Vio770	VIT4	1:200	Miltenyi Biotec
anti-CD8	APC	BW135/80	1:200	Miltenyi Biotec

anti-CD8	PE	RPA-T8 (RUO)	1:100	BD Pharmingen
anti-CD8	PerCP-Cy5.5	RPA-T8	1:200	BD Bioscience
anti-CD19	APC	LT19	1:100	Miltenyi Biotec
anti-CD19	PE-Vio770	LT19	1:100	Miltenyi Biotec
anti-CD25	PE-Vio770	REA570	1:100	Miltenyi Biotec
anti-CD45	BV421	5B1	1:100	Miltenyi Biotec
anti-CD45RA	VioBlue	T6D11	1:100	Miltenyi Biotec
anti-CD45RO	APC	UCHL1	1:100	Miltenyi Biotec
anti-CD62L	PE-Vio770	145/15	1:100	Miltenyi Biotec
anti-CD223(LAG-3)	VioBlue	REA351	1:100	Miltenyi Biotec
anti-CD271(LNGFR)	FITC	ME20.4-1.H4	1:200	Miltenyi Biotec
anti-CD279(PD-1)	PE-Vio770	PD1.3.1.3	1:100	Miltenyi Biotec
anti-CD366(TIM-3)	APC	REA635	1:100	Miltenyi Biotec
anti-His	PE	GG11-8F3.5.1	1:50	Miltenyi Biotec
anti-myc	FITC	SH1-26e7.1.3	1:200	Miltenyi Biotec
anti-TCR	BV421	IP26	1:100	Biolegend
Isotype controls	-	-	-	Miltenyi Biotec, BD Bioscience, Biolegend
Pure anti-CD3	OKT-3		1:100	Miltenyi Biotec
Pure anti-CD28	15E8		1:33	Miltenyi Biotec

4.1.7 Plasmids

Number	Name	Description	Source
P1.01-01	pCMVΔR8.9	HIV-1 packaging plasmid	U. Blömer (Zufferey et al., 1998)
P1.07-01	pMD2.G	Encodes the glycoprotein G of VSV	D. Trono
P2.01-01	pSEW-GFP	HIV-1 transfer vector encoding GFP	M. Grez (Demaison et al., 2002)
P2.01-06	pS-CD19.CAR(28z)-W	HIV-1 transfer vector encoding the CD19.CAR	W. Wels (Oelsner et al., 2017)
P2.01-34	pS-CEA.CAR(28z)-fP2A-dLNGFR	HIV-1 transfer vector encoding the CEA.CAR	(Hombach et al., 2001)
P4.01-04	pHnse-DARPin-CD4.29.2	Encodes MV-HΔ18 fused to the CD4 specific DARPin 29.2	(Zhou et al., 2015)
P4.04-01	pCG-Fnse-Δ30	Encodes MV-FnseΔ30	(Funke et al., 2008)

P4.09-01	pCAGGS-NiV-FΔ22	Encodes NiV-FΔ22	(Bender et al., 2016)
P4.07-02	pCG-NiV-GΔ34 ^{OKT-8}	Encodes the engineered NiV ΔGmut protein in conjunction with the OKT-8-derived CD8-specific scFv	(Bender et al., 2016)
P4.11-16	pCG-NiV-GΔ34 ^{TR66}	Encodes NiV ΔGmut in conjunction with the CD3-specific TR66 scFv	(Frank et al., 2020)
P4.11-20	pCG-NiV-GΔ34 ^{TR66.opt}	Encodes NiV ΔGmut in conjunction with the CD3-specific TR66.opt scFv	(Frank et al., 2020)
P4.11-23	pCG-NiV-GΔ34 ^{HuM291}	Encodes NiV ΔGmut in conjunction with the CD3-specific HuM291 scFv	(Frank et al., 2020)
P2.0-12	pS-Albumin-W	HIV-1 transfer vector encoding WPRE and human albumin as qPCR standard	F. Thalheimer, PEI

4.1.8 Oligonucleotide primers

Number	Name	Sequence (5'-3')
4001	Albumin probe	[6-FAM]-ACG TGA GGA GTA TTT CAT TAC TGC ATG TGT-[BHQ1]
4002	Albumin forward	CAC ACT TTC TGA GAA GGA GAG AC
4003	Albumin reverse	GCT TGA ATT GAC AGT TCT TGC TAT
4020S	WPRE forward	CAC CAC CTG TCA GCT CCT TT
4021S	WPRE reverse	GGA CGA TGA TTT CCC CGA CA
5007	WPRE probe	[Cy5]-CGC CGC CTG CCT TGC CCG CT-[BHQ2]

4.1.9 Consumables

Name	Supplier
BD Micro-Fine™ Insulin syringes (29 gauge)	BD Biosciences
BD Microtainer® Blood Collection Tubes, Lithium Heparin	BD Biosciences
BD Vacutainer® CPT™ Mononuclear Cell Preparation Tubes	BD Biosciences
BD Vacutainer® Safety-Lok Blood Collection Set	BD Biosciences
Cell strainer (40 μm, 70 μm)	Corning
CellStar® conical centrifuge tubes, 15 mL and 50 mL	Greiner Bio-One
Centrifuge tubes, 225 mL	VWR
Cryovial, 2 mL	Greiner Bio-One

E-plates 16	Agilent
Frame Star 96 well plate, Roche style	4titude
LoBind, DNA tubes 1.5 mL	Eppendorf
LoBind, protein tubes 1.5 mL	Eppendorf
Micro-centrifuge tubes, 1.5 mL, 2 mL	Eppendorf
Pasteur pipet, glass, 14.6 cm	VWR
Petri dish, \varnothing 10 cm	Greiner Bio-One
Pipet tips, filtered (10 μ L, 100 μ L, 300 μ L, 1000 μ L)	Biozym
Pipette tips (no filtered)	Sarstedt
Rapid-Flow Bottle Top Filter 0.45 μ m SFCE 500 mL	Thermo Fisher Scientific
Serological pipets (5 ml, 10 ml, 25 ml)	Greiner Bio-One
Syringe filters, Minisart, PTFE (0.45 μ m, 0.2 μ m)	Sartorius
Tissue culture flask (T25, T75, T125)	Greiner Bio-One
Tissue culture plates (6-, 12-, 24-, 48-, 96-well)	Thermo Fisher Scientific
Tubes 1.4 mL	Micronic

4.1.10 Instruments

Name	Company
Cell incubator BBD6220	Heraeus, Thermo Fisher Scientific
Centrifuge multifuge X3	Heraeus, Thermo Fisher Scientific
Freezer (-20°C, -80°C)	New Brunswick, Liebherr, Thermo Fisher Scientific
Fridge	AEG
MACS Quant Analyzer 10 flow cytometer	Miltenyi Biotec
Micropipets research plus®	Eppendorf
Microscopes	Carl Zeiss, Echo
Mr. Frosty™ Freezing container	Nalgene
Multichannel pipets	Thermo Fisher Scientific
NanoDrop™ 2000	Thermo Fisher Scientific
NanoSight™ NS300	Malvern Pananalytic
Nitrogen tank Chronos, Apollo	Messer
Orbital shaker	Celltron
Pipetboy Accu-jet	Brand
Pump Vacusafe	Integra

Spectrophotometer NanoDrop 2000c	Thermo Fisher Scientific
Table centrifuge	Heraeus
Table-top shaker Biometra® WT12	Biometra
Vortex Mixer Vortex Genie® 2	Scientific Industries
XGI-8 Gas Anesthesia system	Perkin Elmer

4.1.11 Software

Name	Company
BioRender	Science Suite Inc.
Citavi 6	Swiss Academic Software
FCS Express, Version 6	De Novo Software
GraphPad Prism 9	GraphPad Software
LEGENDplex™ Data Analysis Software, Version 8	BioLegend
LightCycler® Software 4.1	Roche
Microsoft Office 2016	Microsoft
NTA, Version 3.3	Malvern Pananalytic

4.2 Methods

4.2.1 Molecular biology

4.2.1.1 Isolation of genomic DNA

Genomic DNA was isolated from cell pellets derived from mouse organs and blood using the DNeasy® Blood and Tissue kit (Qiagen) according to the manufacturer's protocol. After isolation, DNA was eluted in 50-100 µL of elution buffer and genomic DNA concentration was determined by UV/Vis spectroscopy using the NanoDrop 2000 spectrophotometer.

4.2.1.2 Quantitative polymerase chain reaction

Quantitative polymerase chain reaction (qPCR) was used to determine the amount of transgene integration per genomic copy of the transduced cells to determine the

vector copy number (VCN). Therefore, a TaqMan-based qPCR assay was performed using the LightCycler® 480 Probes Master kit and analyzed using the LightCycler480® Instrument II (Roche). This method allows the precise measurement of target DNA sequences using fluorescently labelled complementary probes specific for the target sequence. Transgene integration was identified using WPRE-specific primers, while primers specific for the human albumin gene served as an internal reference. Both the WPRE and human albumin were assessed simultaneously in technical duplicates within the same well. The reaction was prepared as described in Table 1 and executed with the following PCR conditions: 1x 95°C for 5 min; 45 cycles of [95°C for 10 sec and 60°C for 40 sec], and subsequently kept cool at 4°C.

The standard curve determined with pS-Albumin-W, which contains one copy of human albumin and one of WPRE, was used to calculate the number of cells and vector integrations. VCN was subsequently calculated as ratio of (copies of WPRE/copies of human albumin). For standardization, all qPCR reactions were performed by the experienced technical staff member Manuela Gallet.

Table 1: Quantitative polymerase chain reaction mixture

Component	Amount
Genomic DNA	50-100 ng
WPRE forward	0.2 µM
WPRE reverse	0.2 µM
WPRE probe	0.2 µM
Human albumin forward	0.2 µM
Human albumin reverse	0.2 µM
Human albumin probe	0.2 µM
LightCycler® 480 Probes Master	1x

4.2.2 Cell culture

4.2.2.1 Freezing and thawing of cells

For freezing of cells, the respective number of cells was centrifuged for 3 min at 350 x g and subsequently resuspended in 1 mL freezing medium (10% DMSO and 90% FBS). The cells were aliquoted in cryovials and transferred to precooled

Mr. Frosty™ containers. These were frozen overnight at -80°C, and the next day the vials were transferred to the liquid nitrogen tank for long-term storage.

For thawing of cells, the cryovials were removed from the liquid nitrogen tank and transferred to a 37°C water bath for a few minutes. The cells were then transferred to 10 mL prewarmed medium, washed twice by centrifugation at 350 x g for 3 min and cultured under appropriate conditions.

4.2.2.2 Cultivation of cell lines

All cells were cultivated at 37°C, 5% CO₂ and 90% humidity and handled under sterile conditions under a laminar flow hood. Adherent cells, including HEK-293T and LS174T cells, were cultivated in Dulbecco's Modified Eagle's Medium (DMEM) supplemented with 10% FBS and 1% L-glutamine (DMEM complete) and split twice a week at a 1:10 ratio. Therefore, the medium was removed, the cells were washed with 10 mL of PBS and detached using 3 mL 0.25% trypsin solution.

Suspension cells, such as Jurkat E6.1 (JE6.1), Molt4.8 and Nalm-6 cells, were cultured in RPMI 1640 supplemented with 10% FBS and 1% L-glutamine (RPMI complete) and split to 1x10⁵ cells/mL three times a week by gentle resuspension.

4.2.2.3 Lentiviral vector production

For the production of lentiviral vectors (LVs), 1.7-2.0x10⁷ HEK-293T cells, Lenti-X-293T or β2M^{-/-}CD47^{high} HEK-293T cells were seeded into T175 flask or 15 cm dishes in 18 mL DMEM complete. The next day, the medium was removed and replaced with 10 mL of DMEM complete supplemented with an additional 5% FBS, prior to plasmid transfection. The plasmid transfection mix was prepared in 2.3 mL DMEM without additives with a total amount of 35 μg DNA (Table 2) and thoroughly mixed with 2.2 mL DMEM without additives containing 140 μL polyethyleneimine (PEI). The plasmid transfection mix was incubated for 10 min at room temperature (RT) and subsequently added to the production cells. After 6-16 hours of incubation at 37°C, the transfection mix was removed from the cells and replaced with 18-20 mL DMEM complete. The cells were further cultivated at 37°C for 48 h. The supernatant containing the released vector particles was harvested after two days and filtered through a 45 μm filter before concentration by centrifugation at 4500 x g for 24 h at 4°C through a

20% sucrose cushion (*w/v* in PBS). After centrifugation, the supernatant was discarded, the pellet was resuspended in 60 μ L PBS and stored at -80°C for later use.

Table 2: Plasmids for lentiviral vector production

	Transfer	Packaging	Envelope
CD3-, CD4-, CD8-LV(GFP)	pS-GFP (15.1 μ g)	pCMVdR8.9 (14.4 μ g)	pCG-NiV-G Δ 34 ^{scFv} (0.9 μ g) pCAGGS-NiV-F Δ 22 (4.5 μ g)
VSV-LV(GFP)	pS-GFP (11.4 μ g)	pCMVdR8.9 (17.5 μ g)	pMD2.G (6.1 μ g)
CD3-LV(CAR)	pS-mycCD19.CAR(28z) or pS-CEA.CAR(28z)-dLNGFR (15.1 μ g)	pCMVdR8.9 (14.4 μ g)	pCG-NiV-G Δ 34 ^{scFv} (0.9 μ g) pCAGGS-NiV-F Δ 22 (4.5 μ g)
VSV-LV(CAR)	pS-mycCD19.CAR(28z) or pS-CEA.CAR(28z)-dLNGFR (11.4 μ g)	pCMVdR8.9 (17.5 μ g)	pMD2.G (6.1 μ g)

4.2.2.4 Titration and particle number detection

The LVs were characterized by their titer determined as transducing units per milliliter (T.U./mL) and their particle concentration. To determine the titer, 4×10^4 cells, either cell lines such as Molt4.8 and JE6.1 or activated PBMCs, were transduced with 5-fold serial dilutions of LV starting with the highest dose of 5 μ L. After three days, the transduction efficiency was determined by flow cytometry. The LV dilutions showing a linear correlation to the number of transduced cells were used to calculate the titer.

To determine the particle numbers, p24 enzyme-linked immunosorbent assay (ELISA) (ZeptoMetrix Corporation) following manufacturer's instruction was used or nanoparticle tracking analysis was performed. The p24 antigen ELISA was used to determine the amount of p24 in the vector stocks and was calculated on the assumption that 1 μ g of p24 proteins corresponds to 1.81×10^{10} viral particles (based on: 2000 p24 molecules per LV and 25.587 kDa per p24). For standardization, all p24 ELISAs were performed by the experienced technical staff member Julia Brynza. For nanoparticle tracking analysis using the NanoSightTM NS3000 instrument (Malvern Pananalytic), the vector stocks were diluted in 0.2 μ m sterile filtered PBS to reach concentrations of 1×10^7 - 1×10^9 particles/mL. The suitable dilutions were loaded into the chamber and measured four times for 60 seconds at 25°C using a custom stop-flow protocol. The NTA3.3 software (Malvern Pananalytic) was used to identify the particles

and determine their size and concentration. The characteristics of the stocks used in this thesis are listed in Table 3.

Table 3: Characteristics of LVs

Vector	Titer (T.U./mL)	Particle Nr./mL	Particles/5 μ L
CD3-LV(GFP)	5x10 ⁶ (on PBMCs) 1x10 ⁶ (on JE6.1)	4-6x10 ¹²	2-3x10 ¹⁰
CD4-LV(GFP)*	6.4x10 ⁶ (on Molt4.8)	-	-
CD8-LV(GFP)	4.15x10 ⁹ (on Molt4.8)	5x10 ¹²	2x10 ¹⁰
VSV-LV(GFP)*	2-3x10 ⁹ (on Molt4.8)	1-2x10 ¹²	0.5-1x10 ¹⁰
CD3-LV(CD19.CAR)	1x10 ⁶ (on PBMCs)	2x10 ¹²	1x10 ¹⁰
CD3-LV(CEA.CAR)*	4x10 ⁶ (on PBMCs)	2x10 ¹²	1x10 ¹⁰
VSV-LV(CD19.CAR)*	5x10 ⁸ (on PBMCs)	1x10 ¹²	5x10 ⁹
VSV-LV(CEA.CAR)*	2x10 ⁹ (Molt4.8)	1x10 ¹²	5x10 ⁹

*Include vector stocks and data provided by former colleagues Annika Frank, Lea Scheib, Naphang Ho and Johanna Gorol.

4.2.2.5 Isolation of human primary blood mononuclear cells

Human peripheral blood mononuclear cells (PBMCs) were isolated from blood of anonymous donors or from buffy coats acquired from DRK Blutspendedienst Baden-Württemberg-Hessen. PBMCs were isolated by density gradient centrifugation using Histopaque®-1077 or Pancoll human gradient or BD Vacutainer® CPT™ tubes according to the manufacturer's instructions. For isolation by density centrifugation, blood was mixed in a 1:1 ratio with PBS and slowly layered onto cold Histopaque®-1077 or Pancoll. The tubes were centrifuged at 1800 rpm and RT for 30 min without brakes, to allow separation of the blood components and the formation of the lymphocyte layer above the Histopaque®-1077 or Pancoll. After centrifugation, the PBMC layer was carefully removed and transferred to a fresh tube where it was resuspended in PBS. PBMCs were pelleted by centrifugation at 300 x g for 10 min and subsequently resuspended in fresh PBS and centrifuged at 200 x g for 10 min for platelet removal. If necessary, the cell pellet was incubated with ammonium chloride (0.86%) for 15-10 min at 37°C to remove residual erythrocytes. Next, the cells were washed twice with PBS by centrifugation for 10 min at 300 x g. Finally, cell numbers were determined and PBMCs were either taken into culture (Section 4.2.2.6) or cryopreserved (Section 4.2.2.1) for later use.

4.2.2.6 Activation and cultivation of human PBMCs

For activation, a 6- or a 24-well plate was coated with 1 µg/mL αCD3 (clone OKT-3) in PBS for two hours at 37°C or overnight at 4°C. After coating, the plate was blocked with blocking solution (2% BSA in PBS, sterile filtered) for 30 min at 37°C and washed twice with PBS. Subsequently, PBMCs were seeded at 1×10^7 cells per 6-well and 2×10^6 cells per 24-well in T cell medium (RPMI complete, 25 mM HEPES, 0.4% P/S; TCM) or 4Cell® Nutri-T medium (4Cell® Nutri-T medium, 0.4% P/S; NutriT medium) supplemented with IL-7 (25 U/mL) and IL-15 (5 U/mL) (IL-7/15), and 3 µg/mL αCD28, for 72 h at 37°C. After activation, PBMCs were further cultured in TCM or NutriT medium supplemented with IL-7/15, which was refreshed every two to three days, and PBMCs were passaged and expanded as needed.

4.2.2.7 Transduction of activated and cytokine-stimulated PBMCs

For the transduction of PBMCs, 8×10^4 activated or cytokine-stimulated cells were seeded in TCM or NutriT medium supplemented with IL-7/15 in a 96-well plate. For transduction in presence of tyrosine kinase inhibitors (TKI) or the endocytosis inhibitor bafilomycin A1 (BflA1), concentrations of 0.39-100 nM of dasatinib, 1 µM bosutinib, 1 µM imatinib, 30 µM genistein or 1-20 nM BflA1 were added to the medium one hour prior to transduction. When indicated, vectofusin-1 (VF-1) (working concentration 10 µg/mL) was incubated for 5-10 min with the vectors before adding the mixture to the cells. The cells were then transduced with 5 µL of targeted vector stocks (delivering GFP, CD19.CAR or CEA.CAR) or serial dilutions for titer determination. To stay below the maximum tolerated dose of 1×10^9 VSV-LV particles (Frank et al., 2020), 5 µL of a 1:10 dilution of VSV-LV was used for transduction. Cells were subsequently centrifuged for 90 min at 850 x g and 32°C. After spinfection, 100 µL of fresh medium supplemented with the according inhibitors was added to the cells. The medium was changed three, five, or seven hours after start of incubation with dasatinib, and five hours after start of incubation with the other inhibitors bosutinib, imatinib, genistein or BflA1. Cells were subsequently cultivated in TCM or NutriT medium supplemented with IL-7/15 and optionally 25 µM UA or DMSO at 37°C and analyzed at the indicated time points.

4.2.2.8 Transduction of whole blood

Whole blood was taken from anonymous donors or from buffy coats acquired from DRK Blutspendedienst Baden-Württemberg-Hessen. The blood was directly transferred to 24-well, distributing 1 mL of blood per well. Next, 100 nM dasatinib or vehicle (DMSO) was added to the blood, which was then incubated on a tumbling table at 120 rpm and 37°C for one hour. After one hour of incubation with dasatinib, 1×10^{11} CD3-LV particles or 3×10^9 VSV-LV particles were added to the blood and incubated on the tumbling table for another six hours. PBMCs were then isolated by density gradient centrifugation as described above (Section 4.2.2.5) and cultivated in TCM or NutriT medium supplemented with IL-7/15 for five to six days prior to analysis.

4.2.2.9 LV binding assay

Activated PBMCs were seeded at 8×10^4 cells per 96-well and incubated with 100 nM dasatinib or without dasatinib. After one hour of incubation with dasatinib, 5 μ L CD3-LVs were added to the cells. The amount of vector particles bound to the cells was determined after seven, 24 and 72 hours by staining the His-tag attached to the binding glycoprotein of LVs and detected by flow cytometry. Due to large differences of MFI levels between the separate measurements, the results were normalized to the values determined after seven hours with HuM291-LV.

4.2.2.10 T cell proliferation assay

Activated PBMCs were cultivated in NutriT medium supplemented with IL-7/15 overnight. The next day, PBMCs were stained with CellTrace® Violet (CTV) (Thermo Fisher Scientific) according to manufacturer's instruction. The stained PBMCs were incubated with or without dasatinib one hour before adding LVs. CTV fluorescence was determined prior to treatment on day zero, after 24 and after 72 hours using flow cytometry.

4.2.2.11 Long-term killing assay

Activated PBMCs were seeded at 1×10^4 cells/well in cytokine-free NutriT medium with 50 nM dasatinib or without dasatinib. After one hour of incubation, 5 μ L CD3-LV(CD19.CAR) was added to the cells and spinfection was performed. After spinfection, cells were cultivated and medium was changed to remove dasatinib after five hours. In line with changing the medium, 1×10^4 CTV-labeled Nalm-6 cells were added to the PBMCs. The co-culture was cultivated at 37°C for eight days. Every other day, samples were removed and used for flow cytometry analysis to determine CAR expression and target cell killing. The remaining wells were topped up with doubling amounts of freshly labeled Nalm-6 cells.

4.2.2.12 Cytotoxicity assay

Prior to the cytotoxic assays, CAR expression was determined by flow cytometry three days post transduction for CD19.CAR T cells and six days post transduction for CEA.CAR T cells. The CAR T cell levels and cell count were used to normalize all conditions to contain equal T and CAR T cell numbers. Cells were washed and resuspended in cytokine-free NutriT medium in which the killing assays were performed. To determine CD19.CAR T cell cytotoxicity, 1×10^4 labeled Nalm-6 cells were added to 5×10^3 CD19.CAR T cells and the amount of dead target cells was determined by flow cytometry after four and 24 hours.

To determine CEA.CAR T cell cytotoxicity, 3×10^4 LS174T cells were labeled and seeded one day prior to the start of the killing assay. The next day, 1×10^4 CEA.CAR T cells were added and the amount of dead target cells was determined 24 hours after start of killing by flow cytometry.

For particular experiments the killing results were calculated as T cell specific lysis (Equation 1) to exclude the effect of viability issues of the target cells.

$$\% \text{ T cell specific lysis} = 100 \times \left(1 - \frac{\% \text{ viable tumor cells in presence of T cells}}{\% \text{ viable tumor cells in absence of T cells}} \right) \quad [1]$$

Upon killing, the supernatant of the co-cultures were harvested and stored at -80°C for latter cytokine assays (Section 4.2.2.13).

4.2.2.13 Cytokine assay

Cytokine levels of frozen cell culture supernatant collected from CAR T cell killing assays were analyzed using a human cytokine customized LEGENDplex™ multiplex assay kit (BioLegend) following the manufacturer's instruction. After sample preparation, the probes were measured using the MACSQuant Analyzer 10 (Miltenyi Biotec) and further analyzed with the LEGENDplex™ data analysis software (Biolegend).

4.2.2.14 Antibody staining and flow cytometry

For flow cytometry analysis, approximately 1×10^5 cells were transferred to micronic tubes and washed twice with FACS wash buffer (PBS, 2% FBS, 2 mM NaN₃). Therefore, 500 μ L FACS wash was added to the cells, the cells were centrifuged at 350 x g and 4°C for 3 min, the supernatant was removed and the cells were carefully resuspended. Prior to staining, cells were optionally treated with human FcR blocking reagent for 10 min at RT. Samples were subsequently stained with the appropriate antibody mix for 30 min at 4°C in the dark. The fixable viability dye eFlour780 was added to the antibody mixture to determine cell viability. After staining, the cells were washed twice with FACS wash buffer, the supernatant was removed, and the cells were resuspended in 100 μ L FACS fix buffer (PBS, 1% formaldehyde). The samples were stored at 4°C until measurement. In addition, single stains were prepared on untreated cells or on compensation beads (UltraComp eBeads™) to allow later compensation of channels with overlapping emission spectra prior to data analysis. Isotype controls were included to differentiate non-specific background signal from specific antibody signal. The samples were measured using MACSQuant Analyzer 10 (Miltenyi Biotec) and data analysis was carried out with FCS Express, Version 6 (De Novo Software).

4.2.3 Experimental mouse work

The mouse work was performed in accordance to the German animal protection law and the respective European Union guidelines. Four- to five-week old female NSG mice (NOD.Cg.PrkdcscidIL2rgtmWjl/SzJ) were purchased from Jackson Laboratories

Germany GmbH and housed in ventilated cages with food and water available *ad libitum*. Mice were handled under sterile conditions in laminar flow hoods.

4.2.3.1 PBMC administration

For humanization of the mice, PBMCs were thawed and activated for three days (Section 4.2.2.6) prior to injection. After three days of activation, PBMCs were pooled and washed twice with PBS by centrifugation for 5 min at 300 x g and 4°C. Cells were counted and the concentration was set to 1×10^8 cells/mL in PBS. Subsequently, mice were intravenously (i.v.) injected with 100 μ L of the cell suspension corresponding to 1×10^7 activated PBMCs per mouse. All injections were performed using 0.5 mL insulin syringes with a fixed 29-gauge needle (BD Bioscience).

4.2.3.2 Blood sampling and cell preparation

For blood sampling, mice were anesthetized with 3% isoflurane and blood was withdrawn by retroorbital (r.o.) sinus bleeding using sterile Pasteur glass pipettes. For monitoring, 50-70 μ L of blood was collected one day prior to treatment. For final analysis, the maximum amount of blood was collected prior to termination by cervical dislocation. Blood was collected in lithium heparin coated BD Microtainer® tubes (BD Biosciences) and washed once with 1 mL PBS by centrifugation at 300 x g and RT for 5 min. The washed blood was transferred to 15 mL falcon and lysed in 10 mL lysis buffer (10% 10x BD PharmLyse buffer + 90% H₂O, cell culture grade) for 15 min at RT. After lysis, cells were washed in 10 mL PBS by centrifugation at 300 x g for 5 min. Cells were further used for flow cytometry analysis (Section 4.2.2.14) and isolation of genomic DNA (Section 4.2.1.1) for qPCR (Section 4.2.1.2).

4.2.3.3 Drug formulation and administration

To test the transduction enhancing effect of dasatinib *in vivo*, 10 mg/kg dasatinib was administered to the mice intraperitoneally (i.p.) one hour prior to vector administration. Calculations were made based on a 20 g mouse receiving 150 μ L of drug formulation to achieve a dose of 10 mg/kg of dasatinib. Therefore, dasatinib was diluted in 4% (*v/v*) DMSO, 33% (*w/v*) PEG300, 5% (*v/v*) Tween® 80 and cell culture

grade H₂O. In addition, vehicle formulation without dasatinib was prepared and administered as a reference.

4.2.3.4 Administration of vector particles

CD3-LV was thawed on ice and resuspended by pipetting. One hour after dasatinib or vehicle administration, CD3-LV was briefly warmed to RT before injection. Mice were restrained and injected with 200 µL CD3-LV (1.2×10^{12} particles) through i.v. tail vein injection. Following treatment, mice were monitored for visual abnormalities and weight measurements were taken.

4.2.3.5 Organ harvest and cell preparation

On the day of final analysis, mice were anesthetized with 3% isoflurane, bled, and killed by cervical dislocation (Section 4.2.3.2). Spleen and leg bones (hip bones, femur and tibia) were harvested from each mouse and stored in RPMI complete for further processing. For cell preparation, the spleen was minced through a 70 µm cell strainer into a 15 mL falcon filled with 10 mL RPMI complete. The leg bones were cleaned from remaining tissue using a scalpel and the ends of the bones were cut off. The cut bones were transferred to pierced 0.5 mL tubes and centrifuged at 4600 rpm x g for 3 min, collecting the cells in 1.5 mL tubes containing 50 µL RPMI complete. The cells were resuspended in 1 mL RPMI complete and put through a 70 µm cell strainer.

Both cell suspensions derived from spleen and bone marrow were washed with 10 mL PBS by centrifugation at 300 x g and 4°C for 5 min and subsequently treated with lysis buffer (10% 10x BD PharmLyse buffer + 90% H₂O, cell culture grade) at RT for 15-20 min. After erythrocyte lysis, the cells were washed twice in PBS by centrifugation at 300 x g and 4°C for 5 min, and residual cell debris was removed by pipetting or, if necessary, by filtering through a 40 µm cell strainer. Cell pellets were resuspended in 2 mL RPMI complete, counted and used for further downstream applications such as flow cytometry (Section 4.2.2.14) and qPCR (Section 4.2.1.2), or cryopreserved for later use (Section 4.2.2.1).

4.2.4 Statistical analysis

Statistical analysis was performed using GraphPad Prism 9 (GraphPad Software Inc.). Data were analyzed for statistical significance using the indicated tests described in the figure legends and were considered significant at $*p < 0.05$. Statistical results were abbreviated as follows ns: non-significant, $*p < 0.05$, $**p < 0.01$, $***p < 0.001$ and $****p < 0.0001$.

5 References

- Abou-El-Enein, M., Elsallab, M., Feldman, S. A., Fesnak, A. D., Heslop, H. E., Marks, P., Till, B. G., Bauer, G., & Savoldo, B. (2021). Scalable Manufacturing of CAR T cells for Cancer Immunotherapy. *Blood Cancer Discovery*, 2(5), 408–422. <https://doi.org/10.1158/2643-3230.bcd-21-0084>
- Acuto, O., & Michel, F. (2003). Cd28-mediated co-stimulation: A quantitative support for TCR signalling. *Nature Reviews. Immunology*, 3(12), 939–951. <https://doi.org/10.1038/nri1248>
- Agarwal, S., Hanauer, J. D., Frank, A. M., Riechert, V., Thalheimer, F. B., & Buchholz, C. J. (2020). In vivo generation of CAR T cells selectively in human CD4+ lymphocytes. *Mol Ther*, 20, 30239-2. <https://doi.org/10.1016/j.ymthe.2020.05.005>
- Akhmetzyanova, I., Zelinsky, G., Schimmer, S., Brandau, S., Altenhoff, P., Sparwasser, T., & Dittmer, U. (2013). Tumor-specific CD4+ T cells develop cytotoxic activity and eliminate virus-induced tumor cells in the absence of regulatory T cells. *Cancer Immunology, Immunotherapy : CII*, 62(2), 257–271. <https://doi.org/10.1007/s00262-012-1329-y>
- Alcover, A., Alarcón, B., & Di Bartolo, V. (2018). Cell Biology of T Cell Receptor Expression and Regulation. *Annual Review of Immunology*, 36, 103–125. <https://doi.org/10.1146/annurev-immunol-042617-053429>
- Al-Haideri, M., Tondok, S. B., Safa, S. H., maleki, A. H., Rostami, S., Jalil, A. T., Al-Gazally, M. E., Alsaikhan, F., Rizaev, J. A., Mohammad, T. A. M., & Tahmasebi, S. (2022). Car-T cell combination therapy: The next revolution in cancer treatment. *Cancer Cell International*, 22(1), 365. <https://doi.org/10.1186/s12935-022-02778-6>
- Amirache, F., Levy, C., Costa, C., Mangeot, P.-E., Torbett, B. E., Wang, C. X., Negre, D., Cosset, F.-L., & Verhoeven, E. (2014). Mystery solved: Vsv-G-LVs do not allow efficient gene transfer into unstimulated T cells, B cells, and HSCs because they lack the LDL receptor. *Blood*, 123(9), 1422–1424. <https://doi.org/10.1182/blood-2013-11-540641>
- Andreux, P. A., Blanco-Bose, W., Ryu, D., Burdet, F., Ibberson, M., Aebischer, P., Auwerx, J., Singh, A., & Rinsch, C. (2019). The mitophagy activator urolithin A is safe and induces a molecular signature of improved mitochondrial and cellular health in humans. *Nature Metabolism*, 1(6), 595–603. <https://doi.org/10.1038/s42255-019-0073-4>
- Arcangeli, S., Bove, C., Mezzanotte, C., Camisa, B., Falcone, L., Manfredi, F., Bezzecchi, E., El Khoury, R., Norata, R., Sanvito, F., Ponzoni, M., Greco, B., Moresco, M. A., Carrabba, M. G., Ciceri, F., Bonini, C., Bondanza, A., & Casucci, M. (2022). Car T cell

- manufacturing from naive/stem memory T lymphocytes enhances antitumor responses while curtailing cytokine release syndrome. *The Journal of Clinical Investigation*, 132(12). <https://doi.org/10.1172/JCI150807>
- Arcangeli, S., Falcone, L., Camisa, B., Girardi, F. de, Biondi, M., Giglio, F., Ciceri, F., Bonini, C., Bondanza, A., & Casucci, M. (2020). Next-Generation Manufacturing Protocols Enriching TSCM CAR T Cells Can Overcome Disease-Specific T Cell Defects in Cancer Patients. *Frontiers in Immunology*, 11, 1217. <https://doi.org/10.3389/fimmu.2020.01217>
- Bender, R. R., Muth, A., Schneider, I. C [Irene C.], Friedel, T., Hartmann, J., Pluckthun, A., Maisner, A., & Buchholz, C. J. (2016). Receptor-Targeted Nipah Virus Glycoproteins Improve Cell-Type Selective Gene Delivery and Reveal a Preference for Membrane-Proximal Cell Attachment. *PLoS Pathog*, 12(6), e1005641. <https://doi.org/10.1371/journal.ppat.1005641>
- Biasco, L., Izotova, N., Rivat, C., Ghorashian, S., Richardson, R., Guvenel, A., Hough, R., Wynn, R., Popova, B., Lopes, A., Pule, M., Thrasher, A. J., & Amrolia, P. J. (2021). Clonal expansion of T memory stem cells determines early anti-leukemic responses and long-term CAR T cell persistence in patients. *Nature Cancer*, 2(6), 629–642. <https://doi.org/10.1038/s43018-021-00207-7>
- Bishop, D. C., Clancy, L. E., Simms, R., Burgess, J., Mathew, G., Moezzi, L., Street, J. A., Sutrave, G., Atkins, E., McGuire, H. M., Gloss, B. S., Lee, K., Jiang, W., Maddock, K., McCaughan, G., Avdic, S., Antonenas, V., O'Brien, T. A., Shaw, P. J., . . . Micklethwaite, K. P. (2021). Development of CAR T-cell lymphoma in 2 of 10 patients effectively treated with piggyBac-modified CD19 CAR T cells. *Blood*, 138(16), 1504–1509. <https://doi.org/10.1182/blood.2021010813>
- Blank, C. U., Haining, W. N., Held, W., Hogan, P. G., Kallies, A., Lugli, E., Lynn, R. C., Philip, M., Rao, A., Restifo, N. P., Schietinger, A., Schumacher, T. N., Schwartzberg, P. L., Sharpe, A. H., Speiser, D. E., Wherry, E. J., Youngblood, B. A., & Zehn, D. (2019). Defining 'T cell exhaustion'. *Nature Reviews Immunology*, 19(11), 665–674. <https://doi.org/10.1038/s41577-019-0221-9>
- Blessing, D., & Deglon, N. (2016). Adeno-associated virus and lentivirus vectors: A refined toolkit for the central nervous system. *Current Opinion in Virology*, 21, 61–66. <https://doi.org/10.1016/j.coviro.2016.08.004>
- Borsotti, C., Borroni, E., & Follenzi, A. (2016). Lentiviral vector interactions with the host cell. *Current Opinion in Virology*, 21, 102–108. <https://doi.org/10.1016/j.coviro.2016.08.016>
- Bosslet, K., Steinsträsser, A., Schwarz, A., Harthus, H. P., Lüben, G., Kuhlmann, L., & Sedlacek, H. H. (1988). Quantitative considerations supporting the irrelevance of circulating serum CEA for the immunoscintigraphic visualization of CEA expressing

- carcinomas. *European Journal of Nuclear Medicine*, 14(11), 523–528.
<https://doi.org/10.1007/BF00286769>
- Braun, A. H., Frank, A. M., Ho, N., & Buchholz, C. J. (2023). Dasatinib is a potent enhancer for CAR T cell generation by CD3-targeted lentiviral vectors. *Mol Ther Methods Clin Dev*, 28, 90–98. <https://doi.org/10.1016/j.omtm.2022.12.002>
- Brehm, M. A., Daniels, K. A., & Welsh, R. M. (2005). Rapid production of TNF-alpha following TCR engagement of naive CD8 T cells. *Journal of Immunology (Baltimore, Md. : 1950)*, 175(8), 5043–5049. <https://doi.org/10.4049/jimmunol.175.8.5043>
- Buck, M. D., O'Sullivan, D., Klein Geltink, R. I., Curtis, J. D., Chang, C.-H., Sanin, D. E., Qiu, J., Kretz, O., Braas, D., van der Windt, G. J. W., Chen, Q., Huang, S. C.-C., O'Neill, C. M., Edelson, B. T., Pearce, E. J., Sesaki, H., Huber, T. B., Rambold, A. S., & Pearce, E. L. (2016). Mitochondrial Dynamics Controls T Cell Fate through Metabolic Programming. *Cell*, 166(1), 63–76.
<https://doi.org/10.1016/j.cell.2016.05.035>
- Call, M. E., Pyrdol, J., Wiedmann, M., & Wucherpfennig, K. W. (2002). The Organizing Principle in the Formation of the T Cell Receptor-CD3 Complex. *Cell*, 111(7), 967–979.
- Call, M. E., & Wucherpfennig, K. W. (2004). Molecular mechanisms for the assembly of the T cell receptor–CD3 complex. *Molecular Immunology*, 40(18), 1295–1305.
<https://doi.org/10.1016/j.molimm.2003.11.017>
- Cappell, K. M., & Kochenderfer, J. N. (2023). Long-term outcomes following CAR T cell therapy: What we know so far. *Nature Reviews. Clinical Oncology*, 20(6), 359–371.
<https://doi.org/10.1038/s41571-023-00754-1>
- Carding, S. R., & Egan, P. J. (2002). Gammadelta T cells: Functional plasticity and heterogeneity. *Nature Reviews. Immunology*, 2(5), 336–345.
<https://doi.org/10.1038/nri797>
- Caruso, H. G., Tanaka, R., Liang, J., Ling, X., Sabbagh, A., Henry, V. K., Collier, T. L., & Heimberger, A. B. (2019). Shortened ex vivo manufacturing time of EGFRvIII-specific chimeric antigen receptor (CAR) T cells reduces immune exhaustion and enhances antglioma therapeutic function. *Journal of Neuro-Oncology*, 145(3), 429–439.
<https://doi.org/10.1007/s11060-019-03311-y>
- Chakraborty, A. K., & Weiss, A [Arthur] (2014). Insights into the initiation of TCR signaling. *Nature Immunology*, 15(9), 798–807. <https://doi.org/10.1038/ni.2940>
- Chapman, N. M., Boothby, M. R., & Chi, H. (2020). Metabolic coordination of T cell quiescence and activation. *Nature Reviews. Immunology*, 20(1), 55–70.
<https://doi.org/10.1038/s41577-019-0203-y>

- Chapman, N. M., & Chi, H. (2018). Hallmarks of T-cell Exit from Quiescence. *Cancer Immunology Research*, 6(5), 502–508. <https://doi.org/10.1158/2326-6066.CIR-17-0605>
- Charitidis, F. T. (2023). *Deploying single-cell transcriptomics for assessing CAR T cell generation: alleviating antiviral restriction factors enhances gene transfer* [Dissertation]. TU Darmstadt, Darmstadt.
- Charitidis, F. T., Adabi, E., Ho, N., Braun, A. H., Tierney, C., Strasser, L., Thalheimer, F. B., Childs, L., Bones, J., Clarke, C., & Buchholz, C. J. (2023). CAR gene delivery by T-cell targeted lentiviral vectors is enhanced by rapamycin induced reduction of antiviral mechanisms. *Advanced Science*. Advance online publication. <https://doi.org/10.1002/advs.202302992>
- Charitidis, F. T., Adabi, E., Thalheimer, F. B., Clarke, C., & Buchholz, C. J. (2021). Monitoring CAR T cell generation with a CD8-targeted lentiviral vector by single-cell transcriptomics. *Mol Ther Methods Clin Dev*, 23, 359–369. <https://doi.org/10.1016/j.omtm.2021.09.019>
- Cibrián, D., & Sánchez-Madrid, F. (2017). Cd69: From activation marker to metabolic gatekeeper. *European Journal of Immunology*, 47(6), 946–953. <https://doi.org/10.1002/eji.201646837>
- Cieri, N., Camisa, B., Cocchiarella, F., Forcato, M., Oliveira, G., Provasi, E., Bondanza, A., Bordignon, C., Peccatori, J., Ciceri, F., Lupo-Stanghellini, M. T., Mavilio, F., Mondino, A [Anna], Bicciato, S., Recchia, A., & Bonini, C. (2013). IL-7 and IL-15 instruct the generation of human memory stem T cells from naive precursors. *Blood*, 121(4), 573–584. <https://doi.org/10.1182/blood-2012-05-431718>
- Cornetta, K., & Anderson, W. F. (1989). Protamine sulfate as an effective alternative to polybrene in retroviral-mediated gene-transfer: Implications for human gene therapy. *Journal of Virological Methods*, 23(2), 187–194. [https://doi.org/10.1016/0166-0934\(89\)90132-8](https://doi.org/10.1016/0166-0934(89)90132-8)
- Coroadinha, A. S. (2023). Host Cell Restriction Factors Blocking Efficient Vector Transduction: Challenges in Lentiviral and Adeno-Associated Vector Based Gene Therapies. *Cells*, 12(5). <https://doi.org/10.3390/cells12050732>
- Curtsinger, J. M., Schmidt, C. S., Mondino, A [A.], Lins, D. C., Kedl, R. M., Jenkins, M. K., & Mescher, M. F. (1999). Inflammatory cytokines provide a third signal for activation of naive CD4+ and CD8+ T cells. *Journal of Immunology (Baltimore, Md. : 1950)*, 162(6), 3256–3262.
- D'Amico, D., Andreux, P. A., Valdés, P., Singh, A., Rinsch, C., & Auwerx, J. (2021). Impact of the Natural Compound Urolithin A on Health, Disease, and Aging. *Trends in Molecular Medicine*, 27(7), 687–699. <https://doi.org/10.1016/j.molmed.2021.04.009>

- Delville, M., Soheili, T., Bellier, F., Durand, A., Denis, A., Lagresle-Peyrou, C., Cavazzana, M., Andre-Schmutz, I., & Six, E. (2018). A Nontoxic Transduction Enhancer Enables Highly Efficient Lentiviral Transduction of Primary Murine T Cells and Hematopoietic Stem Cells. *Molecular Therapy — Methods & Clinical Development*, *10*, 341–347. <https://doi.org/10.1016/j.omtm.2018.08.002>
- Demaison, C., Parsley, K., Brouns, G., Scherr, M., Battmer, K., Kinnon, C., Grez, M., & Thrasher, A. J. (2002). High-level transduction and gene expression in hematopoietic repopulating cells using a human immunodeficiency virus type 1-based lentiviral vector containing an internal spleen focus forming virus promoter. *Hum Gene Ther*, *13*(7), 803–813. <https://doi.org/10.1089/10430340252898984>
- den Braber, I., Mugwagwa, T., Vrisekoop, N., Westera, L., Mögling, R., Boer, A. B. de, Willems, N., Schrijver, E. H. R., Spierenburg, G., Gaiser, K., Mul, E., Otto, S. A., Ruiters, A. F. C., Ackermans, M. T [Mariette T.], Miedema, F., Borghans, J. A. M., Boer, R. J. de, & Tesselaar, K. (2012). Maintenance of peripheral naive T cells is sustained by thymus output in mice but not humans. *Immunity*, *36*(2), 288–297. <https://doi.org/10.1016/j.immuni.2012.02.006>
- Denk, D., Petrocelli, V., Conche, C., Drachler, M., Ziegler, P. K., Braun, A., Kress, A., Nicolas, A. M., Mohs, K., Becker, C., Neurath, M. F., Farin, H. F., Buchholz, C. J., Andreux, P. A., Rinsch, C., & Greten, F. R. (2022). Expansion of T memory stem cells with superior anti-tumor immunity by Urolithin A-induced mitophagy. *Immunity*, *55*(11), 2059-2073.e8. <https://doi.org/10.1016/j.immuni.2022.09.014>
- de Dong, Zheng, L., Lin, J., Zhang, B., Zhu, Y., Li, N [Ningning], Xie, S., Wang, Y [Yuhang], Gao, N., & Huang, Z. (2019). Structural basis of assembly of the human T cell receptor-CD3 complex. *Nature*, *573*(7775), 546–552. <https://doi.org/10.1038/s41586-019-1537-0>
- Escors, D., Bricogne, C., Arce, F., Kochan, G., & Karwacz, K. (2011). On the Mechanism of T cell receptor down-modulation and its physiological significance. *The Journal of Bioscience and Medicine*, *1*(1).
- Eshhar, Z., Waks, T., Gross, G., & Schindler, D. G. (1993). Specific activation and targeting of cytotoxic lymphocytes through chimeric single chains consisting of antibody-binding domains and the gamma or zeta subunits of the immunoglobulin and T-cell receptors. *Proceedings of the National Academy of Sciences of the United States of America*, *90*(2), 720–724. <https://doi.org/10.1073/pnas.90.2.720>
- Fenard, D., Ingrao, D., Seye, A., Buisset, J., Genries, S., Martin, S., Kichler, A., & Galy, A. (2013). Vectofusin-1, a new viral entry enhancer, strongly promotes lentiviral transduction of human hematopoietic stem cells. *Molecular Therapy : The Journal of the American Society of Gene Therapy*, *2*, e90. <https://doi.org/10.1038/mtna.2013.17>

- Finkelshtein, D., Werman, A., Novick, D., Barak, S., & Rubinstein, M. (2013). Ldl receptor and its family members serve as the cellular receptors for vesicular stomatitis virus. *Proc Natl Acad Sci U S a*, *110*(18), 7306–7311. <https://doi.org/10.1073/pnas.1214441110>
- Fraietta, J. A., Lacey, S. F., Orlando, E. J., Pruteanu-Malinici, I., Gohil, M., Lundh, S., Boesteanu, A. C., Wang, Y [Yan], O'Connor, R. S., Hwang, W.-T., Pequignot, E., Ambrose, D. E., Zhang, C [Changfeng], Wilcox, N., Bedoya, F., Dorfmeier, C., Chen, F., Tian, L., Parakandi, H., . . . Melenhorst, J. J. (2018). Determinants of response and resistance to CD19 chimeric antigen receptor (CAR) T cell therapy of chronic lymphocytic leukemia. *Nature Medicine*, *24*(5), 563–571. <https://doi.org/10.1038/s41591-018-0010-1>
- Frank, A. M., Braun, A. H., Scheib, L., Agarwal, S., Schneider, I. C [Irene C.], Fusil, F., Perian, S., Sahin, U., Thalheimer, F. B., Verhoeyen, E., & Buchholz, C. J. (2020). Combining T-cell-specific activation and in vivo gene delivery through CD3-targeted lentiviral vectors. *Blood Adv*, *4*(22), 5702–5715. <https://doi.org/10.1182/bloodadvances.2020002229>
- Frank, A. M., & Buchholz, C. J. (2018). Surface-engineered lentiviral vectors for selective gene transfer into subtypes of lymphocytes. *Mol Ther Methods Clin Dev*, *12*(12), 19–31. <https://doi.org/10.1016/j.omtm.2018.10.006>
- Funke, S., Maisner, A., Mühlebach, M. D., Koehl, U., Grez, M., Cattaneo, R., Cichutek, K., & Buchholz, C. J. (2008). Targeted cell entry of lentiviral vectors. *Mol Ther*, *16*(8), 1427–1436. <https://doi.org/10.1038/mt.2008.128>
- Gattinoni, L., Klebanoff, C. A., & Restifo, N. P. (2012). Paths to stemness: Building the ultimate antitumour T cell. *Nature Reviews Cancer*, *12*(10), 671–684. <https://doi.org/10.1038/nrc3322>
- Gattinoni, L., Lugli, E., Ji, Y., Pos, Z., Paulos, C. M., Quigley, M. F., Almeida, J. R., Gostick, E., Yu, Z., Carpenito, C., Wang, E., Douek, D. C., Price, D. A., June, C. H., Marincola, F. M., Roederer, M., & Restifo, N. P. (2011). A human memory T cell subset with stem cell-like properties. *Nature Medicine*, *17*(10), 1290–1297. <https://doi.org/10.1038/nm.2446>
- Gattinoni, L., Speiser, D. E., Lichterfeld, M., & Bonini, C. (2017). T memory stem cells in health and disease. *Nature Medicine*, *23*(1), 18–27. <https://doi.org/10.1038/nm.4241>
- Geethakumari, P. R., Ramasamy, D. P., Dholaria, B., Berdeja, J., & Kansagra, A. (2021). Balancing Quality, Cost, and Access During Delivery of Newer Cellular and Immunotherapy Treatments. *Current Hematologic Malignancy Reports*, *16*(4), 345–356. <https://doi.org/10.1007/s11899-021-00635-3>

- Germain, R. N. (2002). T-cell development and the CD4-CD8 lineage decision. *Nature Reviews. Immunology*, 2(5), 309–322. <https://doi.org/10.1038/nri798>
- Ghassemi, S., Durgin, J. S., Nunez-Cruz, S., Patel, J., Leferovich, J., Pinzone, M., Shen, F., Cummins, K. D., Plesa, G., Cantu, V. A., Reddy, S., Bushman, F. D., Gill, S. I., O'Doherty, U., O'Connor, R. S., & Milone, M. C. (2022). Rapid manufacturing of non-activated potent CAR T cells. *Nature Biomedical Engineering*, 6(2), 118–128. <https://doi.org/10.1038/s41551-021-00842-6>
- Ghassemi, S., Nunez-Cruz, S., O'Connor, R. S., Fraietta, J. A., Patel, P. R., Scholler, J., Barrett, D. M., Lundh, S. M., Davis, M. M., Bedoya, F., Zhang, C [Changfeng], Leferovich, J., Lacey, S. F., Levine, B. L., Grupp, S. A., June, C. H., Melenhorst, J. J., & Milone, M. C. (2018). Reducing Ex Vivo Culture Improves the Antileukemic Activity of Chimeric Antigen Receptor (CAR) T Cells. *Cancer Immunology Research*, 6(9), 1100–1109. <https://doi.org/10.1158/2326-6066.CIR-17-0405>
- Gibbins, D., & Befus, A. D. (2009). Cd4 and CD8: An inside-out coreceptor model for innate immune cells. *Journal of Leukocyte Biology*, 86(2), 251–259. <https://doi.org/10.1189/jlb.0109040>
- Gogol-Döring, A., Ammar, I., Gupta, S., Bunse, M., Miskey, C., Chen, W., Uckert, W., Schulz, T. F., Izsvák, Z., & Ivics, Z. (2016). Genome-wide Profiling Reveals Remarkable Parallels Between Insertion Site Selection Properties of the MLV Retrovirus and the piggyBac Transposon in Primary Human CD4(+) T Cells. *Molecular Therapy*, 24(3), 592–606. <https://doi.org/10.1038/mt.2016.11>
- Golubovskaya, V., & Wu, L. (2016). Different Subsets of T Cells, Memory, Effector Functions, and CAR-T Immunotherapy. *Cancers*, 8(3), 36. <https://doi.org/10.3390/cancers8030036>
- Groschel, B., & Bushman, F. (2005). Cell cycle arrest in G2/M promotes early steps of infection by human immunodeficiency virus. *Journal of Virology*, 79(9), 5695–5704. <https://doi.org/10.1128/JVI.79.9.5695-5704.2005>
- Gross, G., Waks, T., & Eshhar, Z. (1989). Expression of immunoglobulin-T-cell receptor chimeric molecules as functional receptors with antibody-type specificity. *Proceedings of the National Academy of Sciences*, 86(24), 10024–10028. <https://doi.org/10.1073/pnas.86.24.10024>
- Gu, T., Zhu, M., Huang, H., & Hu, Y. (2022). Relapse after CAR-T cell therapy in B-cell malignancies: Challenges and future approaches. *Journal of Zhejiang University. Science. B*, 23(10), 793–811. <https://doi.org/10.1631/jzus.B2200256>
- Hanenberg, H., Xiao, X. L., Dilloo, D., Hashino, K., Kato, I., & Williams, D. A. (1996). Colocalization of retrovirus and target cells on specific fibronectin fragments

- increases genetic transduction of mammalian cells. *Nature Medicine*, 2(8), 876–882.
<https://doi.org/10.1038/nm0896-876>
- Harrison, S. C. (2015). Viral membrane fusion. *Virology*, 479-480, 498–507.
<https://doi.org/10.1016/j.virol.2015.03.043>
- Hebbar, N., Epperly, R., Vaidya, A., Thanekar, U., Moore, S. E., Umeda, M., Ma, J., Patil, S. L., Langfitt, D., Huang, S., Cheng, C., Klco, J. M., Gottschalk, S., & Velasquez, M. P. (2022). CAR T cells redirected to cell surface GRP78 display robust anti-acute myeloid leukemia activity and do not target hematopoietic progenitor cells. *Nature Communications*, 13(1). <https://doi.org/10.1038/s41467-022-28243-6>
- Höfig, I., Atkinson, M. J., Mall, S., Krackhardt, A. M., Thirion, C., & Anastasov, N. (2012). Poloxamer syneronic F108 improves cellular transduction with lentiviral vectors: Achtung, funktioniert bei mir nicht (Tobi). *The Journal of Gene Medicine*, 14(8), 549–560. <https://doi.org/10.1002/jgm.2653>
- Holzinger, A., & Abken, H [Hinrich] (2017). Car T cells targeting solid tumors: Carcinoembryonic antigen (CEA) proves to be a safe target. *Cancer Immunology, Immunotherapy*, 66(11), 1505–1507. <https://doi.org/10.1007/s00262-017-2045-4>
- Holzinger, A., & Abken, H [Hinrich] (2019). CAR T cells: A Snapshot on the Growing Options to Design a CAR. *HemaSphere*, 3(1), e172.
- Hombach, A., Wierzchowiec, A., Marquardt, T., Heuser, C., Usai, L., Pohl, C., Seliger, B., & Abken, H [H.] (2001). Tumor-specific T cell activation by recombinant immunoreceptors: Cd3 zeta signaling and CD28 costimulation are simultaneously required for efficient IL-2 secretion and can be integrated into one combined CD28/CD3 zeta signaling receptor molecule. *The Journal of Immunology*, 167(11), 6123–6131. <https://doi.org/10.4049/jimmunol.167.11.6123>
- Hornick, A. L., Li, N [Ni], Oakland, M., McCray, P. B., & Sinn, P. L. (2016). Human, Pig, and Mouse Interferon-Induced Transmembrane Proteins Partially Restrict Pseudotyped Lentiviral Vectors. *Human Gene Therapy*, 27(5), 354–362.
<https://doi.org/10.1089/hum.2015.156>
- Huang, J., Brameshuber, M., Zeng, X., Xie, J., Li, Q. J., Chien, Y. H., Valitutti, S [S.], & Davis, M. M [M. M.] (2013). A Single Peptide-Major Histocompatibility Complex Ligand Triggers Digital Cytokine Secretion in CD4(+) T Cells. *Immunity*, 39(5).
<https://doi.org/10.1016/j.immuni.2013.08.036>
- Irving, M., Lanitis, E., Migliorini, D., Ivics, Z., & Guedan, S. (2021). Choosing the Right Tool for Genetic Engineering: Clinical Lessons from Chimeric Antigen Receptor-T Cells. *Human Gene Therapy*, 32(19-20), 1044–1058. <https://doi.org/10.1089/hum.2021.173>
- Jamali, A., Kapitza, L., Schaser, T., Johnston, I. C. D., Buchholz, C. J., & Hartmann, J. (2019). Highly Efficient and Selective CAR-Gene Transfer Using CD4- and CD8-

- Targeted Lentiviral Vectors. *Molecular Therapy — Methods & Clinical Development*, 13, 371–379. <https://doi.org/10.1016/j.omtm.2019.03.003>
- José, E. S., Borroto, A., Niedergang, F., Alcover, A., & Alarcón, B. (2000). Triggering the TCR Complex Causes the Downregulation of Nonengaged Receptors by a Signal Transduction-Dependent Mechanism. *Immunity*, 12(2), 161–170. [https://doi.org/10.1016/S1074-7613\(00\)80169-7](https://doi.org/10.1016/S1074-7613(00)80169-7)
- June, C. H., & Sadelain, M. (2018). Chimeric Antigen Receptor Therapy. *N Engl J Med*, 379(1), 64–73. <https://doi.org/10.1056/NEJMra1706169>
- Jung, I.-Y., Noguera-Ortega, E., Bartoszek, R., Collins, S. M., Williams, E., Davis, M., Jadowsky, J. K., Plesa, G., Siegel, D. L., Chew, A., Levine, B. L., Berger, S. L., Moon, E. K., Albelda, S. M., & Fraietta, J. A. (2023). Tissue-resident memory CAR T cells with stem-like characteristics display enhanced efficacy against solid and liquid tumors. *Cell Reports. Medicine*, 4(6), 101053. <https://doi.org/10.1016/j.xcrm.2023.101053>
- Kajaste-Rudnitski, A., & Naldini, L [Luigi] (2015). Cellular innate immunity and restriction of viral infection: Implications for lentiviral gene therapy in human hematopoietic cells. *Human Gene Therapy*, 26(4), 201–209. <https://doi.org/10.1089/hum.2015.036>
- Kamath, A. V., Wang, J [Jian], Lee, F. Y., & Marathe, P. H. (2008). Preclinical pharmacokinetics and in vitro metabolism of dasatinib (BMS-354825): A potent oral multi-targeted kinase inhibitor against SRC and BCR-ABL. *Cancer Chemotherapy and Pharmacology*, 61(3), 365–376. <https://doi.org/10.1007/s00280-007-0478-8>
- Karwacz, K., Bricogne, C., MacDonald, D., Arce, F., Bennett, C. L., Collins, M., & Escors, D. (2011). Pd-L1 co-stimulation contributes to ligand-induced T cell receptor down-modulation on CD8+ T cells. *EMBO Molecular Medicine*, 3(10), 581–592. <https://doi.org/10.1002/emmm.201100165>
- Katz, S. C., Burga, R. A., McCormack, E., Wang, L. J., Mooring, W., Point, G. R., Khare, P. D., Thorn, M., Ma, Q., Stainken, B. F., Assanah, E. O., Davies, R., Espat, N. J., & Junghans, R. P. (2015). Phase I Hepatic Immunotherapy for Metastases Study of Intra-Arterial Chimeric Antigen Receptor-Modified T-cell Therapy for CEA+ Liver Metastases. *Clinical Cancer Research : An Official Journal of the American Association for Cancer Research*, 21(14), 3149–3159. <https://doi.org/10.1158/1078-0432.CCR-14-1421>
- Kaygisiz, K., & Synatschke, C. V. (2020). Materials promoting viral gene delivery. *Biomaterials Science*, 8(22), 6113–6156. <https://doi.org/10.1039/D0BM01367F>
- Labanieh, L., & Mackall, C. L. (2023). Car immune cells: Design principles, resistance and the next generation. *Nature*, 614(7949), 635–648. <https://doi.org/10.1038/s41586-023-05707-3>

- Larson, R. C., & Maus, M. V. (2021). Recent advances and discoveries in the mechanisms and functions of CAR T cells. *Nature Reviews. Cancer*, 21(3), 145–161. <https://doi.org/10.1038/s41568-020-00323-z>
- Lee, D. W., Gardner, R., Porter, D. L., Louis, C. U., Ahmed, N., Jensen, M., Grupp, S. A., & Mackall, C. L. (2014). Current concepts in the diagnosis and management of cytokine release syndrome. *Blood*, 124(2), 188–195. <https://doi.org/10.1182/blood-2014-05-552729>
- Levine, B. L., Miskin, J., Wonnacott, K., & Keir, C. (2017). Global Manufacturing of CAR T Cell Therapy. *Molecular Therapy — Methods & Clinical Development*, 4, 92–101. <https://doi.org/10.1016/j.omtm.2016.12.006>
- Li, T., Wu, B., Yang, T., Zhang, L., & Jin, K. (2020). The outstanding antitumor capacity of CD4+ T helper lymphocytes. *Biochimica Et Biophysica Acta. Reviews on Cancer*, 1874(2), 188439. <https://doi.org/10.1016/j.bbcan.2020.188439>
- Lissina, A., Ladell, K., Skowera, A., Clement, M., Edwards, E., Seggewiss, R., van den Berg, H. A., Gostick, E., Gallagher, K., Jones, E., Melenhorst, J. J., Godkin, A. J., Peakman, M., Price, D. A., Sewell, A. K., & Wooldridge, L. (2009). Protein kinase inhibitors substantially improve the physical detection of T-cells with peptide-MHC tetramers. *Journal of Immunological Methods*, 340(1), 11–24. <https://doi.org/10.1016/j.jim.2008.09.014>
- Liu, H [H.], Rhodes, M., Wiest, D. L., & Vignali, D. A. (2000). On the dynamics of TCR: Cd3 complex cell surface expression and downmodulation. *Immunity*, 13(5), 665–675.
- Lock, D., Monjezi, R., Brandes, C., Bates, S., Lennartz, S., Teppert, K., Gehrke, L., Karasakalidou-Seidt, R., Lukic, T., Schmeer, M., Schleef, M., Werchau, N., Eyrich, M., Assenmacher, M., Kaiser, A., Prommersberger, S., Schaser, T., & Hudecek, M [Michael] (2022). Automated, scaled, transposon-based production of CAR T cells. *Journal for ImmunoTherapy of Cancer*, 10(9). <https://doi.org/10.1136/jitc-2022-005189>
- Luo, F. R., Yang, Z [Zheng], Camuso, A., Smykla, R., McGlinchey, K., Fager, K., Flefleh, C., Castaneda, S., Inigo, I., Kan, D., Wen, M.-L., Kramer, R., Blackwood-Chirchir, A., & Lee, F. Y. (2006). Dasatinib (BMS-354825) pharmacokinetics and pharmacodynamic biomarkers in animal models predict optimal clinical exposure. *Clinical Cancer Research*, 12(23), 7180–7186. <https://doi.org/10.1158/1078-0432.CCR-06-1112>
- Maiti, A., Cortes, J. E., Patel, K. P., Masarova, L., Borthakur, G., Ravandi, F., Verstovsek, S., Ferrajoli, A., Estrov, Z., Garcia-Manero, G., Kadia, T. M., Noguera-González, G. M., Skinner, J., Poku, R., DellaSala, S., Luthra, R., Jabbour, E. J., O'Brien, S., & Kantarjian, H. M. (2020). Long-term results of frontline dasatinib in chronic myeloid leukemia. *Cancer*, 126(7), 1502–1511. <https://doi.org/10.1002/cncr.32627>

- Mestermann, K., Giavridis, T., Weber, J., Rydzek, J., Frenz, S., Nerreter, T., Maden, A., Sadelain, M., Einsele, H., & Hudecek, M [Michael] (2019). The tyrosine kinase inhibitor dasatinib acts as a pharmacologic on/off switch for CAR T cells. *Science Translational Medicine*, *11*(499), eaau5907.
<https://doi.org/10.1126/scitranslmed.aau5907>
- Meuer, S. C., Hodgdon, J. C., Hussey, R. E., Protentis, J. P., Schlossman, S. F., & Reinherz, E. L. (1983). Antigen-like effects of monoclonal antibodies directed at receptors on human T cell clones. *The Journal of Experimental Medicine*, *158*(3), 988–993. <https://doi.org/10.1084/jem.158.3.988>
- Meyran, D., Zhu, J. J., Butler, J., Tantalò, D., MacDonald, S., Nguyen, T. N., Wang, M [Minyu], Thio, N., D'Souza, C., Qin, V. M., Slaney, C., Harrison, A., Sek, K., Petrone, P., Thia, K., Giuffrida, L., Scott, A. M., Terry, R. L., Tran, B., . . . Neeson, P. J. (2023). Tstem-like CAR-T cells exhibit improved persistence and tumor control compared with conventional CAR-T cells in preclinical models. *Science Translational Medicine*, *15*(690), eabk1900.
<https://doi.org/10.1126/scitranslmed.abk1900>
- Michels, A., Ho, N., & Buchholz, C. J. (2022). Precision medicine: In vivo CAR therapy as a showcase for receptor-targeted vector platforms. *Mol Ther*, *30*(7), 2401–2415.
<https://doi.org/10.1016/j.ymthe.2022.05.018>
- Milani, M., Annoni, A., Moalli, F., Liu, T., Cesana, D., Calabria, A., Bartolaccini, S., Biffi, M., Russo, F., Visigalli, I., Raimondi, A., Patarroyo-White, S., Dräger, D., Cristofori, P., Ayuso, E., Montini, E., Peters, R., Iannacone, M., Cantore, A., & Naldini, L [Luigi] (2019). Phagocytosis-shielded lentiviral vectors improve liver gene therapy in nonhuman primates. *Sci Transl Med*, *11*, eaav7325.
<https://doi.org/10.1126/scitranslmed.aav7325>
- Miyoshi, H., Blömer, U., Takahashi, M., Gage, F. H., & Verma, I. M [I. M.] (1998). Development of a self-inactivating lentivirus vector. *Journal of Virology*, *72*(10), 8150–8157.
- Münch, R. C., Mühlebach, M. D., Schaser, T., Kneissl, S., Jost, C., Plückthun, A., Cichutek, K., & Buchholz, C. J. (2011). Darpins: An efficient targeting domain for lentiviral vectors. *Molecular Therapy : The Journal of the American Society of Gene Therapy*, *19*(4), 686–693. <https://doi.org/10.1038/mt.2010.298>
- Murphy, K. M., Janeway, C. A., Travers, P., Walport, M., Mowat, A., & Weaver, C. T. (2012). *Janeways Immunobiology 8th edition*.
- Naldini, L [Luigi], Trono, D [Didier], & Verma, I. M [Inder M.] (2016). Lentiviral vectors, two decades later. *Science (New York, N.Y.)*, *353*(6304), 1101–1102.
<https://doi.org/10.1126/science.aah6192>

- Newick, K., Moon, E., & Albelda, S. M. (2016). Chimeric antigen receptor T-cell therapy for solid tumors. *Molecular Therapy Oncolytics*, 3, 16006. <https://doi.org/10.1038/mto.2016.6>
- Nishi, T., & Forgac, M. (2002). The vacuolar (H⁺)-ATPases--nature's most versatile proton pumps. *Nature Reviews. Molecular Cell Biology*, 3(2), 94–103. <https://doi.org/10.1038/nrm729>
- Oelsner, S., Friede, M. E., Zhang, C [Congcong], Wagner, J., Badura, S., Bader, P., Ullrich, E., Ottmann, O. G., Klingemann, H., Tonn, T., & Wels, W. S. (2017). Continuously expanding CAR NK-92 cells display selective cytotoxicity against B-cell leukemia and lymphoma. *Cytotherapy*, 19(2), 235–249. <https://doi.org/10.1016/j.jcyt.2016.10.009>
- Palacios, E. H., & Weiss, A [Arthur] (2004). Function of the Src-family kinases, Lck and Fyn, in T-cell development and activation. *Oncogene*, 23(48), 7990–8000. <https://doi.org/10.1038/sj.onc.1208074>
- Petrillo, C., Thorne, L. G., Unali, G., Schioli, G., Giordano, A. M. S., Piras, F., Cuccovillo, I., Petit, S. J., Ahsan, F., Noursadeghi, M., Clare, S., Genovese, P., Gentner, B., Naldini, L [Luigi], Towers, G. J., & Kajaste-Rudnitski, A. (2018). Cyclosporine H Overcomes Innate Immune Restrictions to Improve Lentiviral Transduction and Gene Editing In Human Hematopoietic Stem Cells. *Cell Stem Cell*, 23(6), 820-832.e9. <https://doi.org/10.1016/j.stem.2018.10.008>
- Pfeiffer, A., Thalheimer, F. B., Hartmann, S., Frank, A. M., Bender, R. R., Danisch, S., Costa, C., Wels, W. S., Modlich, U., Stripecke, R., Verhoeyen, E., & Buchholz, C. J. (2018). In vivo generation of human CD19-CAR T cells results in B-cell depletion and signs of cytokine release syndrome. *EMBO Mol Med*, 10(10), e9158. <https://doi.org/10.15252/emmm.201809158>
- Puttini, M., Coluccia, A. M. L., Boschelli, F., Cleris, L., Marchesi, E., Donella-Deana, A., Ahmed, S., Redaelli, S., Piazza, R., Magistrini, V., Andreoni, F., Scapozza, L., Formelli, F., & Gambacorti-Passerini, C. (2006). In vitro and in vivo activity of SKI-606, a novel Src-Abl inhibitor, against imatinib-resistant Bcr-Abl⁺ neoplastic cells. *Cancer Research*, 66(23), 11314–11322. <https://doi.org/10.1158/0008-5472.CAN-06-1199>
- Ramos, C. A., Rouce, R., Robertson, C. S., Reyna, A., Narala, N., Vyas, G., Mehta, B., Zhang, H [Huimin], Dakhova, O., Carrum, G., Kamble, R. T., Gee, A. P., Mei, Z., Wu, M.-F., Liu, H [Hao], Grilley, B., Rooney, C. M., Heslop, H. E., Brenner, M. K., . . . Dotti, G. (2018). In Vivo Fate and Activity of Second- versus Third-Generation CD19-Specific CAR-T Cells in B Cell Non-Hodgkin's Lymphomas. *Molecular Therapy*, 26(12), 2727–2737. <https://doi.org/10.1016/j.jymthe.2018.09.009>

- Rasbach, A., Abel, T., Münch, R. C., Boller, K., Schneider-Schaulies, J., & Buchholz, C. J. (2013). The receptor attachment function of measles virus hemagglutinin can be replaced with an autonomous protein that binds Her2/neu while maintaining its fusion-helper function. *J Virol*, *87*(11), 6246–6256. <https://doi.org/10.1128/JVI.03298-12>
- Remington, R. L., Rix, U., Colinge, J., Hantschel, O., Bennett, K. L., Stranzl, T., Müller, A., Baumgartner, C., Valent, P., Augustin, M., Till, J. H., & Superti-Furga, G. (2009). Global target profile of the kinase inhibitor bosutinib in primary chronic myeloid leukemia cells. *Leukemia*, *23*(3), 477–485. <https://doi.org/10.1038/leu.2008.334>
- Rezaei, R., Esmaili Gouvarchin Ghaleh, H., Farzanehpour, M., Dorostkar, R., Ranjbar, R., Bolandian, M., Mirzaei Nodoshan, M., & Ghorbani Alvanegh, A. (2022). Combination therapy with CAR T cells and oncolytic viruses: A new era in cancer immunotherapy. *Cancer Gene Therapy*, *29*(6), 647–660. <https://doi.org/10.1038/s41417-021-00359-9>
- Ruella, M., Xu, J., Barrett, D. M., Fraietta, J. A., Reich, T. J., Ambrose, D. E., Klichinsky, M., Shestova, O., Patel, P. R., Kulikovskaya, I., Nazimuddin, F., Bhoj, V. G., Orlando, E. J., Fry, T. J., Bitter, H., Maude, S. L., Levine, B. L., Nobles, C. L., Bushman, F. D., . . . Melenhorst, J. J. (2018). Induction of resistance to chimeric antigen receptor T cell therapy by transduction of a single leukemic B cell. *Nat Med*, *24*(10), 1499–1503. <https://doi.org/10.1038/s41591-018-0201-9>
- Sabatino, M., Hu, J., Sommariva, M., Gautam, S., Fellowes, V., Hocker, J. D., Dougherty, S., Qin, H [Haiying], Klebanoff, C. A., Fry, T. J., Gress, R. E., Kochenderfer, J. N., Stroncek, D. F., Ji, Y., & Gattinoni, L. (2016). Generation of clinical-grade CD19-specific CAR-modified CD8+ memory stem cells for the treatment of human B-cell malignancies. *Blood*, *128*(4), 519–528. <https://doi.org/10.1182/blood-2015-11-683847>
- Sakuma, T., Barry, M. A., & Ikeda, Y. (2012). Lentiviral vectors: Basic to translational. *The Biochemical Journal*, *443*(3), 603–618. <https://doi.org/10.1042/BJ20120146>
- Salz, L., Seitz, A., Schäfer, D., Franzen, J., Holzer, T., Garcia-Prieto, C. A., Bürger, I., Hardt, O., Esteller, M., & Wagner, W. (2023). Culture expansion of CAR T cells results in aberrant DNA methylation that is associated with adverse clinical outcome. *Leukemia*, 1–11. <https://doi.org/10.1038/s41375-023-01966-1>
- Schade, A. E., Schieven, G. L., Townsend, R., Jankowska, A. M., Susulic, V., Zhang, R [Rosemary], Szpurka, H., & Maciejewski, J. P. (2008). Dasatinib, a small-molecule protein tyrosine kinase inhibitor, inhibits T-cell activation and proliferation. *Blood*, *111*(3), 1366–1377. <https://doi.org/10.1182/blood-2007-04-084814>
- Seggewiss, R., Loré, K., Greiner, E., Magnusson, M. K., Price, D. A., Douek, D. C., Dunbar, C. E., & Wiestner, A. (2005). Imatinib inhibits T-cell receptor-mediated T-cell proliferation and activation in a dose-dependent manner. *Blood*, *105*(6), 2473–2479. <https://doi.org/10.1182/blood-2004-07-2527>

- Shah, N. P., Tran, C., Lee, F. Y., Chen, P., Norris, D., & Sawyers, C. L. (2004). Overriding imatinib resistance with a novel ABL kinase inhibitor. *Science (New York, N.Y.)*, *305*(5682), 399–401. <https://doi.org/10.1126/science.1099480>
- Shimabukuro-Vornhagen, A., Gödel, P., Subklewe, M., Stemmler, H. J., Schlößer, H. A., Schlaak, M., Kochanek, M., Böll, B., & Bergwelt-Baildon, M. S. von (2018). Cytokine release syndrome. *Journal for Immunotherapy of Cancer*, *6*(1), 56. <https://doi.org/10.1186/s40425-018-0343-9>
- Sommermeier, D [D.], Hudecek, M [M.], Kosasih, P. L., Gogishvili, T., Maloney, D. G [D. G.], Turtle, C. J [C. J.], & Riddell, S. R [S. R.] (2016). Chimeric antigen receptor-modified T cells derived from defined CD8+ and CD4+ subsets confer superior antitumor reactivity in vivo. *Leukemia*, *30*(2), 492–500. <https://doi.org/10.1038/leu.2015.247>
- Srivastava, S., & Riddell, S. R [Stanley R.] (2015). Engineering CAR-T cells: Design concepts. *Trends in Immunology*, *36*(8), 494–502. <https://doi.org/10.1016/j.it.2015.06.004>
- Sterner, R. C., & Sterner, R. M. (2021). Car-T cell therapy: Current limitations and potential strategies. *Blood Cancer Journal*, *11*(4), 69. <https://doi.org/10.1038/s41408-021-00459-7>
- Straus, D. B., & Weiss, A [A.] (1992). Genetic evidence for the involvement of the lck tyrosine kinase in signal transduction through the T cell antigen receptor. *Cell*, *70*(4), 585–593. [https://doi.org/10.1016/0092-8674\(92\)90428-F](https://doi.org/10.1016/0092-8674(92)90428-F)
- Sušac, L., Vuong, M. T., Thomas, C., Bülow, S. von, O'Brien-Ball, C., Santos, A. M., Fernandes, R. A., Hummer, G., Tampé, R., & Davis, S. J. (2022). Structure of a fully assembled tumor-specific T cell receptor ligated by pMHC. *Cell*, *185*(17), 3201-3213.e19. <https://doi.org/10.1016/j.cell.2022.07.010>
- Tantalo, D. G., Oliver, A. J., Scheidt, B. von, Harrison, A. J., Mueller, S. N., Kershaw, M. H., & Slaney, C. Y. (2021). Understanding T cell phenotype for the design of effective chimeric antigen receptor T cell therapies. *Journal for Immunotherapy of Cancer*, *9*(5). <https://doi.org/10.1136/jitc-2021-002555>
- Thistlethwaite, F. C., Gilham, D. E., Guest, R. D., Rothwell, D. G., Pillai, M., Burt, D. J., Byatte, A. J., Kirillova, N., Valle, J. W., Sharma, S. K., Chester, K. A., Westwood, N. B., Halford, S. E. R., Nabarro, S., Wan, S., Austin, E., & Hawkins, R. E. (2017). The clinical efficacy of first-generation carcinoembryonic antigen (CEACAM5)-specific CAR T cells is limited by poor persistence and transient pre-conditioning-dependent respiratory toxicity. *Cancer Immunology, Immunotherapy : CII*. Advance online publication. <https://doi.org/10.1007/s00262-017-2034-7>
- Tokarski, J. S., Newitt, J. A., Chang, C. Y. J., Cheng, J. D., Wittekind, M., Kiefer, S. E., Kish, K., Lee, F. Y. F., Borzilleri, R., Lombardo, L. J., Xie, D., Zhang, Y [Yaqun], &

- Klei, H. E. (2006). The structure of Dasatinib (BMS-354825) bound to activated ABL kinase domain elucidates its inhibitory activity against imatinib-resistant ABL mutants. *Cancer Research*, 66(11), 5790–5797. <https://doi.org/10.1158/0008-5472.CAN-05-4187>
- Toney, A. M., Fox, D., Chaidez, V., Ramer-Tait, A. E., & Chung, S. (2021). Immunomodulatory Role of Urolithin A on Metabolic Diseases. *Biomedicines*, 9(2). <https://doi.org/10.3390/biomedicines9020192>
- Toyoshima, K., & Vogt, P. K. (1969). Enhancement and inhibition of avian sarcoma viruses by polycations and polyanions. *Virology*, 38(3), 414–426. [https://doi.org/10.1016/0042-6822\(69\)90154-8](https://doi.org/10.1016/0042-6822(69)90154-8)
- Turtle, C. J [Cameron J.], Hanafi, L.-A., Berger, C., Gooley, T. A., Cherian, S., Hudecek, M [Michael], Sommermeyer, D [Daniel], Melville, K., Pender, B., Budiarto, T. M., Robinson, E., Steevens, N. N., Chaney, C., Soma, L., Chen, X., Yeung, C., Wood, B., Li, D., Cao, J., . . . Maloney, D. G [David G.] (2016). Cd19 CAR-T cells of defined CD4+:Cd8+ composition in adult B cell ALL patients. *The Journal of Clinical Investigation*, 126(6), 2123–2138. <https://doi.org/10.1172/JCI85309>
- Valitutti, S [S.], Müller, S., Cella, M., Padovan, E., & Lanzavecchia, A [A.] (1995). Serial triggering of many T-cell receptors by a few peptide-MHC complexes. *Nature*, 375(6527), 148–151. <https://doi.org/10.1038/375148a0>
- Valitutti, S [Salvatore], & Lanzavecchia, A [Antonio] (1997). Serial triggering of TCRs: a basis for the sensitivity and specificity of antigen recognition. *Immunology Today*, 18(6), 299–304. [https://doi.org/10.1016/S0167-5699\(97\)80027-8](https://doi.org/10.1016/S0167-5699(97)80027-8)
- van der Donk, L. E. H., Ates, L. S., van der Spek, J., Tukker, L. M., Geijtenbeek, T. B. H., & van Heijst, J. W. J. (2021). Separate signaling events control TCR downregulation and T cell activation in primary human T cells. *Immunity, Inflammation and Disease*, 9(1), 223–238. <https://doi.org/10.1002/iid3.383>
- Verdon, D. J., Mulazzani, M., & Jenkins, M. R. (2020). Cellular and Molecular Mechanisms of CD8+ T Cell Differentiation, Dysfunction and Exhaustion. *International Journal of Molecular Sciences*, 21(19). <https://doi.org/10.3390/ijms21197357>
- Vermeer, L. S., Hamon, L., Schirer, A., Schoup, M., Cosette, J., Majdoul, S., Pastré, D., Stockholm, D., Holic, N., Hellwig, P., Galy, A., Fenard, D., & Bechinger, B. (2017). Vectofusin-1, a potent peptidic enhancer of viral gene transfer forms pH-dependent α -helical nanofibrils, concentrating viral particles. *Acta Biomaterialia*, 64, 259–268. <https://doi.org/10.1016/j.actbio.2017.10.009>
- Vormittag, P., Gunn, R., Ghorashian, S., & Veraitch, F. S. (2018). A guide to manufacturing CAR T cell therapies. *Curr Opin Biotechnol*, 53, 164–181. <https://doi.org/10.1016/j.copbio.2018.01.025>

- Vrisekoop, N., den Braber, I., Boer, A. B. de, Ruiter, A. F. C., Ackermans, M. T [Mariëtte T.], van der Crabben, S. N., Schrijver, E. H. R., Spierenburg, G., Sauerwein, H. P., Hazenberg, M. D., Boer, R. J. de, Miedema, F., Borghans, J. A. M., & Tesselaar, K. (2008). Sparse production but preferential incorporation of recently produced naive T cells in the human peripheral pool. *Proceedings of the National Academy of Sciences of the United States of America*(105), 6115–6120.
- Wang, L., Gong, W., Wang, S [Sanmei], Neuber, B., Sellner, L., Schubert, M.-L., Hückelhoven-Krauss, A., Kunz, A., Gern, U., Michels, B., Hinkelbein, M., Mechler, S., Richter, P., Müller-Tidow, C., Schmitt, M., & Schmitt, A. (2019). Improvement of in vitro potency assays by a resting step for clinical-grade chimeric antigen receptor engineered T cells. *Cytotherapy*, 21(5), 566–578.
<https://doi.org/10.1016/j.jcyt.2019.02.013>
- Wang, X [Xiuyan], & Riviere, I. (2016). Clinical manufacturing of CAR T cells: Foundation of a promising therapy. *Molecular Therapy Oncolytics*, 3, 16015.
<https://doi.org/10.1038/mto.2016.15>
- Watanabe, N., Mo, F., & McKenna, M. K. (2022). Impact of Manufacturing Procedures on CAR T Cell Functionality. *Frontiers in Immunology*, 13, 876339.
<https://doi.org/10.3389/fimmu.2022.876339>
- Weber, E. W., Lynn, R. C., Sotillo, E., Lattin, J., Xu, P., & Mackall, C. L. (2019). Pharmacologic control of CAR-T cell function using dasatinib. *Blood Advances*, 3(5), 711–717. <https://doi.org/10.1182/bloodadvances.2018028720>
- Weber, E. W., Parker, K. R., Sotillo, E., Lynn, R. C., Anbunathan, H., Lattin, J., Good, Z., Belk, J. A., Daniel, B., Klysz, D., Malipatlolla, M., Xu, P., Bashti, M., Heitzeneder, S., Labanieh, L., Vandris, P., Majzner, R. G., Qi, Y., Sandor, K., . . . Mackall, C. L. (2021). Transient rest restores functionality in exhausted CAR-T cells through epigenetic remodeling. *Science (New York, N.Y.)*, 372(6537).
<https://doi.org/10.1126/science.aba1786>
- Weinkove, R., George, P., Dasyam, N., & McLellan, A. D. (2019). Selecting costimulatory domains for chimeric antigen receptors: Functional and clinical considerations. *Clinical & Translational Immunology*, 8(5), e1049. <https://doi.org/10.1002/cti2.1049>
- Xu, Y [Yang], Zhang, M., Ramos, C. A., Durett, A., Liu, E., Dakhova, O., Liu, H [Hao], Creighton, C. J., Gee, A. P., Heslop, H. E., Rooney, C. M., Savoldo, B., & Dotti, G. (2014). Closely related T-memory stem cells correlate with in vivo expansion of CAR.Cd19-T cells and are preserved by IL-7 and IL-15. *Blood*, 123(24), 3750–3759.
<https://doi.org/10.1182/blood-2014-01-552174>
- Yang, J., He, J., Zhang, X [Xian], Li, J [Jingjing], Wang, Z [Zhenguang], Zhang, Y [Yongliang], Qiu, L., Wu, Q., Sun, Z., Ye, X., Yin, W., Cao, W., Shen, L., Sersch, M.,

- & Lu, P. (2022). Next-day manufacture of a novel anti-CD19 CAR-T therapy for B-cell acute lymphoblastic leukemia: First-in-human clinical study. *Blood Cancer Journal*, 12(7), 104. <https://doi.org/10.1038/s41408-022-00694-6>
- Yu, Y.-R., Imrichova, H., Wang, H [Haiping], Chao, T., Xiao, Z., Gao, M., Rincon- Restrepo, M., Franco, F., Genolet, R., Cheng, W.-C., Jandus, C., Coukos, G., Jiang, Y.-F., Locasale, J. W., Zippelius, A., Liu, P.-S., Tang, L., Bock, C., Vannini, N., & Ho, P.-C. (2020). Disturbed mitochondrial dynamics in CD8+ TILs reinforce T cell exhaustion. *Nature Immunology*, 21(12), 1540–1551. <https://doi.org/10.1038/s41590-020-0793-3>
- Zhang, C [Cheng], He, J., Liu, L [Li], Wang, J [Jishi], Wang, S [Sanbin], Liu, L [Ligen], Ge, J., Gao, L [Lei], Gao, L [Li], Kong, P., Liu, Y., Liu, J., Han, Y [Yu], Zhang, Y [Yongliang], Sun, Z., Ye, X., Yin, W., Sersch, M., Shen, L., . . . Zhang, X [Xi] (2022). Novel CD19 chimeric antigen receptor T cells manufactured next-day for acute lymphoblastic leukemia. *Blood Cancer Journal*, 12(6), 96. <https://doi.org/10.1038/s41408-022-00688-4>
- Zhang, C [Chengcheng], Wang, Z [Zhe], Yang, Z [Zhi], Wang, M [Meiling], Li, S., Li, Y., Zhang, R [Rui], Xiong, Z., Wei, Z., Shen, J., Luo, Y [Yongli], Zhang, Q., Liu, L [Limei], Qin, H [Hong], Liu, W., Wu, F., Chen, W., Pan, F., Zhang, X [Xianquan], . . . Qian, C. (2017). Phase I Escalating-Dose Trial of CAR-T Therapy Targeting CEA+ Metastatic Colorectal Cancers. *Molecular Therapy : The Journal of the American Society of Gene Therapy*. Advance online publication. <https://doi.org/10.1016/j.ymthe.2017.03.010>
- Zhang, H [Hao], Hu, Y., Shao, M., Teng, X., Jiang, P., Wang, X [Xiujian], Wang, H [Hui], Cui, J., Yu, J., Liang, Z., Ding, L., Han, Y [Yingli], Wei, J., Xu, Y [Yulin], Li, X., Shan, W., Shi, J., Luo, Y [Yi], Qian, P., & Huang, H. (2021). Dasatinib enhances anti-leukemia efficacy of chimeric antigen receptor T cells by inhibiting cell differentiation and exhaustion. *Journal of Hematology & Oncology*, 14(1), 113. <https://doi.org/10.1186/s13045-021-01117-y>
- Zhao, X., Li, J [Jiarui], Winkler, C. A., An, P., & Guo, J.-T. (2018). Ifitm Genes, Variants, and Their Roles in the Control and Pathogenesis of Viral Infections. *Frontiers in Microbiology*, 9, 3228. <https://doi.org/10.3389/fmicb.2018.03228>
- Zhou, Q., Schneider, I. C [I. C.], Edes, I., Honegger, A., Bach, P., Schönfeld, K., Schambach, A., Wels, W. S., Kneissl, S., Uckert, W., & Buchholz, C. J. (2012). T-cell receptor gene transfer exclusively to human CD8(+) cells enhances tumor cell killing. *Blood*, 120(22), 4334–4342. <https://doi.org/10.1182/blood-2012-02-412973>
- Zhou, Q., Uhlig, K. M., Muth, A., Kimpel, J., Lévy, C., Münch, R. C., Seifried, J., Pfeiffer, A., Trkola, A., Coulibaly, C., Laer, D. von, Wels, W. S., Hartwig, U. F., Verhoeven, E., &

- Buchholz, C. J. (2015). Exclusive Transduction of Human CD4+ T Cells upon Systemic Delivery of CD4-Targeted Lentiviral Vectors. *J Immunol*, 195(5), 2493–2501. <https://doi.org/10.4049/jimmunol.1500956>
- Zufferey, R., Dull, T., Mandel, R. J., Bukovsky, A., Quiroz, D., Naldini, L [L.], & Trono, D [D.] (1998). Self-inactivating lentivirus vector for safe and efficient in vivo gene delivery. *J Virol*, 72(12), 9873–9880.
- Zufferey, R., Nagy, D., Mandel, R. J., Naldini, L [L.], & Trono, D [D.] (1997). Multiply attenuated lentiviral vector achieves efficient gene delivery in vivo. *Nat Biotechnol*, 15(9), 871–875. <https://doi.org/10.1038/nbt0997-871>

6 Abbreviations

Abbreviation	Definition
Abl	Abelson murine leukemia
ALL	acute lymphoblastic leukemia
ANOVA	analysis of variance
APC	Antigen-presenting cell
B cells	B lymphocytes
BCMA	B cell maturation antigen
Bcr	Breakpoint cluster region
BfiA1	Bafilomycin A1
BSA	Bovine serum albumin
CAR	Chimeric antigen receptor
CCL3	C-C Motif Chemokine Ligand 3
CD	Cluster of differentiation
CD3-LV	CD3 receptor-targeted lentiviral vector
CD4-LV	CD4 receptor-targeted lentiviral vector
CD8-LV	CD8 receptor-targeted lentiviral vector
CEA	Carcinoembryonic antigen
CI	Confidence interval
CRC	Colorectal cancer
CRS	Cytokine release syndrome
CTLA-4	T-lymphocyte-associated protein 4
CTV	CellTrace® Violet
CXCL10	C-X-C motif chemokine ligand 10
Dasat.	Dasatinib
DARPin	Designed ankyrin repeat protein
DC	Dendritic cell
DMEM	Dulbecco's Modified Eagle Medium
DMSO	Dimethyl sulfoxide
DNA	Desoxyribonucleic acid
EDTA	Ethylenediaminetetraacetic acid
EGFR	Epithelial growth factor receptor
ELISA	Enzyme-linked immunosorbent assay

EMA	European Medicines Agency
FBS	Fetal bovine serum
FcR	Fc receptor
FDA	Food and Drug Administration
F protein	Fusion protein
GD2	Disialoganglioside 2
GFP	Green fluorescent protein
GM-CSF	Granulocyte-macrophage colony-stimulating factor
GOI	Gene of interest
G protein	Glycoprotein
GvHD	Graft-versus host disease
h	Hour(s)
HEK	Human embryonic kidney
HEPES	N-2-hydroxyethylpiperazine-N'-2-ethanesulfonic acid
HER2	Epidermal growth factor receptor-2
HIV-1	Human immunodeficiency virus-1
HSC	Hematopoietic stem cell
H protein	Hemagglutinin protein
i.p.	Intraperitoneal(ly)
i.v.	Intravenous(ly)
ICANS	immune effector cell-associated neurotoxicity syndrome
ICD	Intracellular domain
IFITM	Interferon-induced transmembrane
IFN	Interferon
IL	Interleukin
ITAM	Immunoreceptor tyrosine-based activation motif
LAG-3	Lymphocyte activation gene 3
Lck	Lymphocyte-specific protein tyrosine kinase
LDL	Low density lipoprotein
LNGFR	Low-affinity nerve growth factor receptor
LTR	Long terminal repeat
LV	Lentiviral vector
MFI	Mean fluorescence intensity
MHC	Major histocompatibility complex
MV	Measles virus

myc	myc-tag
NaN ₃	Sodium azide
NiV	Nipah virus
NK	Natural killer
NSG	NOD.Cg-Prkdc ^{scid} Il2rg ^{tm1Wjl}
NTA	Nanoparticle tracking analysis
PBMC	Peripheral blood mononuclear cell
PBS	Phosphate-buffered saline
PCR	Polymerase chain reaction
PD-1	Programmed cell death 1
PEG300	Polyethylene glycol 300
PEI	Polyethyleneimine
PI3K	Phosphatidylinositide 3-kinase
PRR	Pattern recognition receptor
qPCR	Quantitative polymerase chain reaction
RF	Restriction factor
RNA	Ribonucleic acid
r.o.	Retroorbital(ly)
RPMI	Roswell Park Memorial Institute
RT	Room temperature
RV	Retroviral vector
s.c.	Subcutaneous(ly)
scFv	Single chain variable fragment
SD	Standard deviation
SEM	Standard error of the mean
SFFV	spleen focus forming virus
SIN	Self-inactivating
ssRNA	Single stranded ribonucleic acid
TAA	Tumor associated antigen
T cells	T lymphocyte
TCM	T cell medium
T _{CM}	T central memory
TCR	T cell receptor
T _{EFF}	T effector
T _{EM}	T effector memory

TIM-3	T cell immunoglobulin and mucin domain-containing protein 3
TKI	Tyrosine kinase inhibitor
TLR	Toll-like receptor
TMD	Transmembrane domain
T _N	T naïve
TNF- α	Tumor necrosis factor α
T _{SCM}	T stem cell memory
T.U.	Transducing units
UA	Urolithin A
Ut	Untransduced
VCN	Vector copy number
VF-1	Vectofusin-1
VSV	Vesicular stomatitis virus
VSV-G	Vesicular stomatitis virus glycoprotein
VSV-LV	Lentiviral vector pseudotyped with vesicular stomatitis virus glycoprotein
w/o	without
WPRE	Woodchuck hepatitis posttranscriptional element

7 List of figures and tables

7.1 Figures

Figure 1: CD3 receptor:T cell receptor complex.	14
Figure 2: T cell differentiation.	16
Figure 3: Chimeric antigen receptor designs.	19
Figure 4: CAR T cell manufacturing.....	21
Figure 5: Genetic information of HIV-1 and HIV-1 derived 2 nd generation lentiviral vectors.....	25
Figure 6: Engineering of paramyxoviral envelope glycoproteins for receptor targeting.	27
Figure 7: Transduction enhancers for viral vectors.....	29
Figure 8: Experimental setup for PBMC transduction in presence of dasatinib.	33
Figure 9: Dasatinib increases CD3-LV titers.....	34
Figure 10: Dasatinib increases the transduction of CD3-LV in a time- and dose-dependent manner.	35
Figure 11: Dasatinib does not interfere with T cell viability or proliferation.	37
Figure 12: Dasatinib and vectofusin-1 have a synergistic effect on CD3-LV-mediated gene delivery.	38
Figure 13: Experimental setup for transduction of non-activated PBMCs in presence of dasatinib.	39
Figure 14: Dasatinib increases CD3-LV gene transfer to cytokine-only stimulated cells.	40
Figure 15: Dasatinib increases CD3-LV gene transfer to T cells in whole blood.	41
Figure 16: Experimental design for <i>in vivo</i> CD3-LV transduction in presence of dasatinib.....	41
Figure 17: Humanization of NSG mice.	42
Figure 18: <i>In vivo</i> transgene delivery by CD3-LV in presence or absence of dasatinib.	43
Figure 19: Selectivity of <i>in vivo</i> transduction by CD3-LV in presence or absence of dasatinib.	44
Figure 20: Effect of endocytosis inhibitor Bf1A1 on CD3- and VSV-LV transduction.	46
Figure 21: Effect of dasatinib on receptor-targeted LVs.	47

Figure 22: Dasatinib prevents CD25 upregulation.....	48
Figure 23: Dasatinib increases CD3 receptor availability for CD3-LV binding.	49
Figure 24: Dasatinib increases CD3-LV binding to T cells.....	50
Figure 25: Effect of various tyrosine kinase inhibitors on lentiviral gene delivery.	52
Figure 26: Schematic representation of the CD19.CAR construct.....	53
Figure 27: Dasatinib enhances CD3-targeted CD19.CAR gene transfer.....	54
Figure 28: Dasatinib increases CD3-targeted CD19.CAR gene transfer in a time- and dose-dependent manner.....	55
Figure 29: Long-term tumor killing mediated by transduction with CD3-LV.	56
Figure 30: Experimental setup for CD19.CAR T cell generation in presence of dasatinib.	59
Figure 31: Dasatinib does not compromise CAR T cell activity.	59
Figure 32: Dasatinib mediates the generation of less exhausted CAR T cells.....	60
Figure 33: Dasatinib reduces coincident expression of LAG-3 and TIM-3.....	61
Figure 34: Dasatinib influences the T cell phenotype of CD3-LV transduced cells...	62
Figure 35: Effect of dasatinib on CAR T cells generated with CD3-LV compared to VSV-LV.....	63
Figure 36: Dasatinib reduces the expression of exhaustion markers.	64
Figure 37: Dasatinib and LV transduction affect the T cell phenotype.....	65
Figure 38: Cytokine secretion after a 24 hour killing assay.....	66
Figure 39: Experimental setup for CD19.CAR T cell generation in presence of UA.	68
Figure 40: UA does not affect CAR gene delivery or CAR T cell activity.	69
Figure 41: UA facilitates the expansion of T _{SCM} in CD4 ⁺ , CD8 ⁺ and CAR ⁺ T cells....	70
Figure 42: Schematic representation of the CEA.CAR construct.....	71
Figure 43: Experimental design of CEA.CAR T cell generation in presence of UA and dasatinib.	72
Figure 44: Combination of UA and dasatinib during CEA.CAR gene delivery.	73
Figure 45: Potent killing activity of UA treated CEA.CAR T cells.....	74
Figure 46: Effect of UA on T cell phenotype.	75
Figure 47: Cytokine secretion of UA treated cells after a 24 hour killing assay.	76
Figure 48: Dasatinib as a new transduction enhancer.....	83
Figure 49: Evasion of cellular restriction mechanisms in presence of dasatinib.	85
Figure 50: Small molecules for the refined generation of CAR T cells.....	91

7.2 Tables

Table 1: Quantitative polymerase chain reaction mixture	100
Table 2: Plasmids for lentiviral vector production	102
Table 3: Characteristics of LVs.....	103

8 List of publications

8.1 Original research articles

Charitidis F.T., Adabi E., Ho N., **Braun A.H.**, Tierney C., Strasser L., Thalheimer F.B., Childs L., Bones J., Clarke C. and Buchholz C.J. CAR gene delivery by T-cell targeted lentiviral vectors is enhanced by rapamycin induced reduction of antiviral mechanisms. *Advanced Science* (2023), doi: 10.1002/adv.202302992

Braun A.H., Frank A.M., Ho N., and Buchholz C.J. Dasatinib is a potent enhancer for CAR T cell generation by CD3-targeted lentiviral vectors. *Mol. Ther. Methods Clin. Dev.* (2023), doi: 10.1016/j.omtm.2022.12.002

Denk D., Petrocelli V., Conche C., Drachsler M., Ziegler P.K., **Braun A.H.**, Kress A., Nicolas A.M., Mohs K., Becker C., Neurath M.F., Farin H.F., Buchholz C.J., Andreux P.A., Rinsch C. and Greten F.R. Expansion of T memory stem cells with superior anti-tumor immunity by Urolithin A-induced mitophagy. *Immunity* (2022), doi: 10.1016/j.immuni.2022.09.014

Frank A.M., **Braun A.H.**, Scheib L., Agarwal S., Schneider I.C., Fusil F., Perian S., Sahin U., Thalheimer F.B., Verhoeyen E. and Buchholz C.J. Combining T-cell specific activation and *in vivo* gene delivery through CD3-targeted lentiviral vectors. *Blood Adv.* (2020), doi: 10.1182/bloodadvances.2020002229

8.2 Conference poster presentations

Dasatinib is a potent transduction enhancer of CD3-targeted LVs counteracting CAR T cell exhaustion

Braun A.H., Frank A.M., Ho N. and Buchholz C.J.

4th Rhein Main Cancer Retreat in Glashütten, Germany, 16th - 17th of March 2023

Dasatinib is a potent transduction enhancer of CD3-targeted LVs counteracting CAR T cell exhaustion

Braun A.H., Frank A.M., Ho N. and Buchholz C.J.

European Society of Gene and Cell Therapy (ESGCT) Annual Meeting conference in Edinburgh, Scotland, 11th - 14th of October 2022

Dasatinib enhances gene delivery by T cell-targeted lentiviral vectors through CD3 upregulation

Braun A.H., Frank A.M., Ho N. and Buchholz C.J.

3rd International Conference on Lymphocyte Engineering (ICLE) in Munich, Germany, 31st of March - 2nd of April 2022

8.3 Awards

Langener Nachwuchswissenschaftspreis 2023, Paul-Ehrlich-Institut

Awarded for the publication Braun et. al., 2023

Paper of the Quarter Award Q4 2020, Deutsche Gesellschaft für Gentherapie

Awarded for the publication Braun et. al., 2023

8.4 Patents

WO/2022/214588 - MEANS AND METHODS FOR ENHANCING RECEPTOR-TARGETED GENE TRANSFER

Braun A.H., Frank A.M., Buchholz C.J., filed on 07.04.2022

9 Acknowledgement

Abschließend möchte ich mich bei allen bedanken, die mich in den letzten Jahren begleitet haben.

An erster Stelle möchte ich mich ganz herzlich bei Prof. Dr. Christian Buchholz für die Möglichkeit bedanken, meine Doktorarbeit in seiner Arbeitsgruppe an so interessanten Projekten durchführen zu dürfen. Vielen Dank für die ständige Diskussionsbereitschaft, Unterstützung und hervorragende wissenschaftliche Betreuung.

An zweiter Stelle möchte ich Prof. Dr. Harald Kolmar für die unkomplizierte Betreuung als Erstgutachter seitens der Technischen Universität Darmstadt danken.

Mein besonderer Dank gilt allen Kollegen und mittlerweile Freunden, mit denen ich in den letzten Jahren zusammengearbeitet habe. Annika, Lea, Tati, Laura, Shiwani, Vanessa, Naphang, Filip, Alex, Fine, Iris, Doro, Samuel, Fred, Jessi, Luca, Arezoo, Elham, Mar, Merle, Burak, Fabi, Johanna, Manu, Julia und Gundi, danke für die bedingungslose Hilfsbereitschaft, Unterstützung, die Aufmunterung, die Ratschläge und die gemeinsamen Auszeiten. Eine solche Hilfsbereitschaft und Freundlichkeit wie hier im Labor habe ich noch nirgendwo erlebt und genau das macht diese Arbeitsgruppe so einzigartig.

Außerdem möchte ich mich bei meinen Kooperationspartnern Alena Kress und Henner Farin sowie Dominic Denk und Florian Greten vom Georg-Speyer-Haus für die gute und erfolgreiche Zusammenarbeit bedanken.

Ein großes Dankeschön geht an meine Familie und Freunde, die immer für mich da sind. Danke Mama und Papa, dass ihr mich immer von ganzem Herzen unterstützt und mir zeigt, wie stolz ihr auf mich seid. Danke auch an meinen Bruder Robin, meine Omi Gudi und den Rest meiner Familie. Eure Liebe und Unterstützung bedeuten mir unendlich viel.

Zuletzt möchte ich mich ganze besonders bei dir, Lennart, bedanken. Danke, dass du immer an meiner Seite bist, mir Rückhalt gibst und immer an mich glaubst.

10 Ehrenwörtliche Erklärung

§8 Abs. 1 lit. c der Promotionsordnung der TU Darmstadt

Ich versichere hiermit, dass die elektronische Version meiner Dissertation mit der schriftlichen Version übereinstimmt und für die Durchführung des Promotionsverfahrens vorliegt.

§8 Abs. 1 lit. d der Promotionsordnung der TU Darmstadt

Ich versichere hiermit, dass zu einem vorherigen Zeitpunkt noch keine Promotion versucht wurde und zu keinem früheren Zeitpunkt an einer in- oder ausländischen Hochschule eingereicht wurde. In diesem Fall sind nähere Angaben über Zeitpunkt, Hochschule, Dissertationsthema und Ergebnis dieses Versuchs mitzuteilen.

§9 Abs. 1 der Promotionsordnung der TU Darmstadt

Ich versichere hiermit, dass die vorliegende Dissertation selbstständig und nur unter Verwendung der angegebenen Quellen verfasst wurde.

§9 Abs. 2 der Promotionsordnung der TU Darmstadt

Die Arbeit hat bisher noch nicht zu Prüfungszwecken gedient.

Darmstadt, den

(Name und Unterschrift)